PFC/RR-89-12

The Impact of Blanket Design on Activation and Thermal Safety

Yüksel Parlatan

Plasma Fusion Center
Massachusetts Institute of Technology
Cambridge, MA 02139

June 1989

This work was supported by EG&G Contract C86-110982-TKP-153-87.

THE IMPACT OF BLANKET DESIGN ON ACTIVATION AND THERMAL SAFETY

by

YÜKSEL PARLATAN

B.S. Hacettepe University-Ankara-Turkey 1986

SUBMITTED TO THE DEPARTMENT OF
NUCLEAR ENGINEERING IN PARTIAL FULFILLMENT OF THE
REQUIREMENTS FOR THE DEGREE OF

MASTER OF SCIENCE

at the

MASSACHUSETTS INSTITUTE OF TECHNOLOGY

JUNE 1989

Signature of Author

Department of Nuclear Engineering, June 9,1989

Certified by

Mujid S.Kazimi, Thesis Supervisor

Accepted by

Allan F. Henry,
Chairman, Department Committee

THE IMPACT OF BLANKET DESIGN ON ACTIVATION AND THERMAL SAFETY

by

YÜKSEL PARLATAN

Submitted to the Department of Nuclear Engineering
on June 9, 1989 in partial fulfillment of the
requirements for the Degree of Master of Science in
Nuclear Engineering

Abstract

Activation and thermal safety analyses for experimental and power reactors are presented. The effects of a strong neutron absorber, B_4C, on activation and temperature response of experimental reactors to Loss-of-Cooling Accidents are investigated. Operational neutron fluxes, radioactivities of elements and thermal transients are calculated using the codes ONEDANT, REAC and THIOD, respectively.

The inclusion of a small amount of B_4C in the steel blanket of an experimental reactor reduces its activation and the post LOCA temperature escalation significantly. Neither the inclusion of excessive amounts of B_4C nor enriched ^{10}B in the first walls of an experimental reactor bring much advantage. The employment of a 2 cm graphite tile liner before the first wall helps to limit the post LOCA escalation of first wall temperature.

The effect of replacing a 20 cm thick section of a steel shield of a fusion power reactor with B_4C is also analyzed. The first wall temperature peak is reduced by 100°C in the modified blanket.

The natural convection effect on thermal safety of a liquid lithium cooled blanket are investigated. Natural convection has no impact at all, unless the magnetic field can be reduced. If magnets can be shut off rapidly after the accident, then the temperature escalation of the first wall will be limited. Upflow of the coolant is better than the initial downflow design from a thermal safety point of view.

Activities of three structural materials, OTR stainless steel, SS-316 and VCrTi are compared. Although VCrTi has higher activity for a period of two hours after the accident, it has one to two orders of magnitude less activity than those of the steels in the mid- and long-terms.

Thesis Supervisor: Mujid S. Kazimi
Title: Professor of Nuclear Engineering

Table of Contents

ACKNOWLEDGEMENTS

The author wishes to thank Professor Kazimi for his patient guidance and help throughout the course of this work. Special thanks also go to John Massidda, without his help this work would not have accomplished. I would also like to thank Erol Çubukçu for his computing skills and his constant support. I would also like to thank Professor Osman Kadiroğlu to whom I owe a lot.

The author wishes to acknowledge the financial support of the Turkish Ministry of Education and the Department of Nuclear Engineering.

This work is dedicated to my family, Mehmet, Saliha, Havva, Gülsen and Ahmet, to whom I am grateful.

List of Figures

List of Tables

Chapter 1

Introduction

Fusion energy is believed to be one of the most promising energy sources which may be available for commercial power production in the future. The safety concerns of fusion have at times been considered non-existent. Today, however, it is recognized that even fusion has potential adverse health effects which must be evaluated in relation to other energy options. A proper development path will hopefully minimize the potential hazards of the future fusion power plants [1].

Use of the D-T fusion cycle will result in induced radioactivity in materials surrounding the plasma, especially the structural first wall and blanket. One resulting problem is the potential for public exposure to the radioactive material due to a possible accidental release. Acceptance of fusion as a commercial energy source will be determined partly by environmental considerations. Specifically, the radiological hazards of fusion must be substantially less than those associated with fission in order to offset fusion's greater technological complexity and cost [2,3,4].

Just as reactor blanket choices should decrease costs and enhance fusion's economic attractiveness, so should blanket choices decrease potential risk to the public and enhance fusion's safety and environmental attractiveness. An increase in safety and environmental attractiveness of designs at the current stage of development will tend to increase public support and acceptance, which will translate into some future economic advantages, and increase the general potential of fusion energy [5].

1.1 Definition of the Problem

The function of the primary system of a fusion reactor is to remove the energy deposited in the first wall/blanket region surrounding the plasma. Energy enters the blanket region through the first wall either in the form of neutrons or direct radiation. The neutrons transfer their kinetic energy into thermal energy through collisions and nuclear reactions with the blanket material. Incident radiation is conducted away from the first wall by the blanket medium. Conduits within the blanket structure contain the primary coolant to which the energy deposited in the blanket is transferred [6].

A loss of cooling accident may result from a pump failure or a rupture of a coolant line. The severity of a loss-of-cooling accident depends on the specific failure mode. For instance, the effect of an individual plugged tube causing a loss-of-cooling in the blanket would be localized in the vicinity of the inactive cooling tube. A temperature rise will be expected in this area, but removal of heat by adjacent, operative cooling tubes would assist in the heat removal and limit the extent of the transient.

In the event of a ruptured or leaking coolant line, on the other hand, loss of the coolant serving an entire module could result. The other modules would still operate normally, providing cooling. A worst case, wherein the entire coolant inventory to all modules is lost, can be envisioned. This event is much more serious in that there is no way to remove the heat load. All modules would experience the same transient. The potential for damage and loss of structural integrity exist.

As mentioned earlier, a number of different scenarios can lead to loss-of-cooling, including pump failure, flow blockage, loss-of-site power, and loss-of-coolant. These accidents can be divided into two general groups, namely, Loss-of-Flow Accident (LOFA) and Loss-of-Coolant Accidents (LOCA). In a LOFA, the coolant, which normally is being pumped through the blanket, and is thus removing the heat via forced convection, stops flowing. This can arise because the coolant pump fails, or the coolant flow passage becomes blocked by some structural failure. The result is that the heat, whether operational power or decay heat in the blanket, is no longer being actively removed.

This leads to a temperature rise in the blanket. A LOCA can arise if a coolant tube or a coolant piping ruptures, thus allowing the coolant to leak out of the system. In this case, the coolant will drain out of the blanket, leaving a void in its place. This will obviously cause a termination of active cooling, and a blanket temperature rise [7].

Subsequent to a loss of cooling accident, there are two heat sources of concern. If the plasma is not extinguished, it will continue to deposit energy in the blanket by neutron and surface heating until it is terminated by either entry of impurities into the plasma (e.g, volatilized first wall material, blanket coolant or breeder), the cause of the accident itself (e.g., magnet quench) or an active shutdown mechanism. Prompt and reliable shutdown of the plasma within a short time would minimize the impact of the Loss-of-Cooling accident. Regardless of whether or not the plasma is terminated, the decay afterheat due to induced structural radioactivity will exist as a heat source in the blanket. In both cases, the consequences at the first wall are the major concern, since it receives the highest surface heating and it is the region of highest decay heat density. Large temperature excursions leading to first wall/blanket structural failure and possible radioactive releases can occur if the heat is not passively dissipated from the wall or an auxiliary cooling system is not provided.

The magnitude of the first wall temperature increase subsequent to a Loss-of-Cooling accident is dependent on the length of time of continued plasma burn, and the decay heat density in the blanket and the first wall. It is expected that the plasma will terminate within seconds after the accident has been initiated. The decay afterheat source, however , will be present over many hours to days, so that the transient may extend over a long period of time. The first wall temperature may rise high enough to result in melting or volatization. If the vacuum vessel is breached, oxygen may enter and oxides may form. These oxides are generally more volatile than the elements from which they are formed, so that they may become mobilized at a lower temperature. With a breached vacuum vessel, there is a pathway to the reactor wall. If the reactor building has not maintained its integrity, the released activity can enter the environment and

reach the public domain.

1.2 Motivation for This Work

In a *fission* plant, the fundamental hazard source is the radioactivity caused by the fissioning process. The material selection and design significantly influence the possible accident scenarios and overall risk. However, the radioactive fission products and actinides are sources of hazards largely independent of the structure or coolant.

In a *fusion* plant, it appears that material selection is more important. The fundamental hazard sources are the presence of a radioactive fuel (e.g., tritium) and induced structural radioactivity. Fortunately, this induced radioactivity is material dependent. Thus, with proper selection of materials, acceptable levels of radiation may be achieved.

Keeping the activation levels low in the blanket and shield is very important for several reasons [8]:

- To minimize the dose rate around the reactor and to maintenance workers;
- To diminish the problems of waste handling;
- To limit the potential escalation in temperature following shutdown, which may cause structural failure possibly with subsequent radioactive isotope release; and
- To lower the potential adverse health effects in case of a severe accident.

Power/cooling mismatch is one of the accidents which can cause plant damage. The problem stems from the fact that undercooling or increased power would cause the temperature in the first wall/blanket region of the reactor to rise. If the temperatures get too high, the structural elements in the first wall/blanket will weaken and subsequently suffer structural failure and possibly melt. In severe cases, this could also lead to the release of some of the activation product inventory.

The goal of this study is to explore the thermal safety characteristics of fusion reactor blankets in various designs. The design alternatives aim to enhance thermal safety by limiting activation levels, which also limits decay heat generation rates.

1.3 Results of Previous Studies

The issue of the potential hazards of fusion reactor operation has been the focus of a number of studies. Many of these have concentrated on defining the risks associated with fusion. Many different quantitative measures of hazard have been used in developing a calculational methodology for comparing the accidents, occupational and waste disposal hazards of fusion reactor designs [2].

There are two levels of safety concerns. The first level involves the risk to public health from a release of radioactivity from the plant. Two sources of radiation in a fusion power plant are tritium and neutron activation products. The total inventory of these activation products depends on the fuel cycle and the reactor materials. Comparison of activity levels, as well as the general safety characteristics of various fuel cycles is made in reference [6]. The influence of steel type on the activation and decay of fusion reactor first wall has been investigated in another study [9]. In that study, five steels (PCA, HT-9, thermally stabilized 2.25Cr-1Mo, Nb stabilized 2.25Cr-1Mo, and 2.25Cr-1V) are compared as a function of time from the viewpoints of activation, afterheat, inhalation biological hazard potential (BHP), ingestion BHP, and feasibilty of disposal by shallow land burial. The PCA steel is found to be the worst choice and 2.25Cr-1V to be the best choice by substantial margins from all five viewpoints. The HT-9 and two versions of 2.25Cr-1Mo are roughly the same at intermediate values. The 2.25Cr-1V has about the same afterheat as those three steels, but its waste disposal feasibility is considerably better. In another study, 316 SS, V-15Cr-Ti and TZM were compared from a potential public health effects point of view. The effects of 316 SS is found to be two orders of magnitude higher than others [4]. However, the probabilities for release of these materials were not addressed in that study.

In other studies, researchers have attempted to reduce the consequence of such a release by minimizing the activation inventory, primarily through the use of low activation materials. If the combination of probability and consequence of a radiation release can be reduced such that there is no threat (or a minute threat) to the public

safety, then the plant can be considered safe with regard to this matter. For instance, a preliminary conceptual design study for a very low activation fusion plasma core experimental facility was presented by Cheng *et al,* [10]. In that study, low activation is achieved by using only very low activation materials in the inner shield (graphite blocks), vacuum vessel (Al/Si composite alloy), outer shield (SiC/B_4C) and magnets (Aluminum). Problem areas, however, are defined such as the need for further development of the aluminum alloy and composite materials for the vacuum vessel, and in cost reduction of high purity low activation materials.

A more recent study by Piet [12] compared the influence of blanket material choice on potential accident consequences in seven different major areas: cooling transients, plasma disruptions, tritium inventory and control, public health effects from release of structural radioactivity, relative rates of structural oxidation and volatility in thermal transients, chemical reactivity, and corrosion product inventory.

The results of the Blanket Comparison and Selection Study (BCSS) [5] categorizes all the materials in terms of the process that is controlling the level of activation relevant for accident analysis. In that study, it was found that *low activation* steels have small influence on accident-relevant activation, which may be either positive (likely for Modified HT-9) or negative (likely for Tenelon). Among the materials investigated in BCSS, only VCrTi is found to be a low activation material.

1.4 Scope of This Work

To prevent a possible accident which can destroy the plant and threaten the public health, there is a strong incentive to design fusion reactors which are passively safe. Passively safe means that in the event of a severe accident, such as complete loss of cooling, no external intervention or other additional means of accident mitigation would be required to prevent either a radiological release or substantial plant damage.

This study investigates some of the thermal aspects of fusion reactor safety, by comparing the thermal response of fusion reactor blankets to power/cooling mismatches.

The purpose of this study is to identify some elements of blanket design which enhance thermal safety.

In early experimental reactors the emphasis will be on a better understanding of the physics and engineering aspects of the plasma and the blanket rather than on power and tritium production. Thus, a shield-blanket may surround the plasma, one that does not contain lithium. Because of the need to protect the magnets and personnel, the shield-blanket may essentially be a massive steel structure cooled by water or helium. This structure will operate at a wall loading of about 1 MW/m^2, and be subjected to a total fluence of less than 1 to 3 $MW.yr/m^2$ [5].

The reasons for keeping the activation levels low in the blanket and shield are discussed in Section 1.2. The limitation on structural activation may be accomplished by including in the structure of strong neutron absorbers. A major part of this study is devoted to the investigation of the effects of a strong absorber on thermal safety of fusion blankets. B_4C is chosen to be the neutron absorber. Various amounts of B_4C, with two B^{10} enrichment levels, are included in the shield-blanket design. Then, by employing three computer codes, namely ONEDANT [12], REAC [13], and THIOD [7] successively, the temperature response of these shield-blankets to Loss-of-Cooling transient are calculated. The methods of analysis in these calculations are presented in Chapter Two. Also included in Chapter Two are the assumptions behind these methods and other relevant issues such as structural considerations.

In the first part of Chapter Three, effects of B_4C in shield-blanket designs for early experimental fusion reactors are presented. The second part of Chapter Three is devoted to the effects of a carbon tile before the first wall on thermal safety of fusion reactor blankets. The last part of Chapter Three investigates the effect of inclusion of B_4C in the shield of a fusion *power* reactor blanket. Here B_4C is included both to decrease the neutron fluence at magnet coils and to improve the thermal response characteristics of the blanket under transient events.

Heat removal by natural circulation can be very helpful to ease the consequences of

a Loss-of-Flow accident. Natural convection strongly depends on the coolant employed for heat removal purposes, and on density gradient. Gases, for example, are not as good as liquid metals from natural convection point of view. Liquid lithium and lithium lead are considered as both a tritium breeder and a coolant in some blanket designs [5,14]. Since they are electrically conductive, they experience large pressure drops under a magnetic field. In some designs, the direction of fluid flow is downwards. Thus, in case of a LOFA, a flow reversal may occur. And during this transition, the temperature of the blanket may reach high levels. Natural convection effects on thermal safety of liquid lithium cooled blankets are discussed in Chapter Four.

In Chapter Five, three types of structural materials, SS-316, VCrTi, and a Soviet steel are discussed from an activation point of view [15,16,17]. A Soviet blanket design proposed for ITER is considered in this part of the study. In Chapter Six, summary and conclusions drawn from this study are presented.

Chapter 2

Method of Analysis

Loss-of-cooling accidents can be divided into two groups: Loss-of-Flow Accidents (LOFA), and Loss-of-Coolant Accidents (LOCA). In this chapter, the temperature response of a blanket to undercooling transients (i.e., LOFA, LOCA) is analyzed with a simple, one dimensional model that only considers heat conduction and radiation. Heat transfer by natural convection is not considered in this part of the study. Natural convection cooling is accounted for in Chapter 4.

The first step in calculating the temperature is to determine the heat source present within the system. It is assumed that a fairly rapid plasma shutdown can always be achieved in the event of an accident. Thus, the bulk of the heat will come from the decay of the radionuclides which have been created in the blanket as a result of neutron interactions.

The chapter begins with a brief discussion about blanket selection, geometric assumptions, and structural considerations. Description of accidents, and decay heat generation and deposition are discussed next. In the last part of the chapter, the method of transient temperature calculations is presented.

2.1 Blanket Selection

The blankets investigated in this study were chosen from a variety of sources. The shield-blankets numbered Blanket#1 through #8 were taken from the work of Brereton [6] with some manipulation. The original blanket configuration is intended to be a blanket of D-D type reactor. Blanket #1 has exactly the same geometry and configuration as the original blanket does with the exception that neutron energy flux distribution on the first wall surface is of a D-T spectrum, and its wall load is much

lower ($\approx$ 0.84 MW/m^2) than the orginal blanket to represent experimental reactor conditions. Figure 2.1 shows a one-dimensional schematic top view of Blanket #1. A big part of the study is devoted to this blanket and its modifications to investigate the effects of a strong neutron absorber and of a graphite tile liner. Different amounts of B_4C are added into Blanket #1 to investigate its effect on thermal safety and activation (Blanket #2, #3, #4, and #5). Blanket #6 and #1, and Blanket #7 and #2, and Blanket #8 and #4 are the same except for the addition of a 2 cm. thick carbon tile liner to Blankets #6, #7, and #8 to investigate that liner's effects on temperature. Table 2.1 shows common reactor parameters of Blankets #1 through #8. In Table 2.2, differences among these blankets are shown.

Table 2.1 Reactor Parameters For Blanket #1 Through #8

Parameter	*Value*
Major Radius	952 cm
Minor Radius	248 cm
Inboard/Outboard	
Blanket Shield Thickness	91/202 cm
Neutron Wall Loading	0.84 MW/m^2
Total Wall Loading	1.01 MW/m^2
Blanket Operating Lifetime	
Before The Accident	1 year

Blanket #9 is essentially a design developed during the Blanket Comparison and Selection Study (BCSS) [5]. In Blanket #10 , a 20 cm. thick section of Fe1422 shield, which is 62 cm thick in Blanket #9, is replaced by B_4C to investigate its effects on shield design. All other design parameters and operating conditions are kept the same for these two blankets, as shown in Table 2.3.

Figure 2.1 One Dimensional Schematic of Blanket #1.

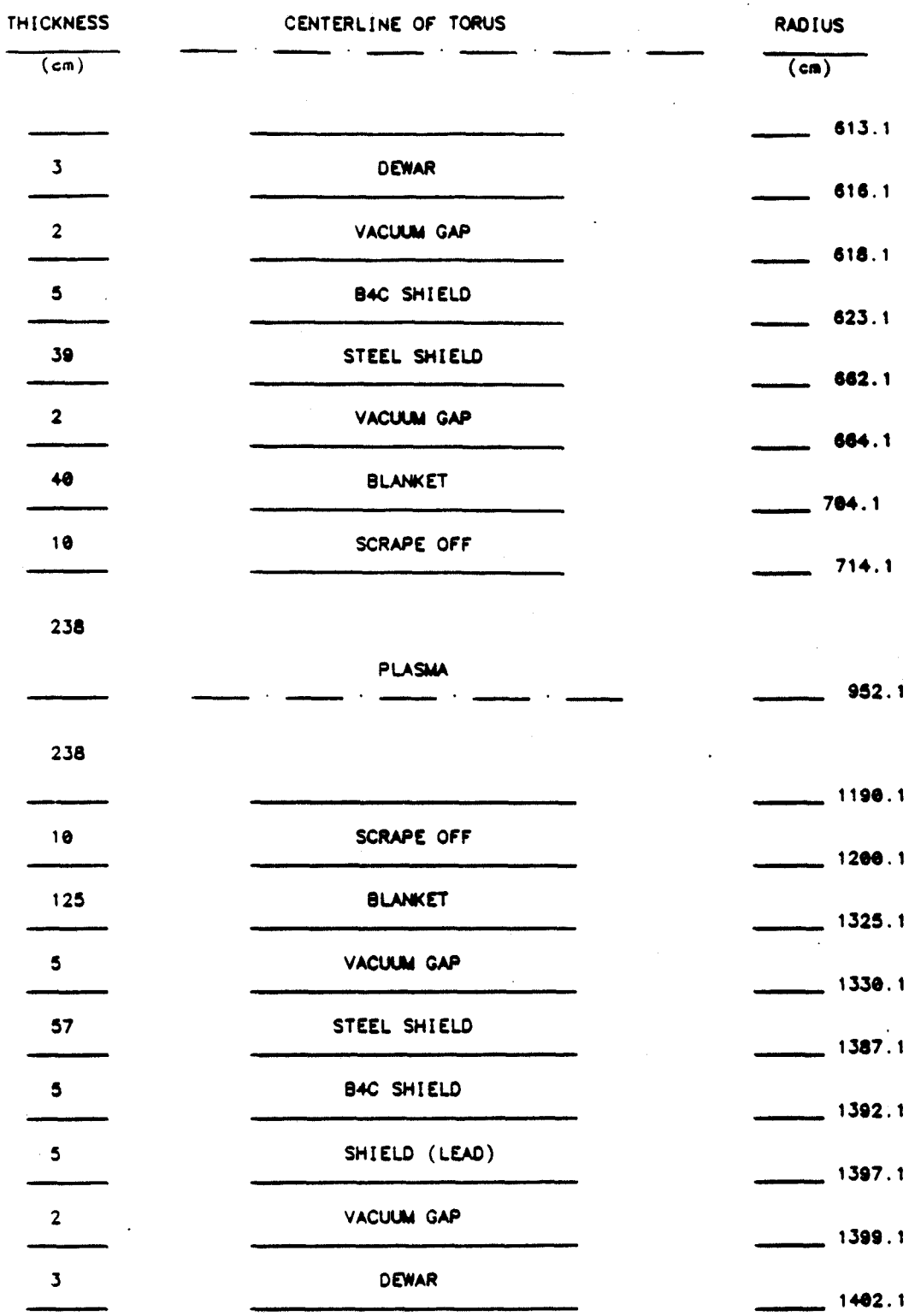

Table 2.2 Differences Among Blankets #1 Through #8

Blanket #	*B_4C Vol. Frac.*	*B^{10} enr. a/o*	*C Tile Liner*
1	0.0	N/A	No
2	12.5	19.8*	No
3	12.5	50.0	No
4	40.0	19.8	No
5	40.0	50.0	No
6	0.0	N/A	Yes
7	12.5	19.8	Yes
8	40.0	19.8	Yes

* Natural Abundancy of B^{10} in Boron

Table 2.3 Reactor Design Parameters And Operating Conditions for Blankets #9 and #10

Parameter	*Value*
Major Radius	7 m
Minor Radius	2.14 m
First Wall Heat Flux	1 MW/m^2
Neutron Wall Loading	5 MW/m^2
Inboard/Outboard Bl. Thick.	64/84 cm
Inboard Shield Thick.	
Blanket #9 Steel/B_4C	42/20 cm
Blanket #10 Steel	62 cm
Outboard Shield Thick.	95 cm
Structure/Breeder/Coolant	VCrTi/Li/Li
Blanket Lifetime	3 years
Tritium Breeding Ratio	1.33
Energy Mult. Factor	1.16

Blanket #11 was chosen from the work of Massidda [7]. His studies includes the effects of magnetic field on natural convection. In the original design, the liquid lithium coolant rises as it passes through coolant channels in the blanket in normal operating conditions (vertically upflow). In this study, the effects of an initially vertical downflow on natural convection is analyzed. Flow reversal from downflow to upflow is expected to take place in this case [19], because heated downflow is an unstable flow configuration in the absence of an external driving force as is the case in LOFA. Since the thermal-hydraulic code (THIOD) used in this analysis does not allow downflow conditions, the initial mass flow rate is assumed nil to represent downflow conditions. This approximation turns out to be a good approximation, because extremely strong MHD pressure drop brings the flow rate to very low values in a very short time after the accident [20]. Table 2.4 gives reactor design parameters and operating conditions for Blanket #11.

Table 2.4 Reactor Design Parameters and Operating Conditions for Blanket #11

Parameter	*Value*
Major Radius	422.5 cm
Minor Radius	65 cm
First Wall Heat Flux	3 MW/m^2
Neutron Wall Loading	15 MW/m^2
Inboard (Outboard)	
Blanket Thickness	31.5 cm
Shield Thickness	45 cm
Structure/Breeder/Coolant	VCrTi/Li/Li
Blanket Lifetime	1 year
Tritium Breeding Ratio	1.32
Energy Mult. Factor	1.16

Blanket #12 through #14 were chosen from ITER Safety and Environmental impact work packages [16,17,18]. These blankets have similar geometric dimensions. The only difference among them is their structural materials. The purpose of this part of the study is to analyze the effects of structural materials on activation. Three structural materials, V-15Cr-5Ti, SS-316, and 03X11H1OM2 (a Soviet steel) are compared from an activation point of view. No temperature calculations were done for these blankets. Table 2.5 shows reactor design parameters and design conditions for Blankets #12 through #14.

Table 2.5 Reactor Design Parameters and Operating Conditions for Blankets #12 through #14

Parameter	*Value*
Major Radius	6.3 m
Minor Radius	2.0 m
First Wall Heat Flux	1.6 MW/m^2
Neutron Wall Load	7.96 MW/m^2
Inboard Blanket + Shield Thickness	102 cm
Outboard Blanket + Shield Thickness	130 cm
Structure/Breeder/Coolant	
Blanket #12	$VCrTi/Li_{17}Pb_{83}/H_2O$
Blanket #13	$SS\text{-}316/Li_{17}Pb_{83}/H_2O$
Blanket #14	$O3X11H1OM2^*/Li_{17}Pb_{83}/H_2O$

* See Table 2.6

Table 2.6 Composition of O3X11H1OM2 Steel

Element	*Weight Frac. %*
Fe	~74
Cr	11
Ni	10
Mo	2.5 - 3.0
Mn	1.5
Ti	0.4
Co	0.01

2.2 Geometry of Blankets

Three dimensional calculations would take considerably long computer times, and were thought unnecessary for this comparative study. A one dimensional cylindrical geometry is used for neutron flux calculation, and a one dimensional slab geometry is used for temperature calculations. The torus is represented as a vertical cylinder as viewed from the top, (Figure 2.2). The innermost region is the inboard shield/blanket; just outside of this is the plasma; and outside the plasma is the outboard blanket/shield. The magnets were not considered in this study.

The validity of the slab approximation in temperature calculations is verified by comparing the slab model results with results obtained using cylindrical geometry [7]. It was found that on the inboard side, slab geometry turns out to be a good approximation to the real toroidal geometry. On the outboard side, slab approximation overpredicts the temperature rise. The difference between the slab and cylindrical results scales as the ratio of the blanket thickness to the major and minor radii. The conclusion is that the difference between the models is small, and the error introduced by using a slab geometry is acceptable.

Fig. 2.2 Top View of a Tokamak.

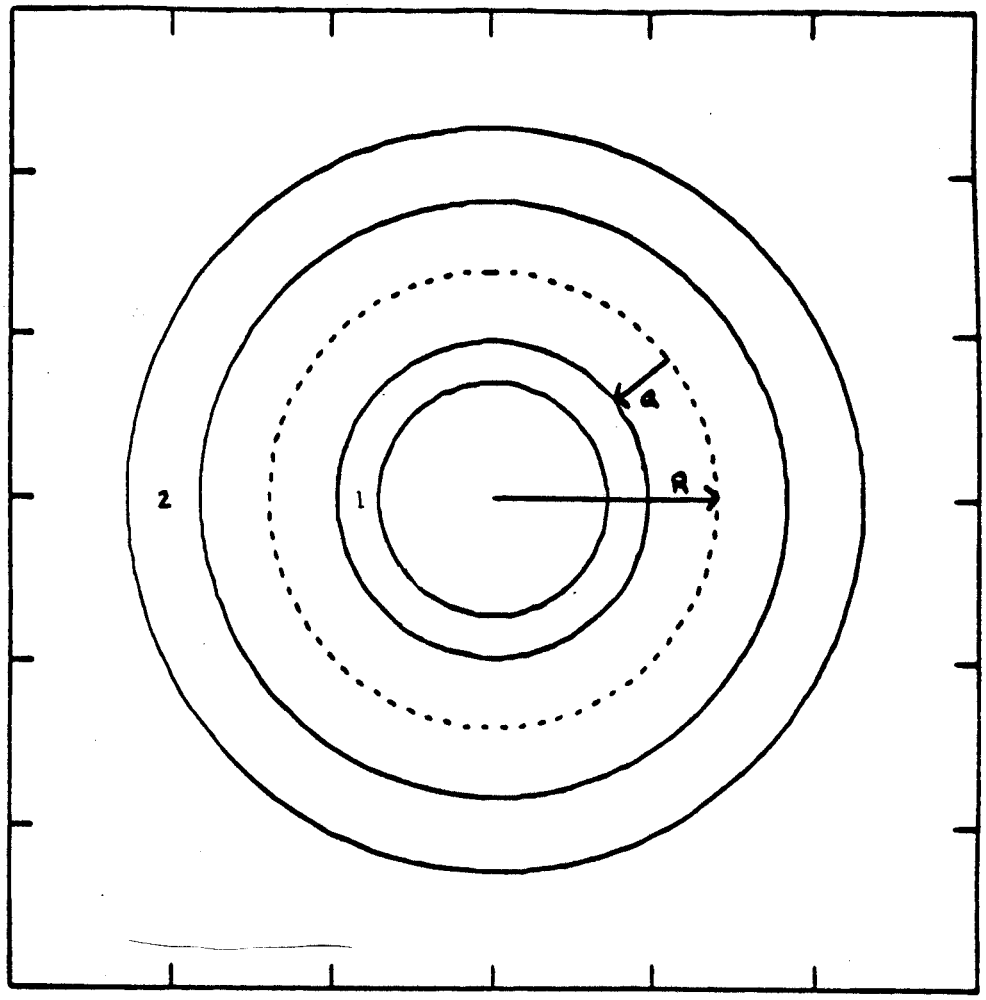

Y

X

a = Minor Radius

R = Major Radius

1= Inboard Blanket.

2= Outbord Blanket.

2.3 Structural Considerations

The basic approach of this investigation involves calculating the temperature response of a blanket to undercooling transients. Once the temperature response is known, a determination can be made as to whether the blanket will suffer structural damage, and whether there exists significant potential for the release of radioactivity.

In the event of a transient which leads to elevated temperatures, the material limits of interest involve Ultimate Tensile Strength (UTS), creep resistance, and oxidation characteristics of the structural materials as a function of temperature. Elevated temperatures in structural materials can cause melting, acute structural failure, thermal creep induced failure, and oxidation or volatization, all of which could lead to the release of radioactive isotopes. Even though the melting points of possible structural materials are relatively high, most of them exhibit a decrease in the yield strength at temperatures lower than their melting points. Figure 2.3 shows the UTS and yield stress of HT-9 versus temperature [21]. Thus, at elevated temperatures, UTS of a structural material may become lower than the applied stress leading to an acute failure. There are two types of stresses which must be taken into account: primary stresses due to external loads such as pressurized coolant in the coolant channels, and thermal stresses due to temperature gradients [22,23]. In a pump-failure LOFA or LOCA, the pressure inside the coolant channels decreases, resulting in reduced primary stresses, and wider margin for temperature. For gas coolants, where natural convection can be neglected, LOCA is less dangerous than LOFA, because of the large coolant pressure in the LOFA case.

Thermal creep can also cause acute structural failure, even if the applied stress never exceeds the yield stress. Creep rate does strongly depend on the temperature. A material at high temperatures for a certain time period may creep excessively, and rupture eventually. The time required to rupture exponentially decreases with temperature according to Larson-Miller parameter: [22]

$$P = (T)\ (C + log_{10}\ t_r) \tag{2.1}$$

Figure 2.3 UTS and Yield Stress of HT-9 as a Function of Temperature.

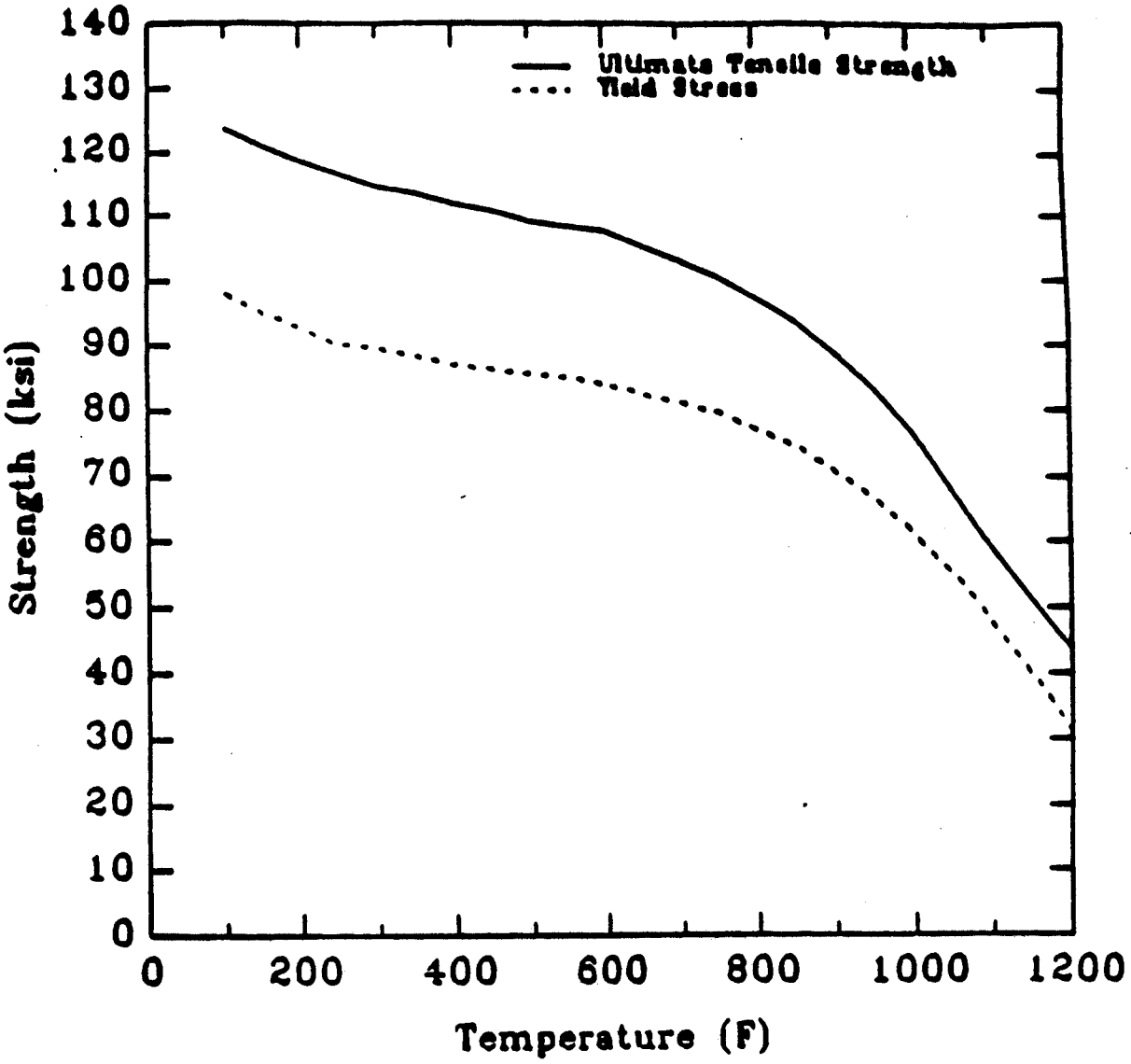

where

P = Larson-Miller parameter, constant for a given material and stress level,

T = temperature (R),

C = constant (usually about 20), and

t_r = time to rupture or to reach a specified value of creep strain (h).

P can be determined from creep tests. Then, knowing the temperature, the time-to-rupture t_r can be found from equation (2.1). If the time spent at a particular temperature is greater than rupture time for that specific temperature, material will fail because of thermal creep. One important thing to remember is that, for a time dependent temperature distribution, failure will occur when the cumulative fraction of time over rupture time exceeds unity. A good discussion can be found in Ref [21,23].

Another mechanism resulting in radiation release is that radioactive isotopes can be mobilized and thus be released into the atmosphere due to increased oxidation and volatization at elevated temperatures.

2.4 Description of Accidents

In this analysis the plasma is assumed either (1) to shut off immediately or (2) to remain at full power until one second after the accident, and then ramp linearly down to zero after five seconds. In either case, this heat source turns out to be small. Zero time defined as the time that the accident begins. The accident is assumed to happen at the end of the life of the blanket to represent the worst case conditions. Figure 2.4 shows the second kind of behavior. If the shown plasma shut off behavior is assumed to take place, a first peak may be observed due to continuous plasma burn in the first few seconds. The effect of continued plasma burn is very small for thermally well-coupled blankets, and is as large as causing a 25 °C difference in peak temperature for not so well-coupled blankets. A thermally well-coupled blanket has good heat transfer properties in the radial direction.

Even if the plasma shuts off rapidly, there is another heat source in the blanket.

Figure 2.4 Fractional Plasma Power After the Accident.

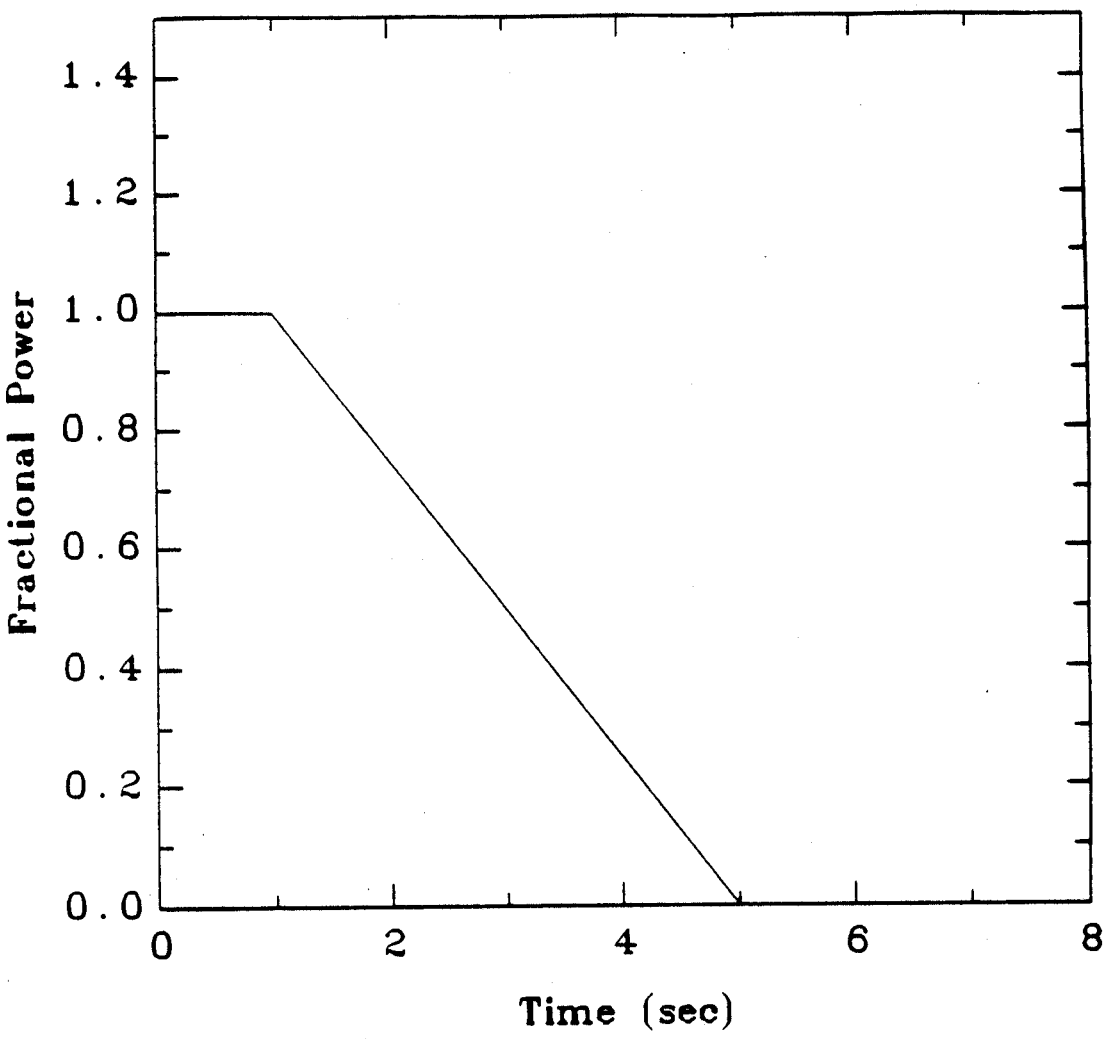

This heat source is due to the decay of radioactive isotopes. Since the neutron flux distribution throughout the blanket is not constant, and different regions in the blanket contain different materials, the radioactivity and the decay heat will be a function of the distance from the first wall. (See Sections 2.5 and 2.7)

In a Loss-of-Flow case, it is assumed that the coolant becomes stagnant at accident initiation and remains stagnant in an entire module. Possible heat transfer in azimuthal direction is not allowed by the code which is used for temperature calculations in this study. Since the heat dissipation to surrounding modules would result in lower temperatures, this approximation is a conservative one. LOFA in all modules at the same time, which is very unlikely, would be represented directly by the assumption. In this case, the heat transfer mechanism across the coolant is by conduction since no convection is allowed.

In a Loss-of-Coolant case, the coolant is assumed to be drained out immediately at accident initiation leaving a void in its place in an entire module. Again, the heat dissipation to the surrounding modules is not allowed, representing a conservative approximation, or representing a LOCA in all the modules at the same time. The heat transport mechanism across the gap is by radiation: no convection or conduction is assumed to take place in coolant channels. In this scenario, there are no blowdown or time-to-drain effects. Allowing for a coolant drain time would result in smaller temperature rises, since the draining coolant cauces heat removal. This approximation is found to be not overly conservative by Piet [12]. The radiative view factor is taken equal to 1 to represent the slab geometry approximation.

Radiation heat transport is assumed to take place across the vacuum gaps and across the coolant channels in case of LOCA. The surfaces of coolant channels are *shiny* (non-oxidized), because, in normal operation, they are in contact with a coolant that does not contain oxygen. The radiative emissivity of such a surface is very low [25]. $\epsilon = 0.10$ for this case. On the other hand, vacuum gap surfaces are assumed to be exposed to the air which would result in the formation of an oxide layer. The oxide

layer increases the radiative emissivity, ϵ, chosen to be 0.50 for these surfaces.

In LOCA and non-convection LOFA , the heat generated in the blanket eventually flows to the magnet coils by radiation. Since the magnet coils cooling system is separate from the blanket cooling system, the coils do not lose cooling even if the latter system fails. Thus, the coils essentially represent a constant temperature heat sink, to which the shield can radiate heat. The coil temperature is assumed to remain at 100 °C which is much higher than the operating superconducting temperature and about the same as an operating resistive magnet.

The material properties ρ and ϵ are assumed to be constant with temperature. However, c_p and k depend on temperature. They are assumed to be linear functions of temperature. If more than one material is included in one region, volumetric heat capacity ρc_p of that region is calculated by volume averaging, and thermal conductivity of that region is found by weighing each conduction path by its area.

2.5 Decay Heat Generation and Deposition

The temperature distribution calculation is needed to predict whether a structural failure will occur and to improve the design of blankets from the thermal safety point of view. To perform this calculation, we need to know decay heat density as a function of time and space. During plasma operation, the material present in the blanket is under bombardment of neutrons of 14.1 MeV for a D-T fuel cycle, which emerges from the following fusion reaction:

$$D + T \longrightarrow He + n + 17.6\ MeV \tag{2.2}$$

As a result, most of the isotopes become radioactive depending on their neutron absorption cross sections. These transmuted isotopes decay with a characteristic half-life, called λ. The decay energy appears as photons and kinetic energy associated with particles and isotopes involved in the decay process, and is deposited as heat in the vicinity of the decaying isotope. Thus, the heat generation rate depends on the decay energy

and half-life of those isotopes. This is why material selection is very important to limit radioactivity levels in fusion reactors.

The β and γ radiations emerge in a decay process. Most of the time one or more γ emission(s) follow a β decay. In a decay process, a certain part of the binding energy of a nucleus is released, and emerges as kinetic energy of the decay products. From the conservation of linear momentum and of energy, the particles' shares the total available energy can be determined, and are inversely proportional to their masses. Therefore, in case of γ and β decay, the kinetic energy of the recoil isotope may be neglected because of its very large mass compared to the electron mass.

Since a β particle is electrically charged (β is either an electron or a positron), it will be stopped almost immediately by the surrounding medium after the decay. Thus, its energy will be deposited as heat at the location of the parent isotope. However, γ is basically a highly energetic photon, and so it has no charge. The energy loss mechanisms of a photon are through pair-production and Compton scattering at higher energies, and through photo-electric effect at lower energies. These mechanisms are weaker, so that a γ ray may travel very long distances compared to a β particle. Before it is absorbed in the photo-electric effect, the γ-ray deposits its energy along its path [27].

In this study, it is assumed that all the energy liberated in a decay reaction is deposited instantly at the location of the parent isotope. This assumption is indeed appropriate for β particles, since they will be stopped in a very short distance. However, the γ energy deposition does have a distribution over space. Also, activation of isotopes is a direct function of neutron flux. Since the neutron flux is higher near the first wall, the decay source rate will be higher also. The net effect of this transport of energy associated with γ's is that the heat generation and deposition rates are not the same for a specific location. Fortunately this makes the heat deposition rates more uniform in the blanket, and yields lower peak heat deposition rates and temperatures near first wall. The local energy deposition approximation is a conservative one because it results

in higher temperatures than it would be if the energy transport by γ's would have been taken into account. Massidda and Kazimi discussed this issue [7], and found out that this approximation is a good one, and its effect on the temperature is minimal.

2.6 Operational Neutron Flux and Activation Computations

Three computer codes are run successively to find the temperature responses of the blankets. These are ONEDANT [13], REAC [14], and THIOD [7]. The first step is the calculation of the operational neutron fluxes. **ONE Dimensional Diffusion Accelerated Neutron Transport** code, ONEDANT, is employed for this purpose. ONEDANT is developed by R.D. O'Dell *et al* at Los Alamos National Laboratory. It solves the one-dimensional multigroup neutron transport equation in plane, cylindrical, spherical, and two-angle plane geometries. The discrete-ordinates approximation is used for treating the angular variation of the particle distribution and the diamond-difference scheme is used for phase space discretization. This code is run with 42 neutron energy groups and with P_3S_{12} approximation. Neutron current coming from plasma is given as a boundary condition at the plasma facing surface of the first wall. This code, in turn, yields the operational neutron flux distribution in the blanket.

The second step involves the calculation of the activation levels by using REAC, an activation/transmutation code developed by F.M. Mann at Hanford Engineering Development Laboratory [26]. REAC solves the following differential equation for each isotope :

$$\begin{aligned}
\frac{dN_i(t)}{dt} &= \varphi(t) \sum_j N_j(t)\, \sigma_{j\to i}(t) && \text{(gain from reactions)} \\
&\quad + \sum_k \lambda_{k\to i}\, N_k(t) && \text{(gain from decay)} \\
&\quad - \varphi(t)\, N_i(t) \sum_l \sigma_{i\to l}(t) && \text{(loss from reactions)} \\
&\quad - N_i(t) \sum_m \lambda_{i\to m} && \text{(loss from decay)} \qquad (2.3)
\end{aligned}$$

where:

$N_i(t)$: number density of nuclide type i

$\sigma_{n\to p}(t)$: spectrum averaged microscopic cross section, see below for changing nuclide n into nuclide p

$\varphi(t)$: total flux, see below

$\lambda_{q\to r}$: decay constant for nuclide q changing into nuclide r

The spectrum-averaged cross-section is obtained by collapsing multigroup cross sections $[(\sigma_{n\to p})_s]$ with the multigroup flux $[\ \varphi_s(t)\ ]$, which is calculated by ONEDANT:

$$\sigma_{n\to p}(t) = \sum_s \varphi_s(t)\ (\sigma_{n\to p})_s\ /\varphi(t) \qquad (2.4)$$

$$Note: \qquad \varphi(t) = \sum_s \varphi_s(t)$$

In a time period which is defined as an irradiation time having constant flux, the code assumes that no reaction can occur on a reaction or decay product. To prevent significant errors from this assumption, the code is run for a series of time periods. In this study, three of four month periods are used for a total irradiation time of one year.

The neutron flux output of ONEDANT is an input to the REAC code. For a given irradiation time, REAC calculates the specific activity (Ci/cm^3.sec) of each radionuclide produced at selected positions in the blanket for selected times after shutdown. REAC assumes that every isotope given in its input has an atomic density of 0.08 atoms/barn.cm, (1 barn = 10^{-28} m^2). Two auxiliary computer programs are used to convert these specific activities to the actual activities by multiplying with the activation concentration in the blanket.

2.7 Decay Heat Distribution

The next step is the calculation of decay heat density distribution in the blanket from the output of REAC. The decay heat density as a function of time for any position in the blanket can be expressed as:

$$\dot{q}'''_{decay}(t) = \sum_i a_i \, e^{-\lambda_i t} \tag{2.5}$$

where the sum is over all the isotopes present at that blanket position. The activity calculated by REAC is a direct function of the neutron flux which decreases exponentially as a function of distance from the first wall. This leads to the expression:

$$\dot{q}'''_{decay}(t) = \sum_i a_i \, e^{-\lambda_i t} \, e^{-\mu_i x} \tag{2.6}$$

where x is the distance from the first wall. The parameters a_i and μ_i are found by manipulation of the REAC output [7]. The summation in equation (2.6) is over all isotopes in the particular blanket region of interest. It will change for other blanket regions to correspond to the isotopes involved in these regions. The operational neutron fluxes and decay heat distributions are plotted in the following chapters for some of the blankets analyzed in this study.

2.8 Temperature Distribution

The last step is to calculate the temperature responses of a blanket as a function of time and position. The one-dimensional THIOD code is used for this purpose. The THIOD code, which was developed by Massidda [7], considers conduction and radiation heat transfer mechanisms in case of a LOCA . It has two options in case of LOFA: (1) conduction and radiation only and (2) conduction, radiation and convection. The latter one requires much more computation time than the former does. Convection heat transfer is taken into account only in Chapter Four.

Basically, THIOD solves the following form of the equation for heat transport by employing finite difference methods to find the blanket temperature distribution:

$$\rho(\mathbf{r}) \, c_p(\mathbf{r}, T) \, \frac{\partial T(\mathbf{r}, t)}{\partial t} = \dot{q}'''_{decay} + \nabla \cdot k(\mathbf{r}, T) \, \nabla T(\mathbf{r}, t) \tag{2.7}$$

where

ρ is the coolant density (kg/m^3),

c_p is heat capacity of the coolant under constant pressure (J/kg.K), and

k is the heat conduction coefficient of the material at that part of the blanket.

By applying the one dimensional slab approximation, we get the following equation:

$$\rho(x)\ c_p(x,T)\ (\frac{\partial T(x,t)}{\partial t})\ =\ \dot{q}'''\ +\ (\frac{\partial}{\partial x}\ k(x,T)\ \frac{\partial T(x,t)}{\partial x}) \tag{2.8}$$

The blanket is then broken up into a fine mesh to obtain a numerical solution, and the above equation is integrated over a mesh distance Δx. The resulting heat balance equation includes the heat flux leaving or entering a mesh zone at the zone boundaries (such as the vacuum/gap/shield interface) due to radiative heat transfer. This radiation term is actually the boundary condition for the solution, and can be shown as:

$$\dot{q}''_{i\rightarrow j}(x_{i+}, x_{j-}, t) = \sigma\epsilon_{ij}(T_i^4 - T_j^4) \tag{2.9}$$

where

$$\epsilon_{ij} = ((\frac{1}{\epsilon_i}) + (\frac{1}{\epsilon_j}) - 1)^{-1} \tag{2.10}$$

σ = Boltzmann's number,

ϵ_i and ϵ_j surface emissivities of the surfaces of adjacent regions of the blanket, and

i and j show the regions next to each other. x_{i+} and x_{j-} are repectively the furthest point in region i and closest point in region j from the first wall. (See Figure 2.5).

2.9 Summary

In this study, temperature responses of blankets in LOCA and LOFA are computed using three codes, ONEDANT, REAC, and THIOD. ONEDANT computes operational neutron fluxes. By using the output of ONEDANT, REAC computes the specific activity of isotopes in the blanket, which determines the decay heat density distribution. Finally, THIOD is employed to find the temperature response of blankets.

Figure 2.5 Schematic of Regions for Radiation Heat Flux Boundary Condition.

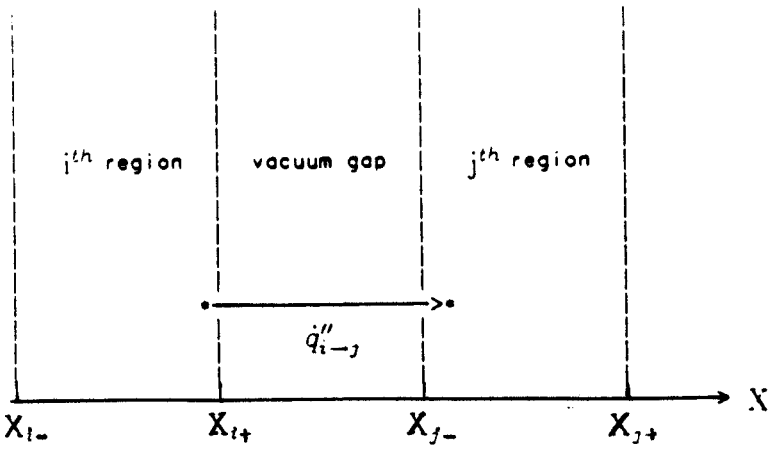

Chapter 3

The Impact of B_4C on Activation and Thermal Response of Blankets

This chapter is devoted to presenting the results of the analysis of the B_4C effects on activation and thermal response of Blankets #1 through #10. The method of analysis presented in the last chapter is used to calculate both short- and long-term radioactivity after shutdown. Temperature responses of those blankets to loss-of-cooling accidents as a function of time after shutdown at some selected points in the blankets are also analyzed.

In the first part of the chapter, activation and temperature responses of Blankets #1 through #8 are presented and compared. These blankets are similar in geometry and operating conditions. For early experimental reactors designed to investigate plasma physics and engineering properties of the plasmas and blankets, there is no need for production of either power or tritium. If low activation materials such as SiC and graphite are not chosen for blanket structures then safety, maintenance and waste disposal issues will be a concern. However, these low activation materials need much research and development; their use for structural materials requires more experience. On the other hand, conventional steels and ceramic B_4C have an enormous database, and they are used under high neutron irradiation in fission reactors. By including B_4C in the structure, the neutron flux level, and consequently activation and decay heat level, can be limited. Hence, safety, maintenance and waste disposal problems will be eased.

A one-dimensional schematic figure, which is used in neutronic and temperature calculations to represent the geometry of the first eight blankets under consideration, will be given. Then, the operational neutron flux, which is the output of ONEDANT

[13], as a function of distance from the first wall, is shown. This neutron flux is an input to the REAC code which calculates the level of activation for each isotope at shutdown. Both short- and long-term total activation are given as a function of time for each blanket. Decay heat as a function of time after shutdown is also given for some of the blankets.

Finally, THIOD [7] is employed to calculate the temperature distribution in the blankets as a function of time. Decay heat generation rates are an input to this code. Temperatures at selected points as a function of time are also plotted.

Section 3.3 compares all eight blankets. Operational neutron fluxes, activation levels and temperature responses are compared.

Two possible plasma shutdown behavior; (1) prompt shutdown at the time of the accident, and (2) linearly decreasing function of plasma shutdown in five seconds after the accident, are compared. The effect of plasma shutdown behavior and the effect of the type of the accident are investigated in Section 3.4. The impact of operating time of the blanket on the temperature is also investigated in Section 3.4

Natural convection effects are not accounted for in this chapter. Since the helium coolant of the first eight blankets does not have good physical properties from a natural convection point of view [7]. The only difference, then, between LOCA and LOFA is the heat conduction by He across the coolant channels. This is expected to have a small influence on the temperature response. LOCA and LOFA are also compared in Section 3.4

In Section 3.5, effects on thermal safety of including B_4C in the shields are investigated. A 20 cm section of a 62 cm thick steel shield is replaced by B_4C of a power reactor blanket design. Also calculated are the short- and long-term activation levels after shutdown from safety, maintenance and waste management standpoints.

3.1 Blankets #1 through #5

Figure 3.1 shows a one dimensional schematic of the inboard side of Blankets #1

through #5. The geometry of all five blankets is the same. The only difference among these blankets is the composition of the first wall. The first wall of Blanket #1 does not include any B_4C. Other blankets have different amounts of B_4C and different levels of enrichment of ^{10}B. Table 2.1 and 2.2 show the design parameters and operating conditions as well as the differences among these blankets.

The volumetric fraction of B_4C in Blankets #2 and #3 is 12.5%, whereas that of Blankets #4 and #5 is 40.0%. The enrichment of ^{10}B in B_4C in Blankets #3 and #5 is 50%. That is HT-9 is replaced by B_4C, (See Table 3.1). The volumetric fraction of coolant is kept constant in the first wall. B_4C is assumed to be distributed homogeneously in the first wall. In real blanket designs, successive layers of HT-9 and B_4C would be employed. This approximation is valid if the thickness of those layers small enough. The computation time, which increase sharply with the number of zones, would be very high if such a layered geometry had been used.

Table 3.1 and 3.2 shows the density and atomic fractions of elements of structural and breeder materials used in this study, [7].

Figure 3.2 shows the normalized operational total neutron flux in the inboard blanket as a function of distance from the first wall. Note that the flux scale is logarithmic. The neutron flux exponentially decreases with distance. This behavior is more pronounced with increasing amounts of B_4C and ^{10}B. The slope of the curves shows the rate of decrease of flux. It is important to note that the difference among the flux levels at the front of the first wall is much smaller than that at the end of the first wall. While there is a factor of two difference between the fluxes of Blankets #1 and #2 at the front, that difference is three at the end of the first wall. By inclusion of more B_4C and ^{10}B enriched boron, the flux is further decreased. Flux of Blanket #1 is 20 times higher than that of Blanket #5, at the back of first wall.

The short term specific activation levels of the first five blankets at the front of first wall are shown in Figure 3.3. The short term activation levels are important from a safety point of view, because the decay heat rate is a direct function of activation as

Figure 3.1 Blankets #1 through #5.

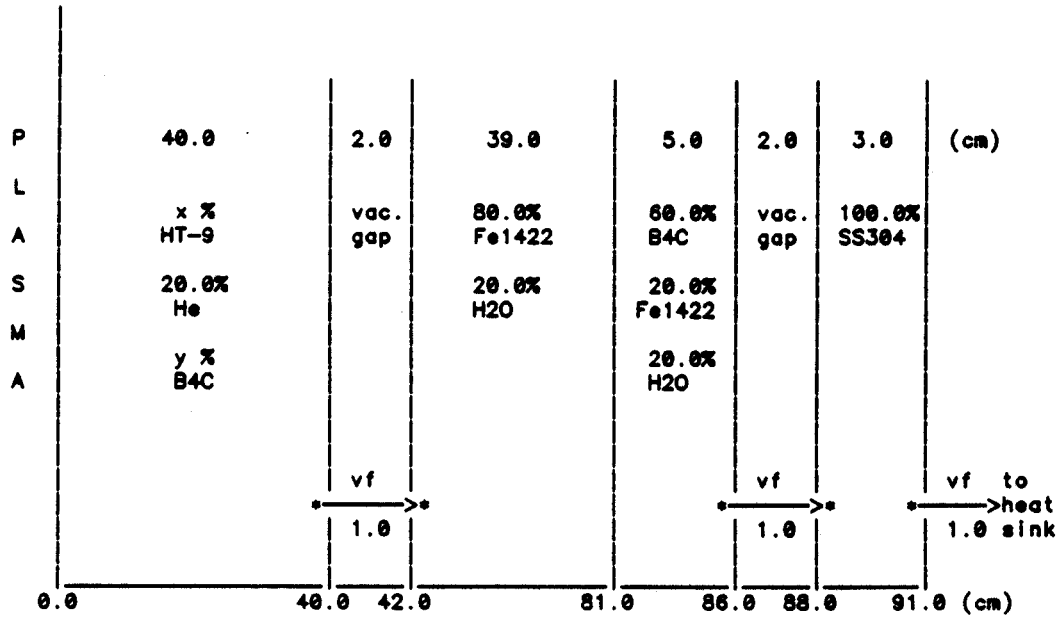

One-dimensional schematic of HT-9/He/B4C inboard blanket for neutronics and 1-D thermal transport modeling.

Arrows connecting asterisks indicate radiation paths. The vf parameters indicate the view factor for that particular radiation path.

Blanket #	x% MT-9	y% B_4C	B^{10} enrich.
1	80.0	0.0	N/A
2	67.5	12.5	19.9[1]
3	67.5	12.5	50.0
4	40.0	40.0	19.9[1]
5	40.0	40.0	50.0

1 Natural Abundancy of B^{10} in B.

Table 3.1 Composition of Structural Materials Used in This Study.

Density	VCrTi	SS304	HT-9	Fe1422	SS316
(atoms/barn.cm)	$7.217\ 10^{-2}$	$8.602\ 10^{-2}$	$8.494\ 10^{-2}$	$8.794\ 10^{-2}$	$8.685\ 10^{-2}$
Element					
C	$8.460\ 10^{-4}$	$2.108\ 10^{-3}$	$9.187\ 10^{-3}$	$2.628\ 10^{-2}$	$2.133\ 10^{-3}$
N	$1.813\ 10^{-3}$	$1.493\ 10^{-3}$	—	$7.379\ 10^{-4}$	$2.070\ 10^{-3}$
O	$1.587\ 10^{-3}$	—	—	—	—
Al	$7.520\ 10^{-5}$	—	—	—	—
Si	$5.440\ 10^{-4}$	$9.209\ 10^{-3}$	$7.856\ 10^{-3}$	$4.453\ 10^{-3}$	$7.528\ 10^{-3}$
P	$1.640\ 10^{-4}$	$4.620\ 10^{-4}$	$3.563\ 10^{-3}$	$2.634\ 10^{-4}$	$1.617\ 10^{-3}$
Ti	$5.300\ 10^{-2}$	$3.447\ 10^{-4}$	—	—	—
V	$7.953\ 10^{-1}$	—	$3.248\ 10^{-3}$	—	—
Cr	$1.465\ 10^{-1}$	$1.873\ 10^{-1}$	$1.220\ 10^{-1}$	$2.102\ 10^{-2}$	$1.819\ 10^{-1}$
Fe	$9.090\ 10^{-5}$	$6.954\ 10^{-1}$	$8.396\ 10^{-1}$	$7.907\ 10^{-1}$	$6.670\ 10^{-1}$
Ni	$8.650\ 10^{-6}$	$8.718\ 10^{-2}$	$4.699\ 10^{-3}$	$1.797\ 10^{-2}$	$1.144\ 10^{-1}$
Nb	$1.366\ 10^{-5}$	—	—	—	—
Mo	$7.142\ 10^{-5}$	$1.893\ 10^{-3}$	$5.750\ 10^{-3}$	—	$1.351\ 10^{-2}$
Mn	—	$1.172\ 10^{-2}$	$5.523\ 10^{-3}$	$1.386\ 10^{-1}$	$9.314\ 10^{-3}$
Cu	—	$1.732\ 10^{-3}$	—	—	$8.753\ 10^{-4}$
S	—	$2.060\ 10^{-4}$	$3.441\ 10^{-4}$	$3.392\ 10^{-5}$	$1.215\ 10^{-4}$
W	—	—	$1.500\ 10^{-3}$	—	—
Co	—	$9.338\ 10^{-4}$	—	—	$1.038\ 10^{-3}$
B	—	—	—	—	$6.187\ 10^{-5}$

Table 3.2 Compositions of Breeder Materials Used in This Study.

Density (atoms/barn.cm)	Lithium $4.514\ 10^{-2}$	Li_2O $1.211\ 10^{-1}$	$Li_{17}Pb_{83}$ $3.381\ 10^{-2}$
Element			
C	$5.783\ 10^{-6}$	$3.314\ 10^{-6}$	—
N	—	$1.421\ 10^{-5}$	—
O	—	$3.325\ 10^{-1}$	—
Si	$1.979\ 10^{-5}$	$1.416\ 10^{-5}$	—
V	$4.091\ 10^{-7}$	$1.952\ 10^{-7}$	—
Cr	$2.672\ 10^{-6}$	$1.912\ 10^{-7}$	—
Fe	$1.244\ 10^{-6}$	$7.122\ 10^{-7}$	—
K	$3.553\ 10^{-5}$	$3.104\ 10^{-5}$	$5.308\ 10^{-6}$
Cu	—	—	$5.445\ 10^{-6}$
Li	$9.997\ 10^{-1}$	$6.674\ 10^{-1}$	$1.701\ 10^{-1}$
Na	$9.064\ 10^{-5}$	$4.323\ 10^{-5}$	$1.354\ 10^{-5}$
Ca	$5.199\ 10^{-5}$	$2.481\ 10^{-5}$	$7.768\ 10^{-6}$
Pb	—	—	$8.269\ 10^{-1}$

Figure 3.2 Operational Neutron Flux of Blankets #1 through #5.

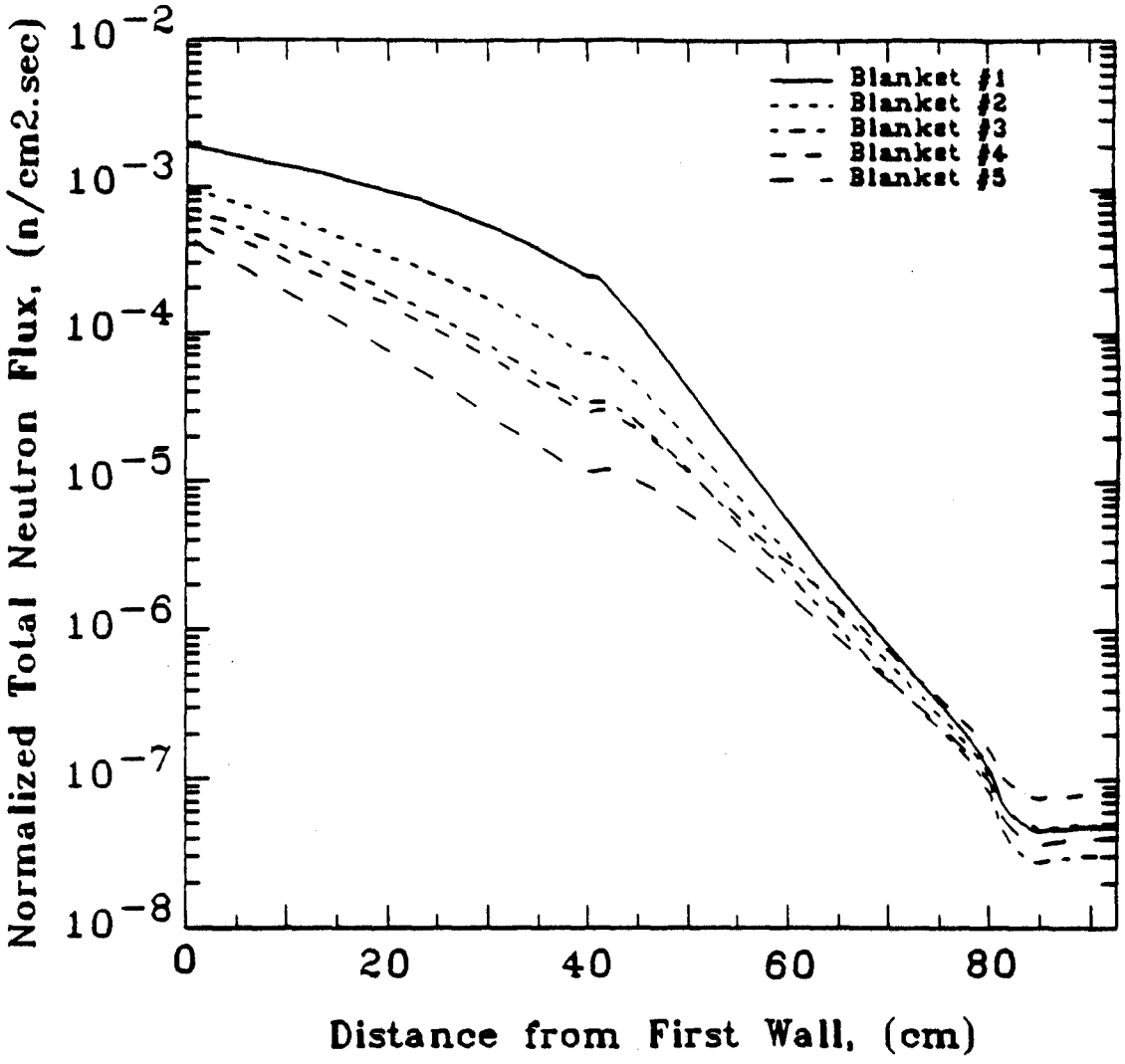

explained in Chapter 2. A number of conclusions can be drawn from this figure. The activity level in the first 10 hours decays very fast, and then becomes constant over a long period of time. The asymptotic values of activation levels of blankets are directly proportional to the concentration of HT-9 in the structure. This means that activation after 10 hours is solely due to the isotopes in HT-9. The asymptotic activation levels are 20,16, and 10 Ci/cm^3.sec for the three different composition levels of HT-9. By remembering that the concentration of HT-9 is 80% for Blanket #1, 67.5% for Blankets #2 and #3, and 40% for Blankets #4 and #5, we can see the same ratio in activation levels. Therefore, the conclusion is that activation at the front of the first wall does not depend on ^{10}B enrichment and is directly proportional to the HT-9 concentration. After 5 hours the radioisotopes created from the elements contained in B_4C die away.

The short term specific activation levels for the first five blankets at the back of the first wall as a function of time after shutdown are shown in Figure 3.4. The effect of B_4C on the activation can be seen from this figure. The activation of Blanket #1 at the back of the first wall is about 10 times smaller than that at the front of first wall,(20 Ci/cm^3.sec and $\sim$1.5 Ci/cm^3.sec). This ratio is about 100 for other blankets, (e.g., 10 Ci/cm^3.sec and 0.10 Ci/cm^3.sec for Blanket #3). Since the activation is a function of neutron flux, and the neutron flux exponentially decreases with distance from the first wall, we expect that activation decreases exponentially with distance from the first wall. This assumption is used to calculate the decay heat generation input to THIOD.

Altough the activation levels of Blankets #2 through #5 are different and proportional to the ^{10}B concentration, their absolute values are very small compared to that of Blanket #1, (0.2 to 0.07 Ci/cm^3.sec versus 3.0 Ci/cm^3.sec, respectively). Therefore 12.5% B_4C with no enrichment is enough to suppress the short-term activation, and hence, decay heat generation. There is no need to use either larger amounts of B_4C or ^{10}B enrichment. This conclusion is important from a safety point of view.

The long-term specific activation levels at the front and at the back of first wall are shown in Figures 3.5 and 3.6, respectively. These figures are important from a

Figure 3.3 Short-Term Activation of Blankets#1 through #5 at the Front of the First Wall.

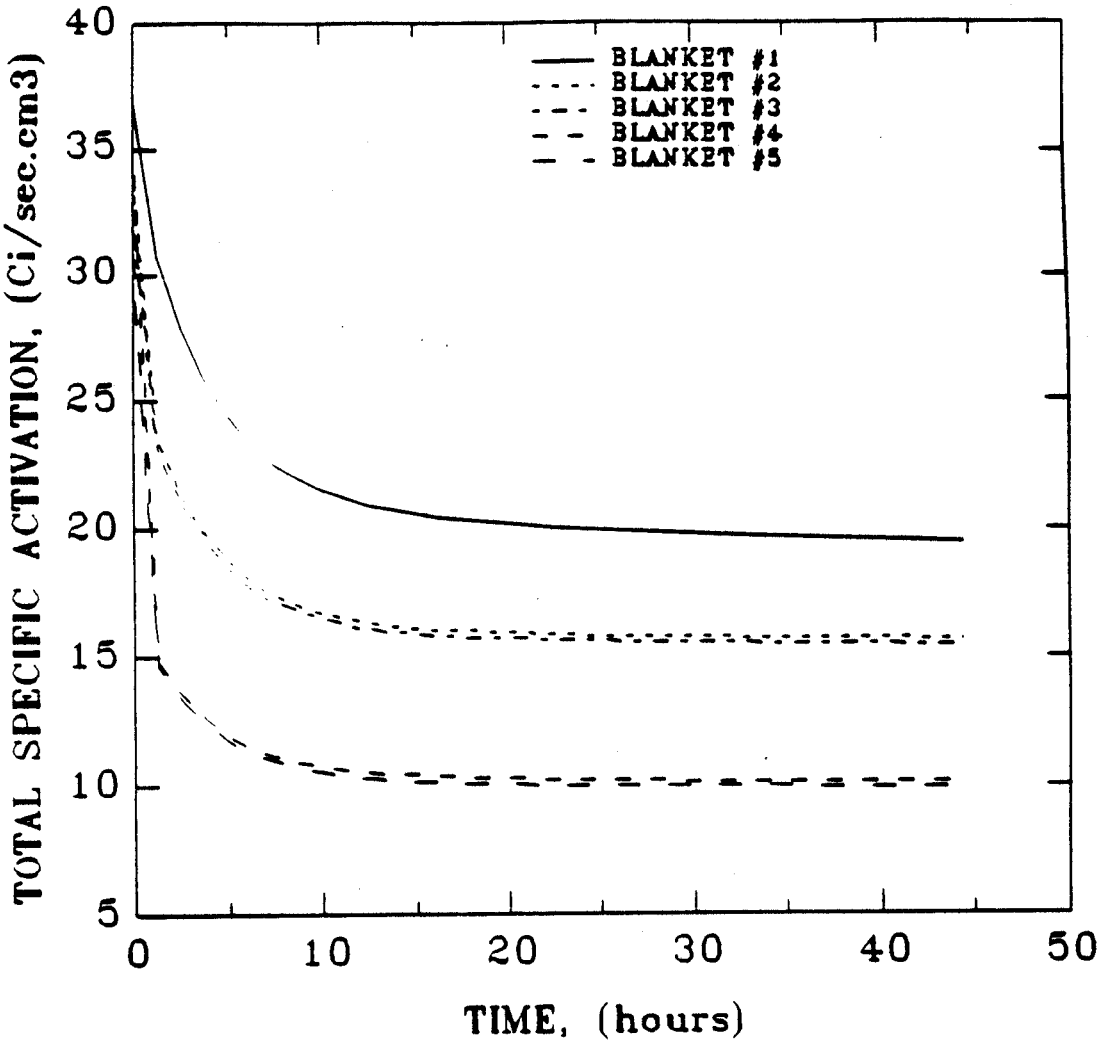

Figure 3.4 Short-Term Activation of Blankets #1 through #5 at the Back of the First Wall.

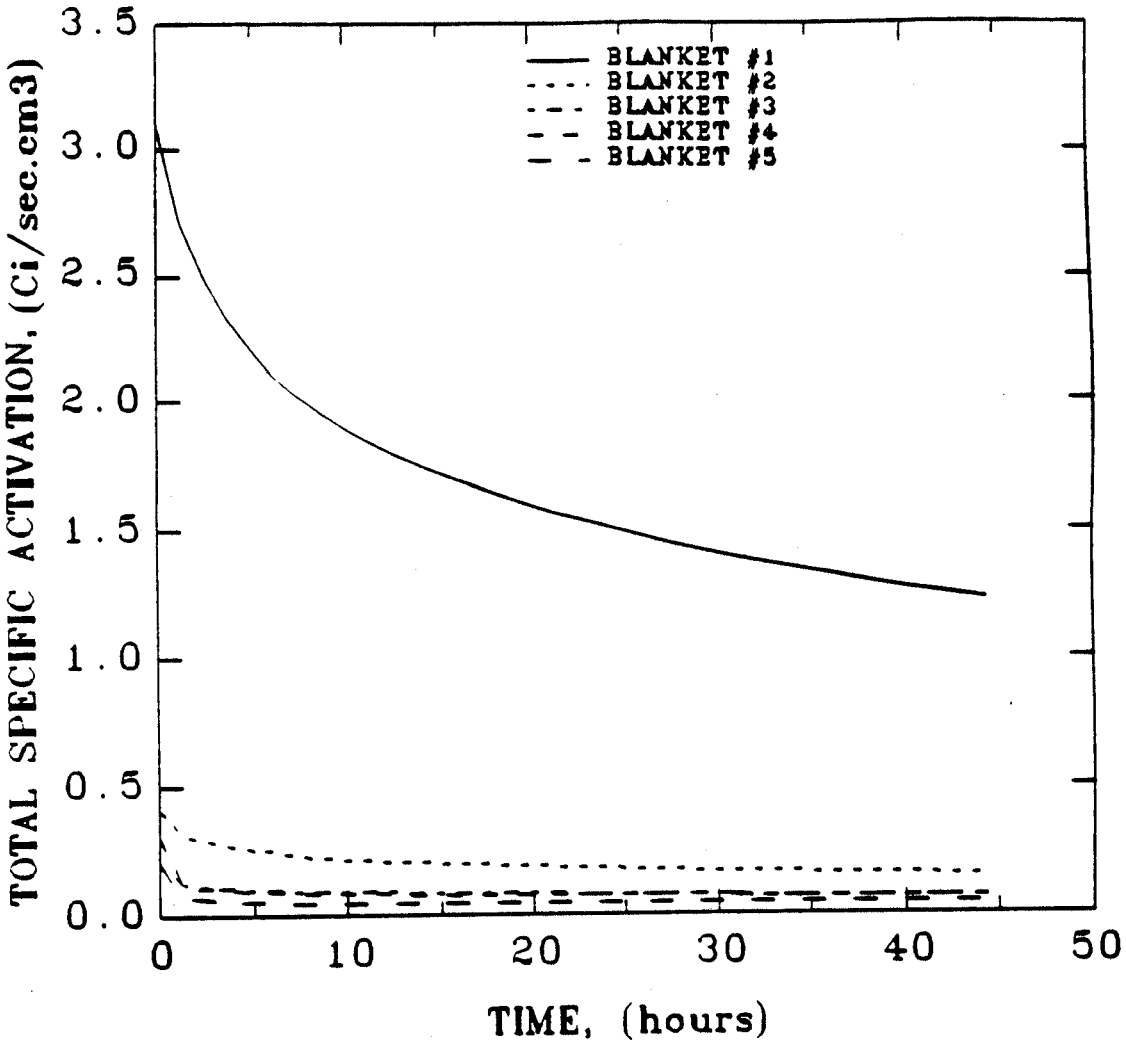

waste disposal point of view. Again, we can see that B_4C has almost no effect on the activation at the front of the first wall, and activation is directly governed by the amount of HT-9. However, at the back of the first wall, B_4C shows its impact on the activation, and at least an order of magnitude less activation can be achieved by using different amounts of B_4C and of ^{10}B enrichment. At about one year ($3.17\ 10^7$ seconds), the activation levels of Blankets #2 through #5 are very close to each other and there is almost an order of magnitude difference between those and that of Blanket #1. The same conclusion can be drawn from these figures: There is no need to use either high amounts of B_4C or ^{10}B enrichment.

Figures 3.7 and 3.8 show the decay heat densities as a function of time after shutdown at the front and at the back of the first wall, respectively. At the front of the first wall, decay heat densities of Blankets #2 and #3 are the same, as are those of Blankets #4 and #5, which means that ^{10}B enrichment has no effect on decay heat production rate at the front of the first wall. The order of decay heat generation rate is about 10^{-2} MW/m^3 at the front, whereas it is on the order of $3\ 10^{-3}$ to $4\ 10^{-5}$ for Blankets #1 and #5, at the back respectively. By employing 12.5% B_4C with natural boron, a factor of 10 less heat generation rates are achievable. By employing the same amount of B_4C with 50% enriched ^{10}B or 40% boron with natural boron, that factor is about 30.

Figures 3.9, 3.10 and 3.11 show the temperature response of Blankets #1 through #5 at the front, at the mid-point, and at the back of the first wall respectively. The temperature of the front of the first wall is the most important from a safety point of view, because it is the most limiting part of the first wall and the total blanket. A peak temperature of 650 °C is observed at about ten hours after shutdown for Blanket #1. This shows a 110 °C increase over its assumed operating temperature. The temperature of the other blankets first exhibit a drop due to stored heat redistribution. Then, they experience an increase. However, those temperatures never exceed 520 °C even for Blanket #2 which has only 12.5% B_4C. Moreover, the difference in temperature

Figure 3.5 Long-Term Activation of Blankets #1 through #5 at the Front of the First Wall.

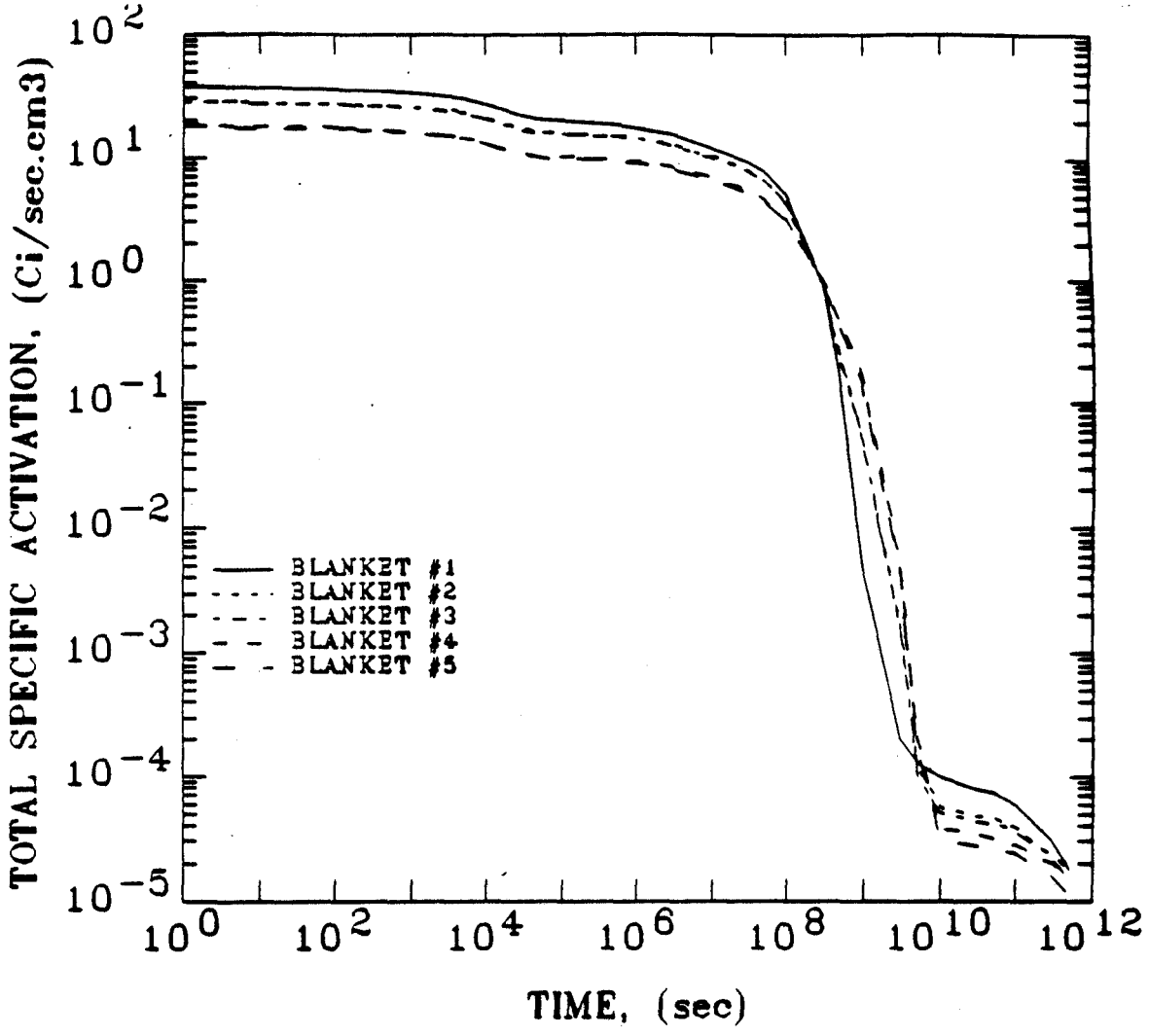

Figure 3.6 Long-Term Activation of Blankets#1 through #5 at the Back of the First Wall.

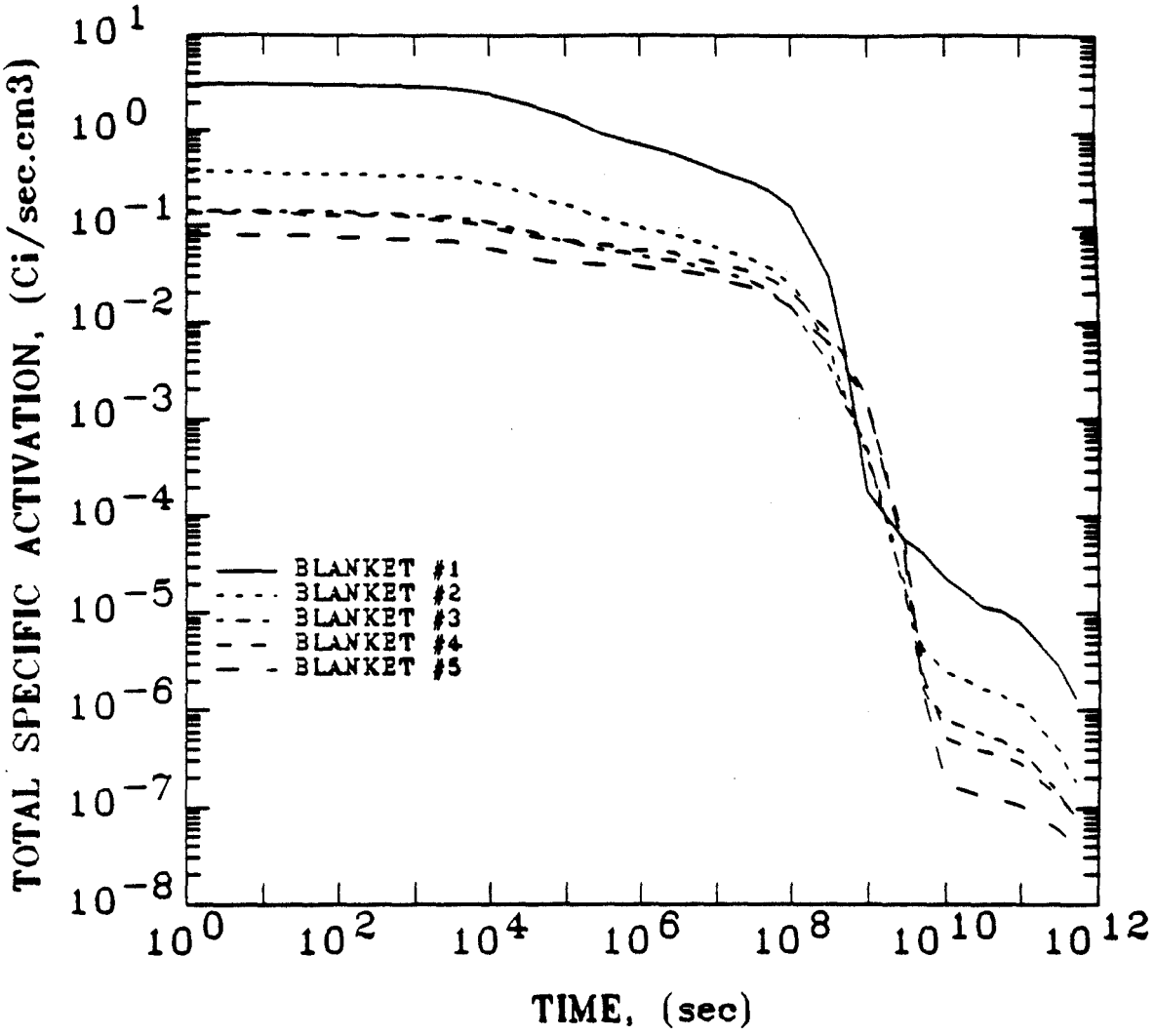

Figure 3.7 Decay Heat Density of Blankets#1 through #5 at the Front of the First Wall.

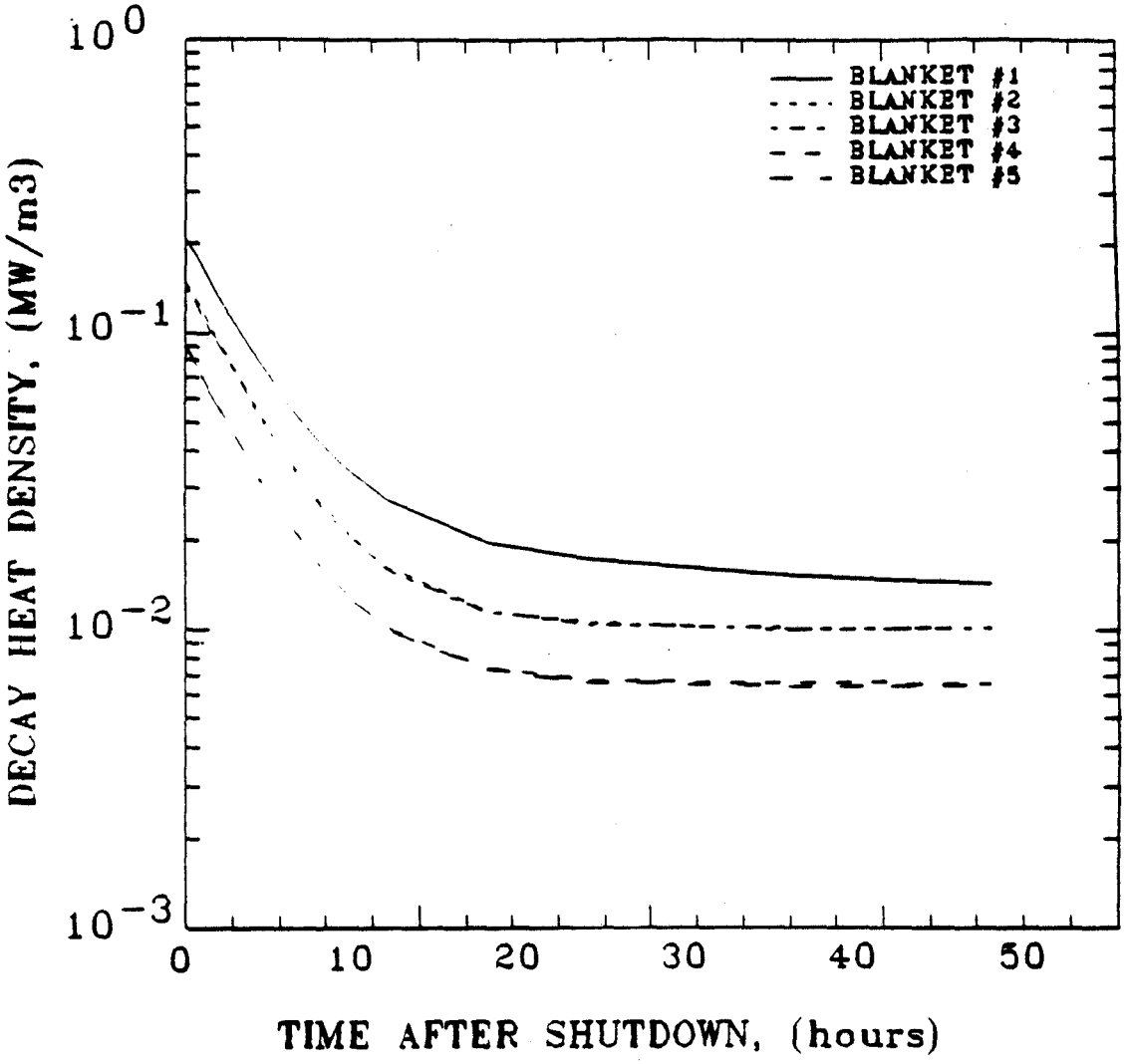

Figure 3.8 Decay Heat Density of Blankets#1 through #5
at the Back of the First Wall.

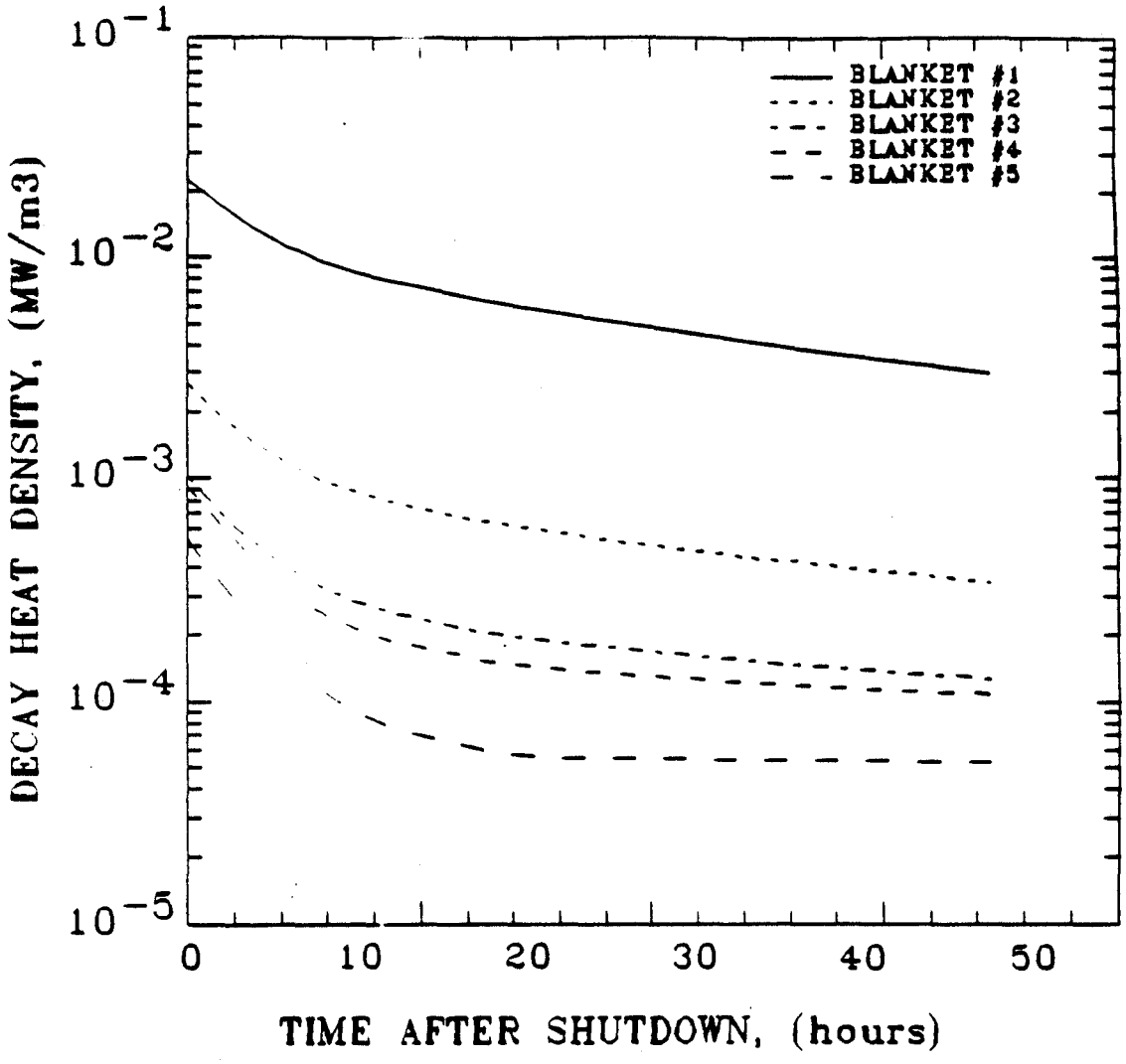

Figure 3.9 Temperature Response of Blankets#1 through #5 at the Front of the First Wall.

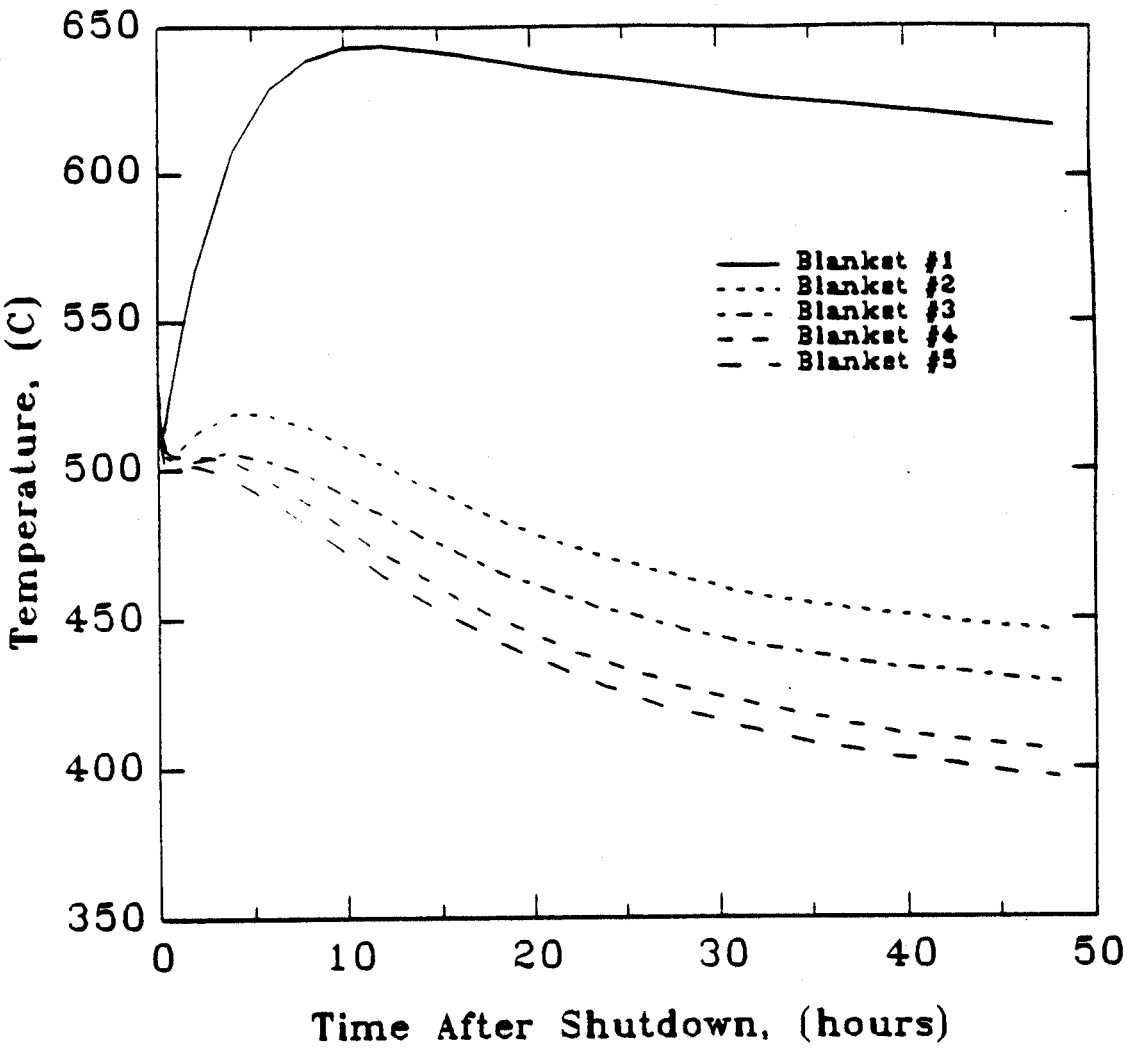

Figure 3.10 Temperature Response of Blankets#1 through #5 at the Mid-point of the First Wall.

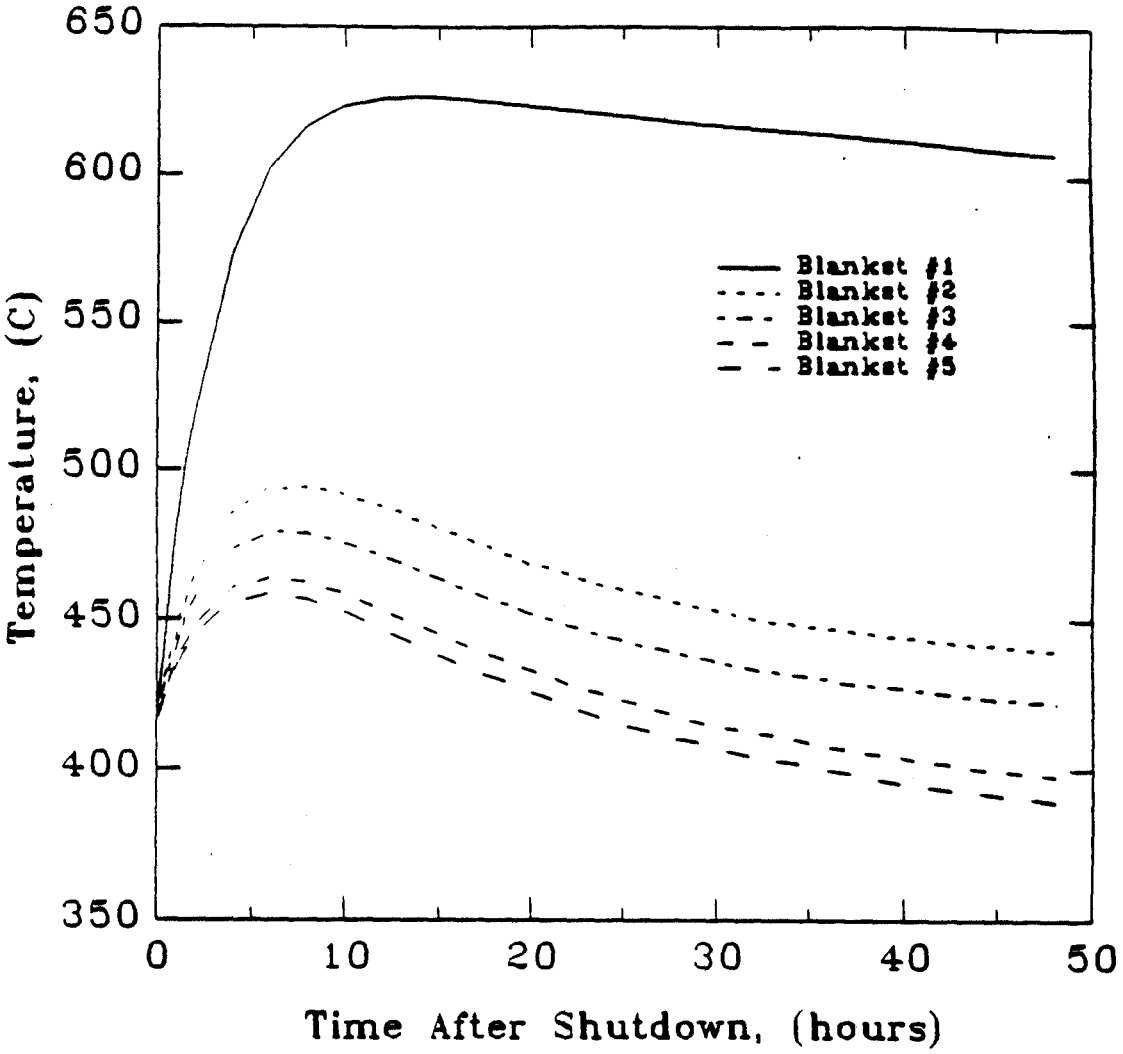

Figure 3.11 Temperature Response of Blankets #1 through #5 at the Back of the First Wall.

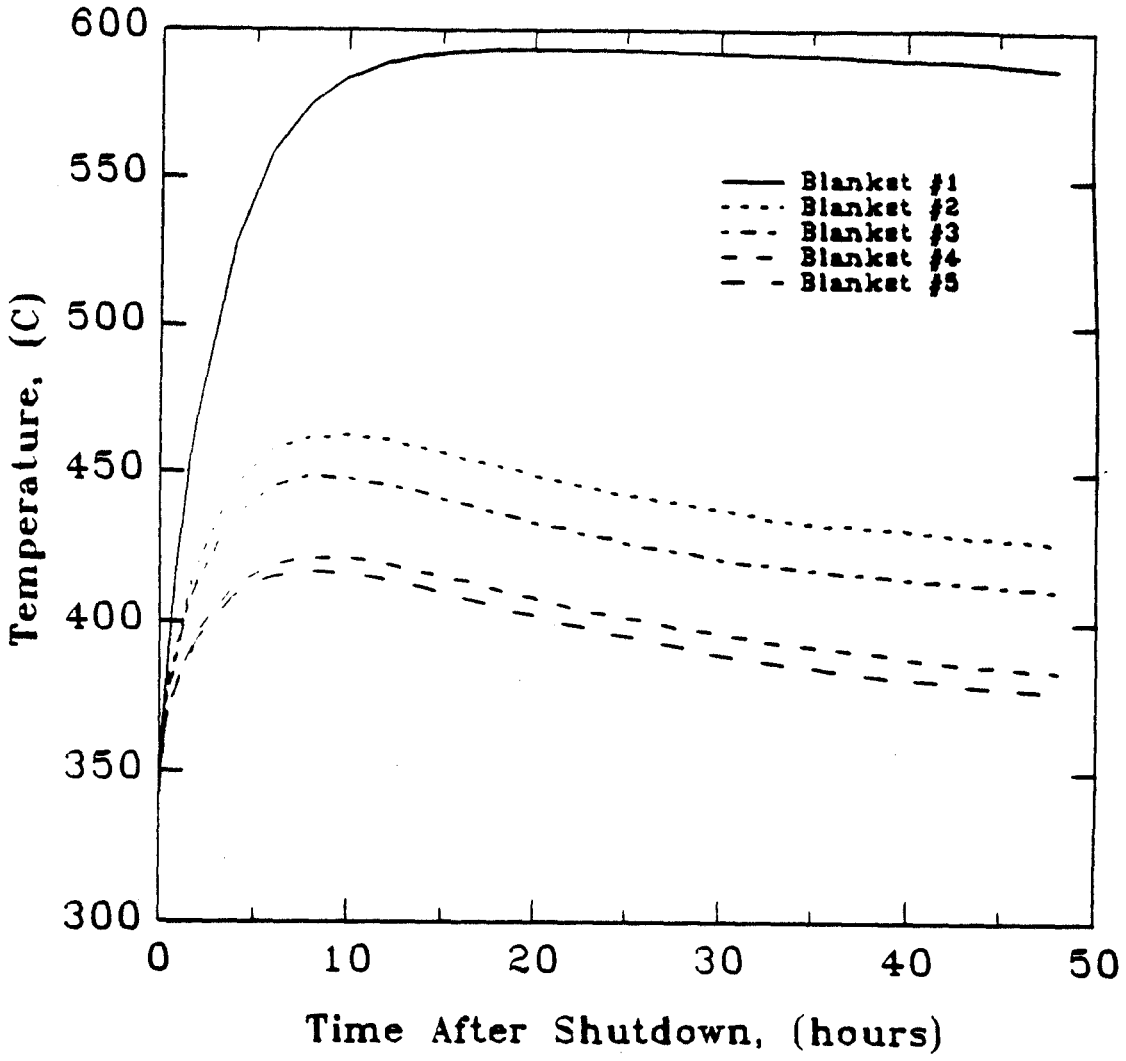

between Blanket #2, and Blanket #3, #4 and #5 is very low ($\sim$ 10 - 15 °C). Therefore, Blanket #2 seems to have the optimum concentration of B_4C and ^{10}B enrichment also from a thermal safety point of view. The temperature response at other points shows a similar behavior.

3.2 The Effect of Graphite Tile Liner

At equilibrium, the power produced in the plasma and the power loss from the plasma must be equal. The major power loss mechanisms are heat transport to the first wall and by Brehmstrahlung radiation. Brehmstrahlung loss can get very high values, if the concentration of high atomic number materials, such as the ones used in conventional steels, reaches certain values. Therefore, to prevent the Brehmstrahlung radiation loss from quenching the plasma, it is essential to limit the impurity atom concentration in the plasma chamber, especially the impurities with high atomic number.

A carbon tile liner inside the first wall is proposed to prevent the high atomic number first wall materials from entering the plasma. However, this tile can affect the thermal response of the blankets to loss of cooling accidents. Its effects on activation and thermal response are investigated in this section. Blanket #1 , #2 and #4 are modified such that those effects can be analyzed. A 2 cm thick section of a graphite liner is added inside both first walls. It was shown in the last section that ^{10}B enrichment does not affect the temperature and thermal response of the blankets. Hence, those enriched blankets, Blanket #3 and #5, are not considered to offer enough incentive to use and are not retained for this part of the study.

Figure 3.12 shows a one dimensional schematic of the Blankets #6, #7 and #8. Their only difference with Blankets #1, #2 and #4 is the addition of a 2 cm thick graphite liner. In Figure 3.13 and 3.14, short- and long-term activation levels for Blanket #6 are shown as a function of time after shutdown. Point 4, 5 and 6 correspond to the back of the first wall, front of the first wall and the mid-point of the graphite

tile, respectively. The activation level of the graphite is lower than that of HT-9 after 1 hour. The activation level of HT-9 in Blanket #6 is 50% less than that of HT-9 in Blanket #1 for short-term. The same information can be obtained from the long-term activation plot.

The temperature of the graphite tile (labeled at *1 cm from first wall*), front of first wall, mid-point of first wall and back of first wall (labeled as *3 cm, 20 cm, and 40 cm from first wall*) for Blanket #6 are shown in Figure 3.15. The temperature of the graphite and the front of the first wall overlap each other. This is because of the high thermal conductivity coefficient of the graphite ($k_{grap} = 152\ W/cm.°C$) and very low decay heat heat generation in the graphite. The temperature at these points exhibit a drop in the first few minutes after the accident due to stored heat redistribution. After that, they rise up to 600 °C and stay at that level for about two days after the accident with a small decrease. The mid-point and the back of the first wall temperatures rise to over 550 °C in ten hours after the accident and stay at that temperature for the rest of the transient.

Total specific activation levels of Blanket #7 as a function of time after shutdown both for short- and long-term are plotted in Figures 3.16 and 3.17, respectively. The difference between the activation of graphite tile and that of the first wall is about five orders of magnitude. The activation level of the back of the first wall (Point 4)is about 0.1 $Ci/cm^3.sec$, which is an order of magnitude less than that of Blanket #6 due to the inclusion of B_4C.

Temperature responses of the various points in Blanket #7 to a LOCA are shown in Figure 3.18. It is very interesting to note that there is no peak in the temperature of the front of the first wall and graphite wall after stored heat redistribution. This blanket can be compared with either Blanket #2 (the difference between them is the graphite tile) or Blanket #6 (the difference between them is the 12.5% B_4C inclusion to the first wall). Both of these blankets exhibit a peak in the temperature after stored heat redistribution, (520 °C for Blanket #2 and 600 °C for Blanket #6). Therefore, Blanket

Figure 3.12 Blankets #6 through #8

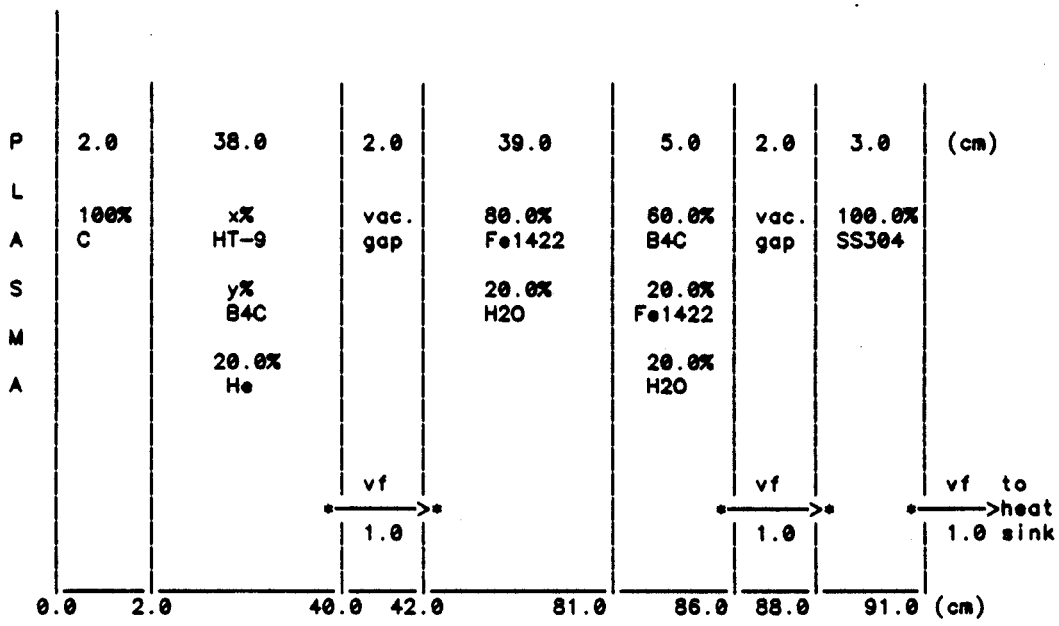

One-dimensional schematic of HT-9/He with C tile inboard blanket for neutronics and 1-D thermal transport modeling.

Arrows connecting asterisks indicate radiation paths. The vf parameters indicate the view factor for that particular radiation path.

Blanket #	x% HT-9	y% B_4C
6	80.0	0.0
7	67.5	12.5
8	40.0	40.0

Figure 3.13 Short-Term Activation of Blanket #6 at the Front and at the Back of the First Wall and the Graphite Tile Liner.

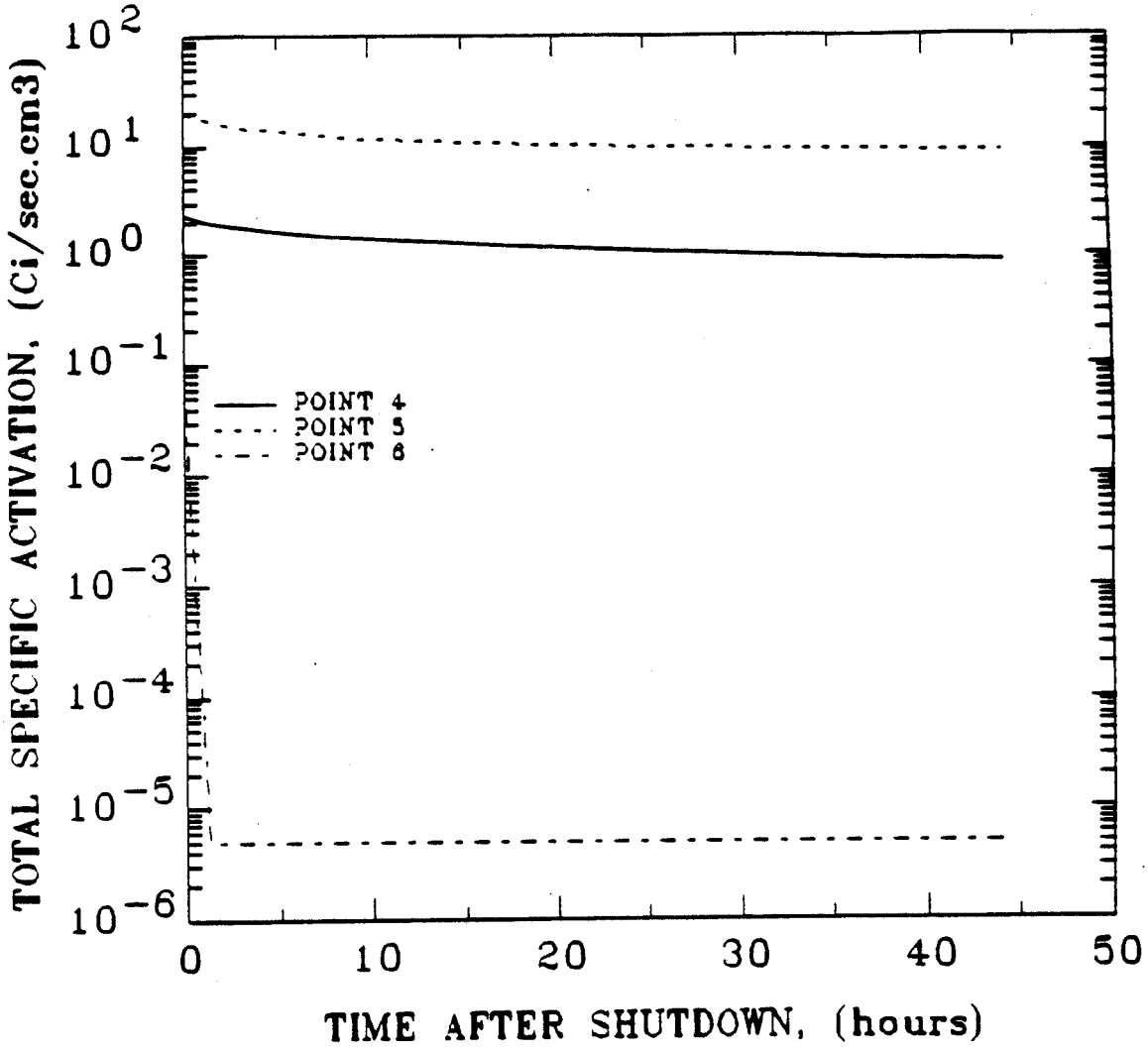

Figure 3.14 Long-Term Activation of Blanket #6 at the Front and at the Back of the First Wall and the Graphite Tile Liner.

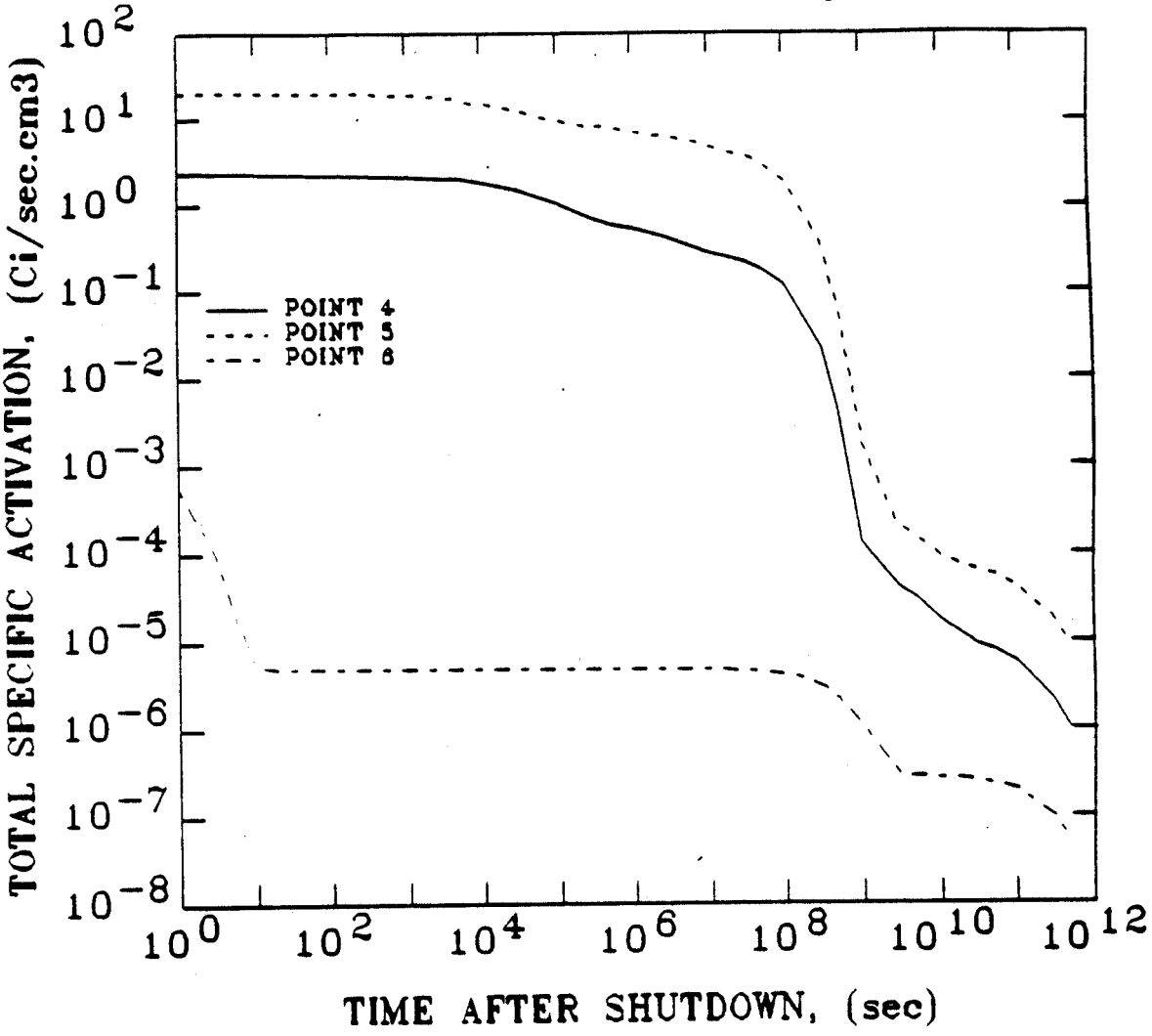

Figure 3.15 Temperature Response of Blanket #6.

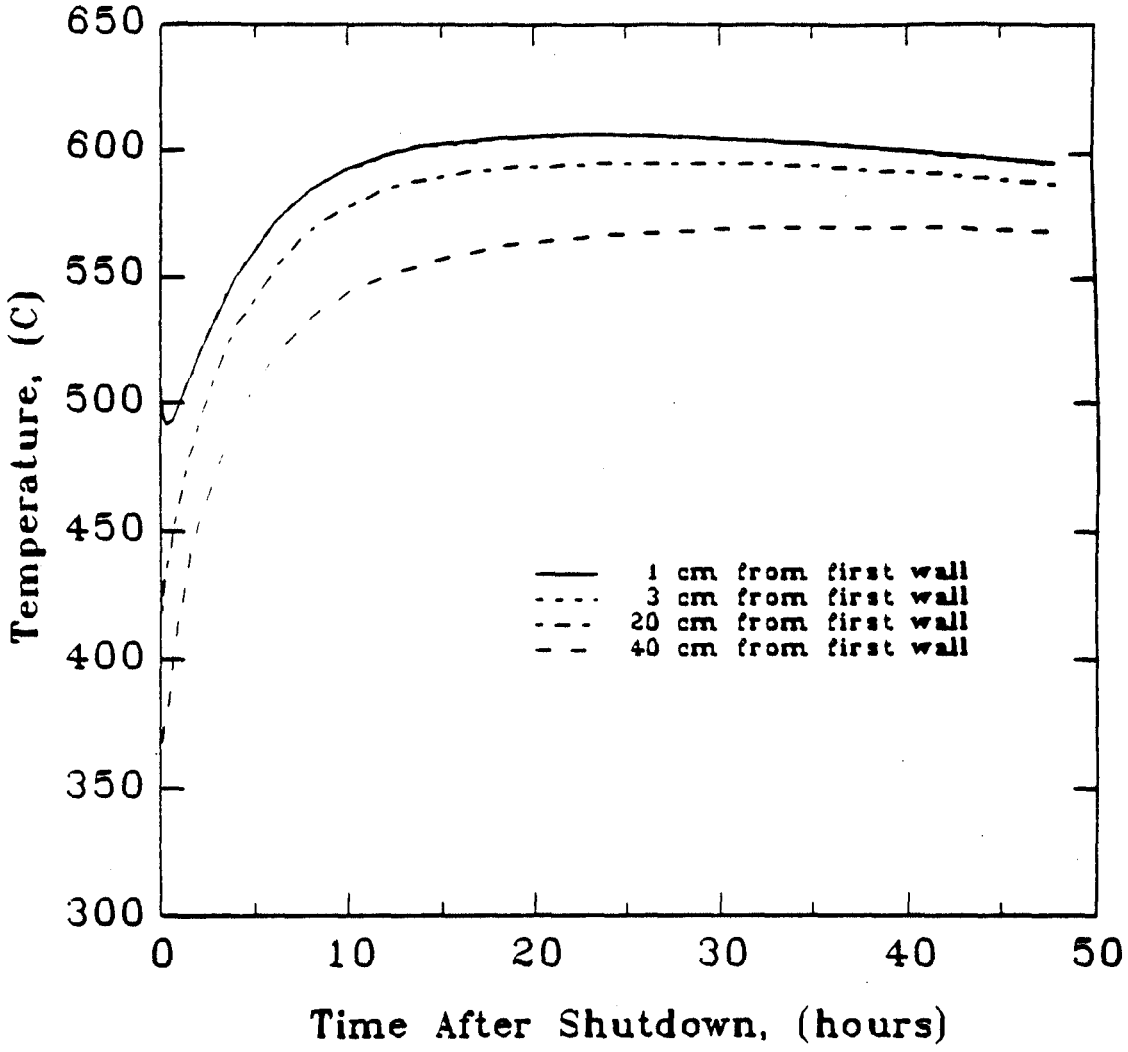

Figure 3.16 Short-Term Activation of Blanket #7 at the Front and the Back of the First Wall and at the Graphite Tile Liner.

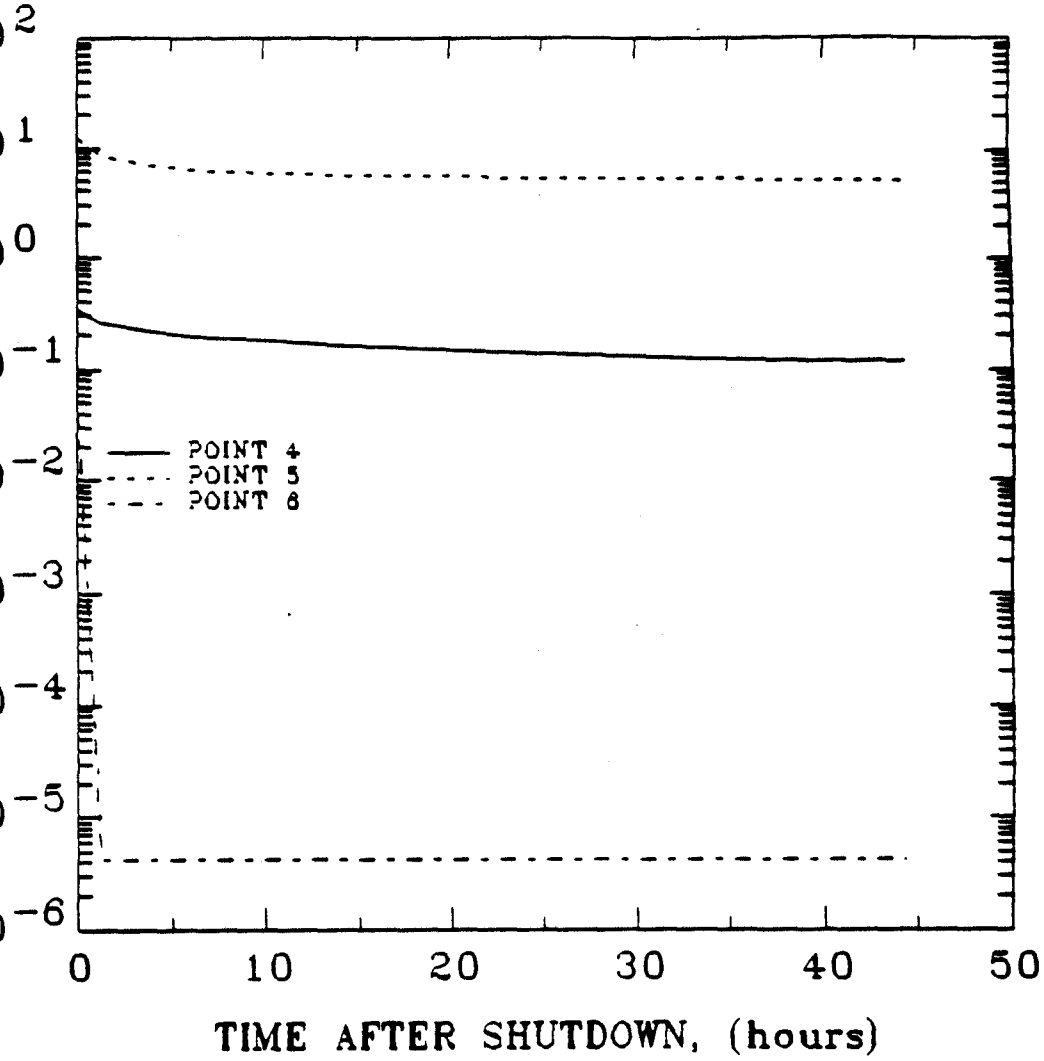

Figure 3.17 Long-Term Activation of Blanket #7 at the Front and at the Back of the First Wall and the Graphite Tile Liner.

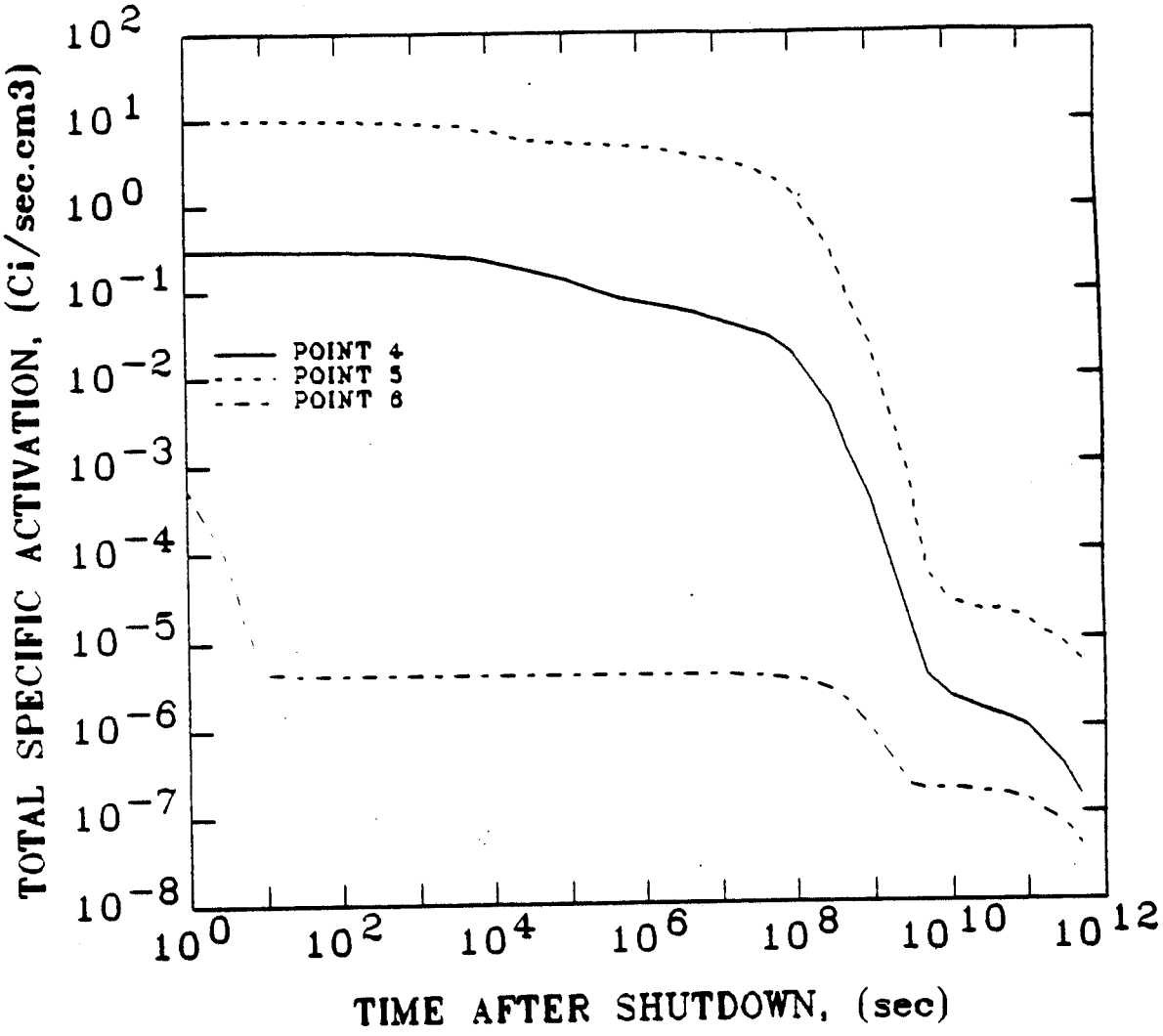

Figure 3.18 Temperature Response of Blanket #7.

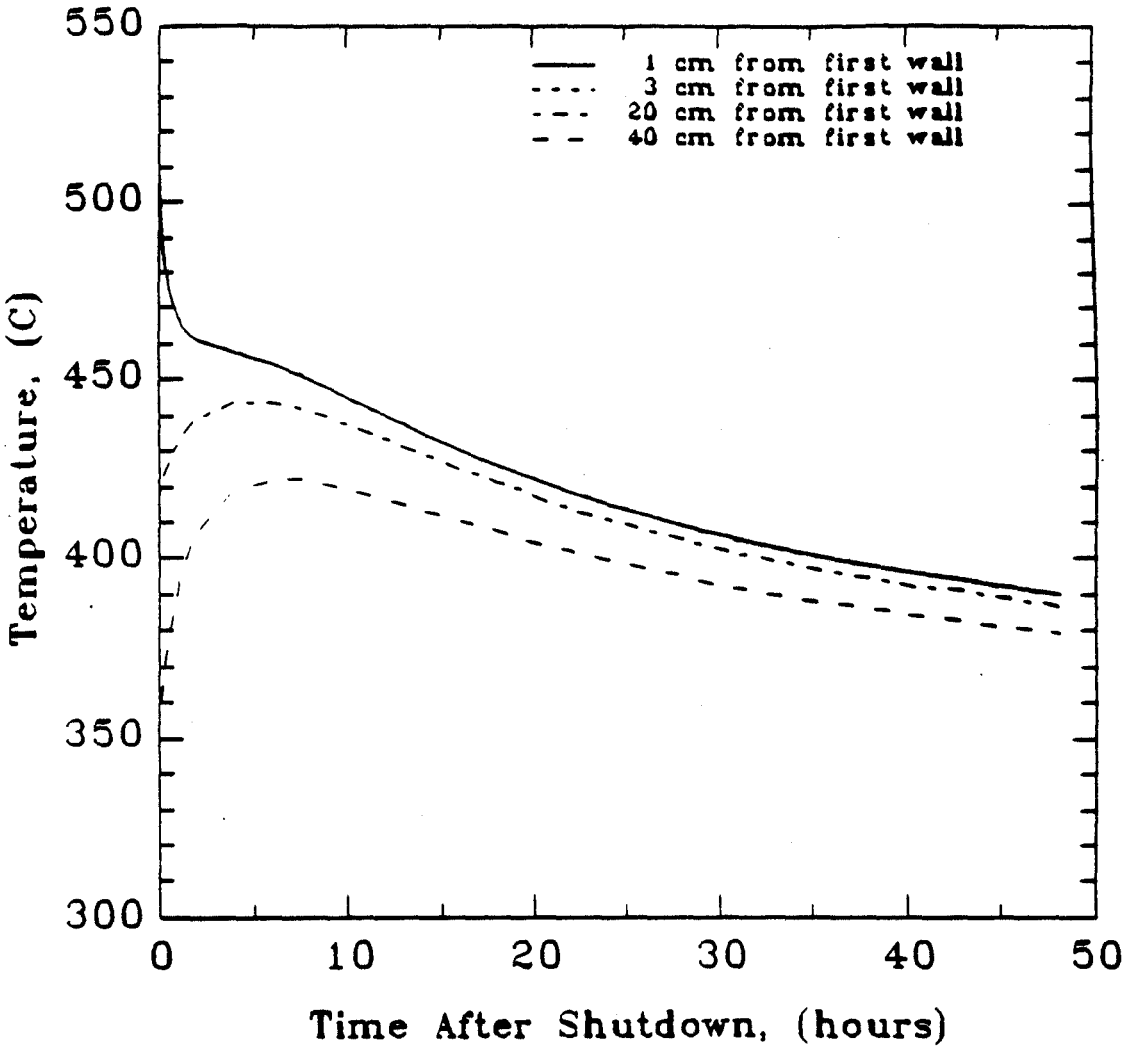

#7 has a clear advantage over other blankets as far as thermal safety is concerned.

The temperature responses of Blanket #8 at various points to a LOCA are shown in Figure 3.19. The temperatures of those points in this blanket decrease rapidly to about 350 °C two days after shutdown.

3.3 Comparison of Blankets #1 through #8

In Section 3.1, a comparison between Blankets #1 through #5 has been done from activation and thermal safety standpoints. It has been seen that there is not much advantage to using ^{10}B enriched B_4C instead of B_4C with natural boron. Then, Blankets #3 and #5 were not considered as a variation to Blankets #2 and #4. In this section Blankets #6, #7 and #8 are compared among themselves and with Blankets #1 and #2. Since the comparisons from an activation and thermal safety points of view result in the same conclusion, only a thermal safety comparison will be made in this section. Moreover, since the most limiting temperature occurs at the point which is closest to the plasma, only the highest temperatures will be compared.

Figure 3.20 shows the highest temperatures of Blankets #6, #7 and #8. Those temperatures are located in the graphite tile. The temperature of the front of the first wall was shown to be equal to the graphite tile temperatures in the last section. The effect of B_4C is clearly seen from the figure. While Blanket #6 shows a very high peak about 600 °C during the transient, Blankets #7 and #8 show a rapid decrease. Blankets #7 and #8 show essentially the same behavior. Therefore, Blankets #4 and #8 are no longer considered as options to improve safety.

Figure 3.21 shows the highest temperatures of the Blankets #1, #2, #6 and #7 as a function of time after the accident initiation (or shutdown). The comparison between the highest temperatures of Blankets #1 and #6 lead us to conclude that using a graphite tile helps limit the temperature escalation by about 50 °C for about 10 hours after the accident initiation. Therefore, the use of graphite tile is beneficial from activation and thermal safety points of view.

Figure 3.19 Temperature Response of Blanket #8.

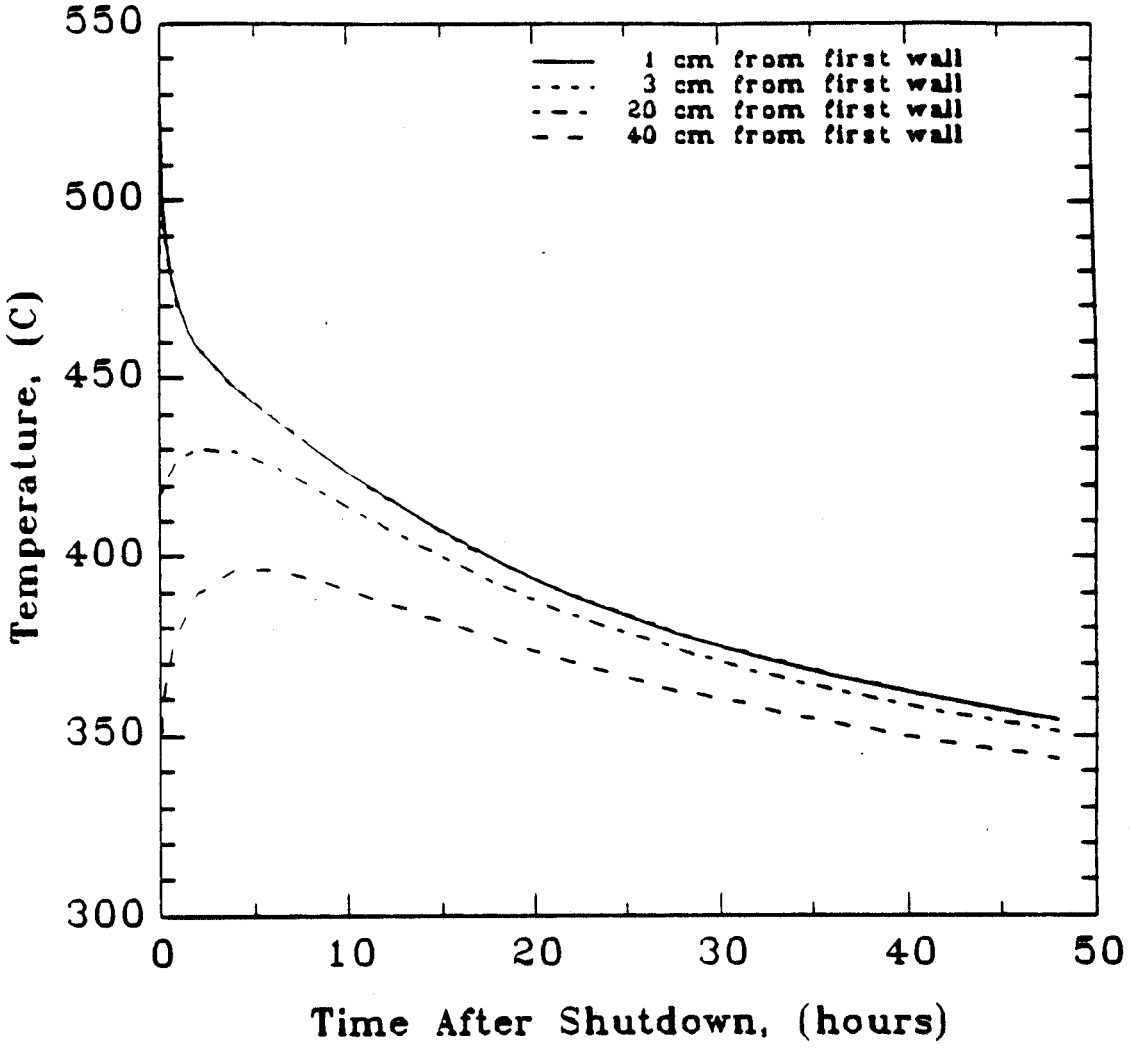

Figure 3.20 Highest Temperatures of Blankets #6 through #8.

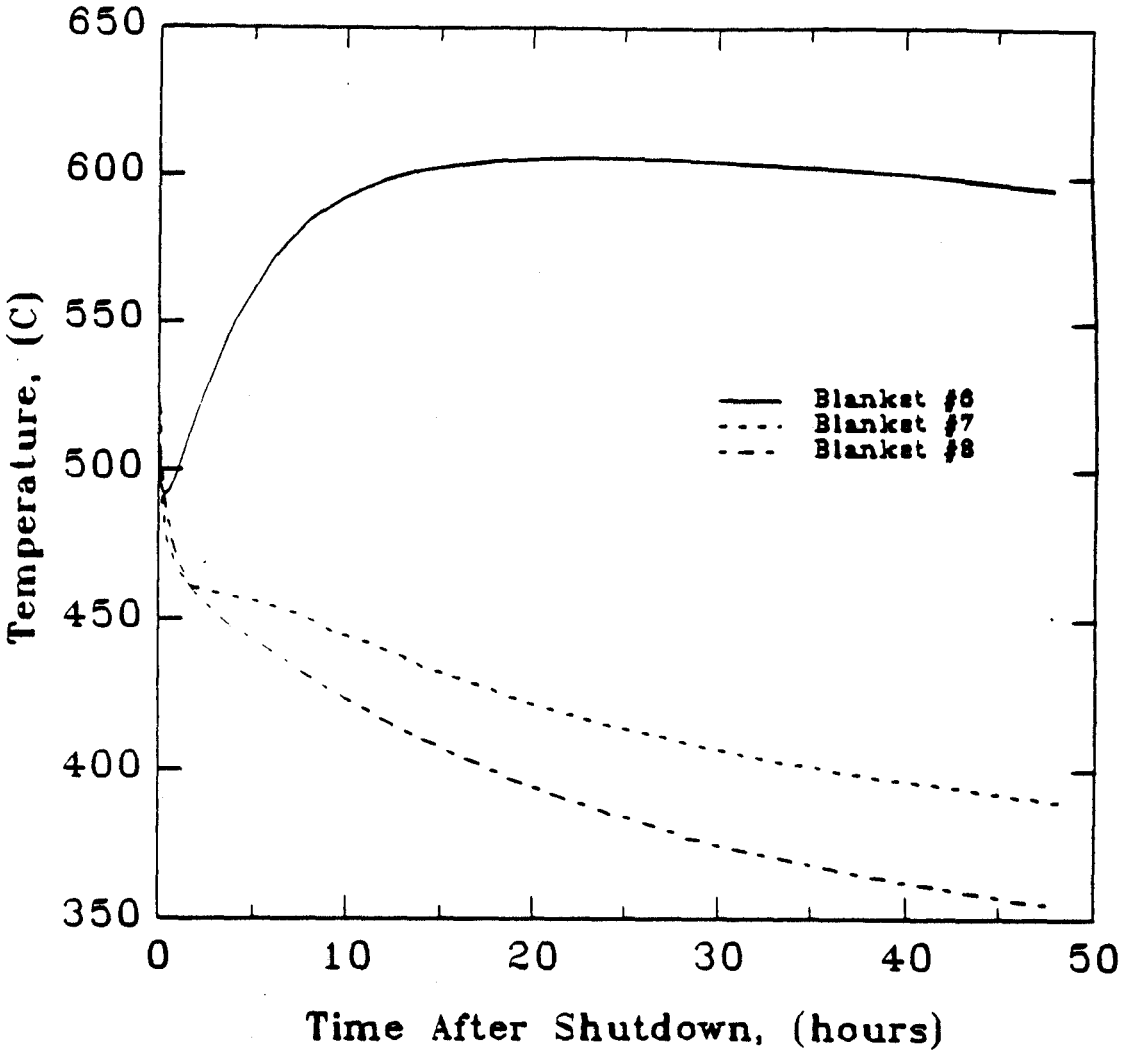

Figure 3.21 Highest Temperatures of Blankets #1,#2,#6,#7.

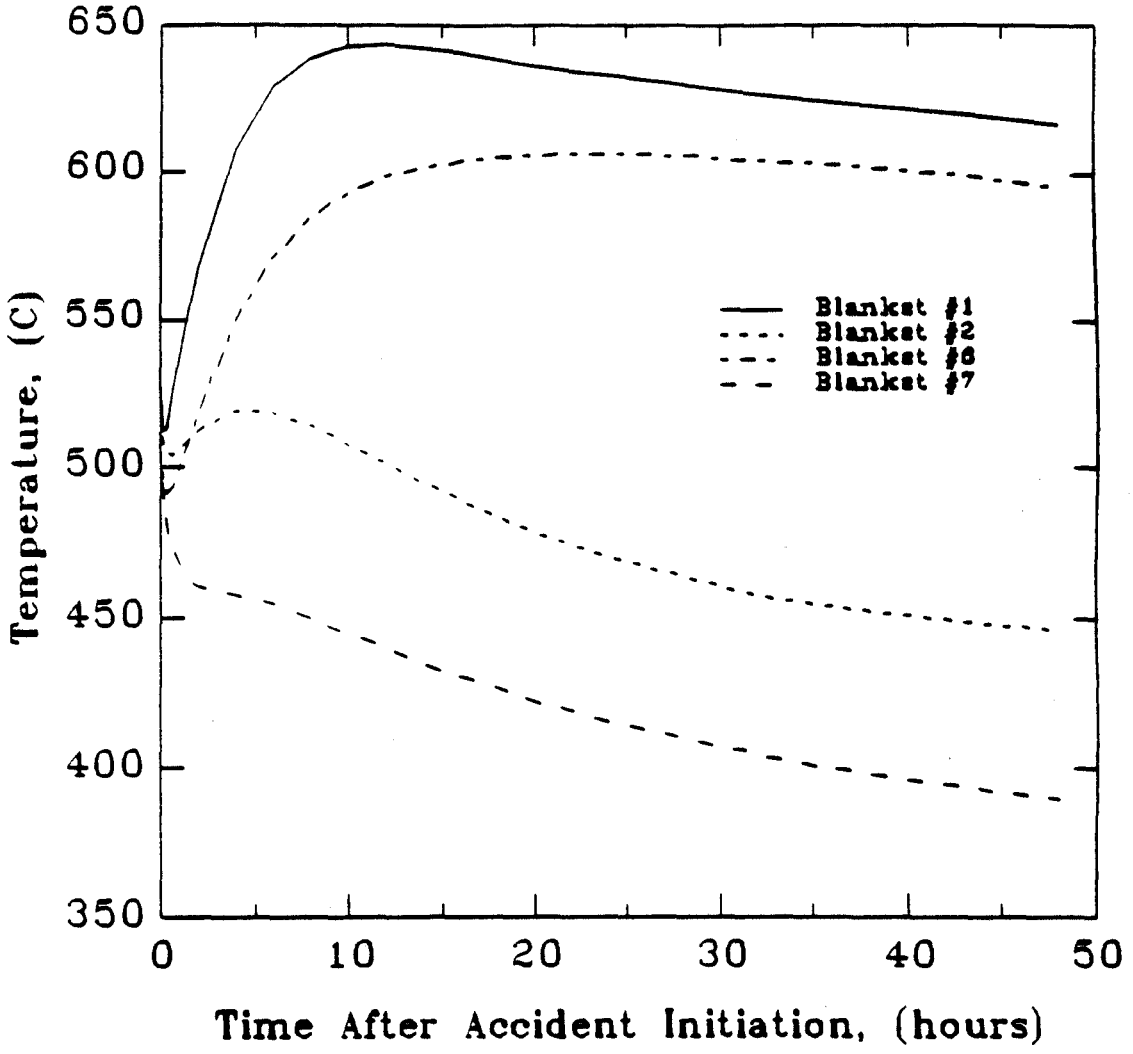

The comparison of the highest temperatures of Blankets #2 and #7 shows that using the neutron absorber and the graphite tile at the same time results in an advantage of a difference of 50 °C in the temperature response over only using the neutron absorber. Therefore, if it feasible from other viewpoints, such as strength, fabricability and irradiation resistance, the use of B_4C and graphite tile at the same time are recommended. If one of them is not feasible to use, the other can still bring advantages alone.

3.4 Verification of Some of the Approximations

The accident assumed to be the worst case is LOCA as defined in Chapter 2. The assumption was that the coolant in all modules is lost at the beginning of the accident. This assumption is necessary because the code THIOD, which computes transient temperatures, uses one dimensional geometry to simulate the blanket. Therefore, the assumption is equivalent to not allowing heat transfer in poloidal and toroidal directions.

The worst case LOFA can be defined with the same analogy; the coolant in all modules stops flowing at the initiation of the accident. In this section, the effect of the type of the accident is analyzed for Blanket #5.

Figure 3.22 shows the temperature response of the Blanket #5 to LOCA and to LOFA. The two exactly overlap each other. This is due to very low activation of He and the low thermal conductivity of He. Remember that natural convection is not allowed in this part of the study.

The neutron bombardment duration may affect the activation, and therefore, the temperature response of the first wall. In this analysis, activation is calculated for one year of irradiation time. Temperature response of Blanket #5 to two bombarding times, one year and three year, is shown in Figure 3.23. In the first five hours, there is no difference between the temperatures. After five hours, the temperature of 3 year operation time is about ~5 °C higher that that of 1 year operation time. This can be

Figure 3.22 First Wall Temperature Response of Blanket #5: LOCA vs. LOFA.

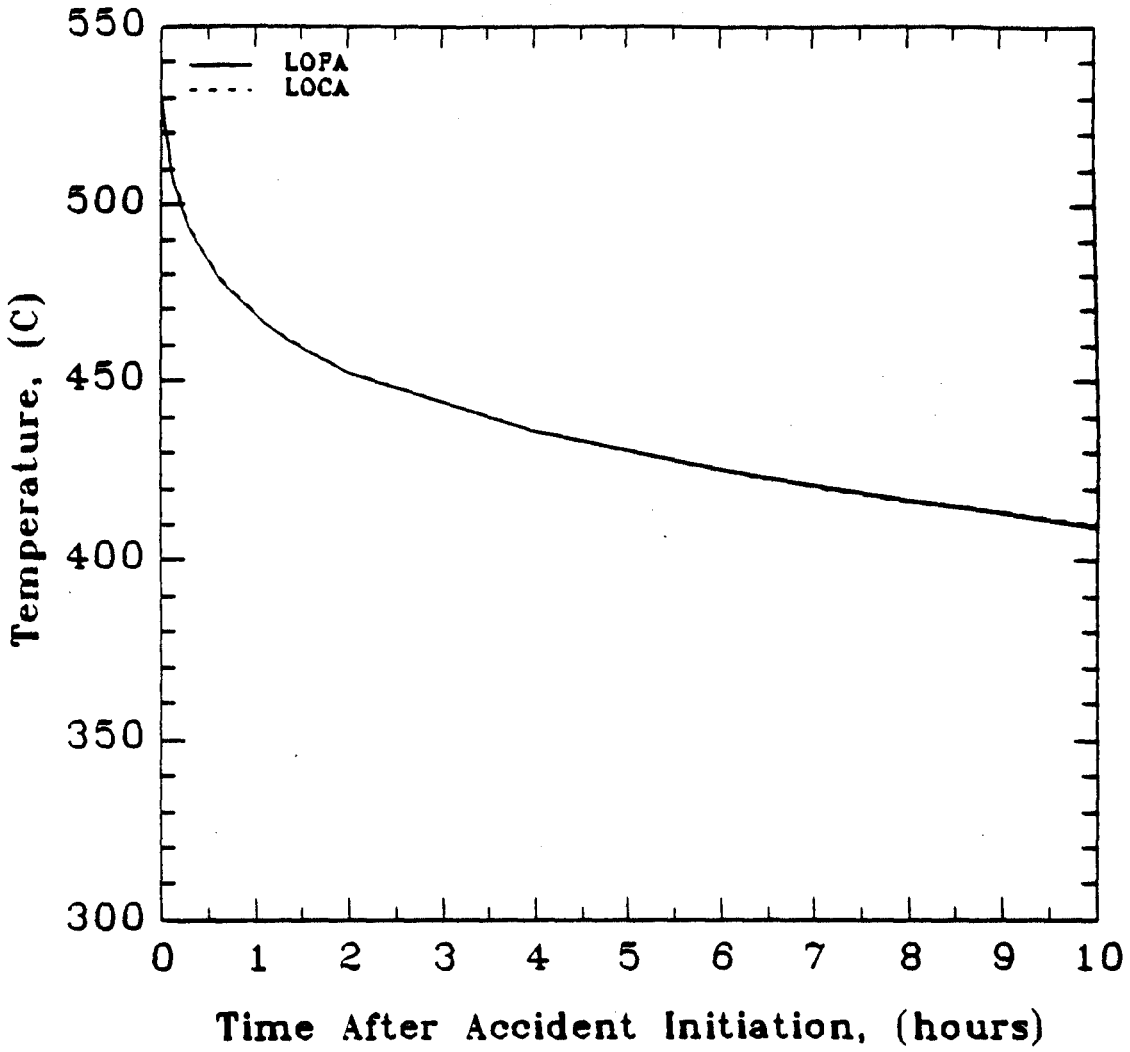

explained as follows; The radioisotopes with long half-lives reach saturation at a longer time than those with shorter half-lives [27]. Long half-life isotopes decay at a slower rate. In the first five hours after the accident, the decay heat is mainly generated by the decay of the radioisotopes with short half-lives. The decay energy emitted by the decay of the long half-live isotopes shows its effect only after the radioisotopes with short half-lives die away. Since, the concentration of radioisotopes with long half-lives is higher after 3 years of operation, the decay heat, and therefore the temperature, get higher five hours after the accident.

In the previous sections, the plasma is assumed to shut off immediately after the accident so that there is no heat flux to the first wall from the plasma. Another plasma shutdown scenario was presented in Chapter 2. In that, plasma heat flux was assumed to exist for 1 second, and then to go to zero linearly, (see Figure 2.4). In this case, the total heat input to the first wall is higher. In Figure 3.24, temperature response of first wall is plotted according to the two different plasma shutdown scenarios. Due to the excess heat flux to the first wall, the temperature experiences a $\sim$10 °C peak in a very few seconds after the accident. One hour after the accident, the effect of the extra plasma heat flux is negligible.

3.5 The Impact of B_4C Before a Steel Shield

The first eight blankets can only be employed for experimental fusion reactors which do not aim to produce power or tritium. However, the goal of fusion power reactors is to generate electricity. To make that possible, tritium breeding in the blanket is a must. Therefore, a neutron absorber in the blanket where tritium is bred can not be included. In some cases, moreover, a neutron multiplier such as Be can be employed to achieve the neccessary tritium breeding ratio (TBR).

To limit the irradiation of the magnets, and to limit the temperature rise in case of loss-of-cooling accidents, a B_4C layer can be inserted before the steel shield. In this part of the study, the effects of such an insertion is investigated.

Figure 3.23 First Wall Temperature Response of Blanket #5:
Impact of Neutron Bombarding Time.

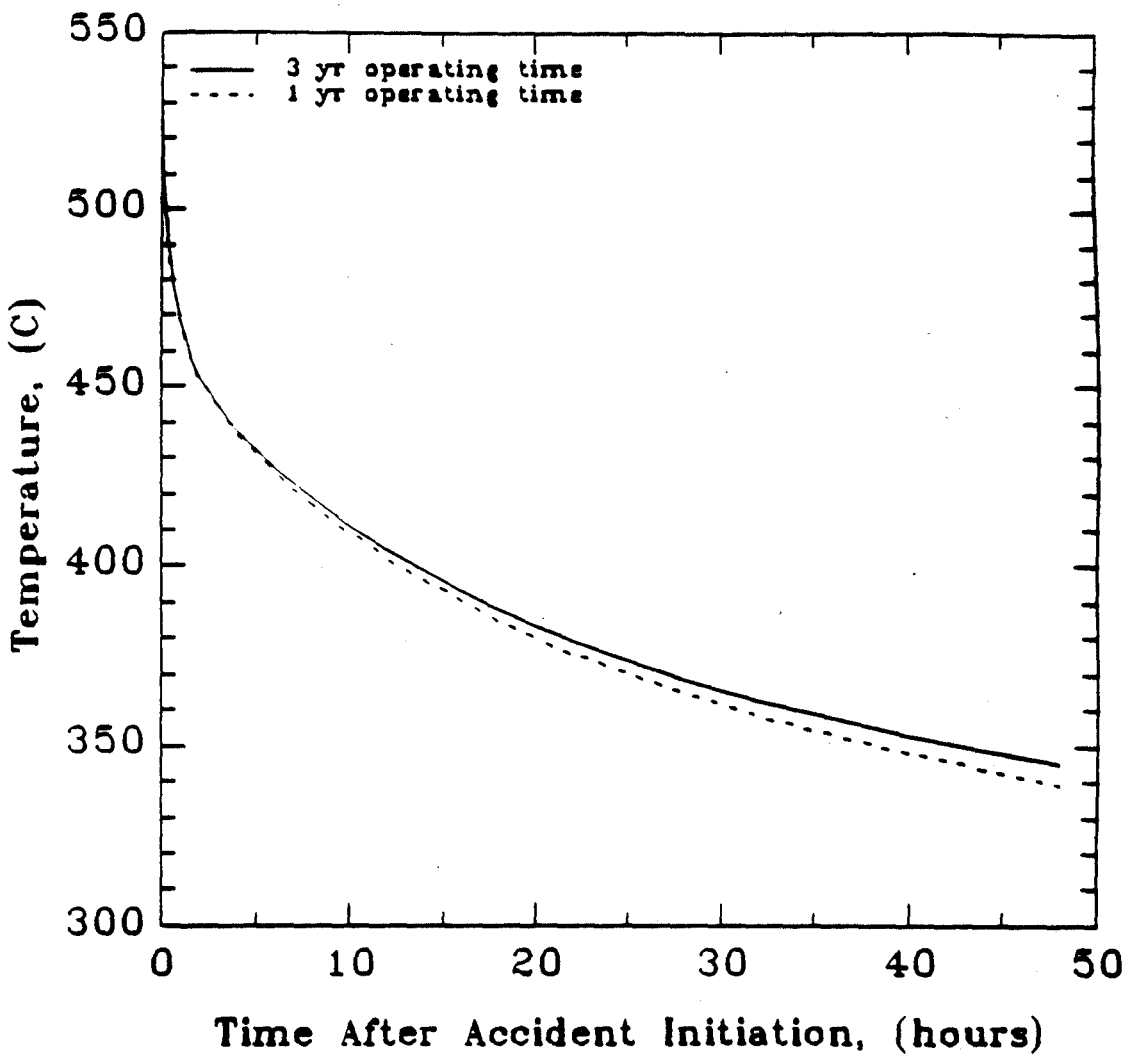

Figure 3.24 First Wall Temperature Response of Blanket #5:
Impact of Plasma Shut-down Behavior.

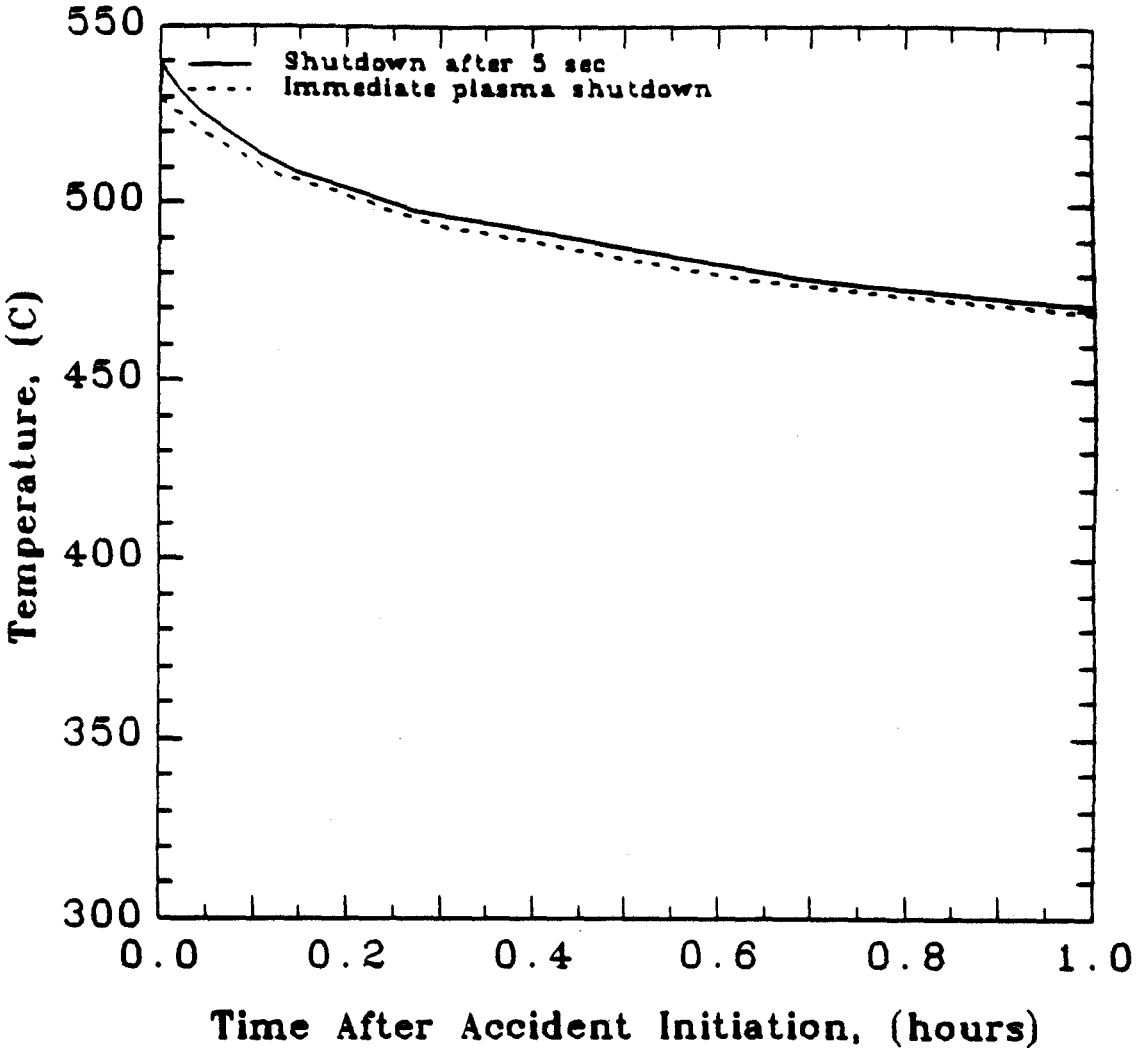

Blanket #9 and #10 are the reference blankets for this analysis. Blanket #9 is essentially a design developed during the Blanket Comparison and Selection Study [5]. The design parameters and operating conditions are shown in Table 2.3. The only difference between these two blankets is that a 20 cm thick steel shield in Blanket #9 is replaced by a 20 cm thick B_4C shield, Figure 3.25.

The method of analysis which is described in Chapter 2 is performed to calculate the temperature response of these blankets to a LOFA accident. Because of the limitation of the codes used in this study, a worst case LOFA is assumed, as discussed before. The impact of natural convection is also neglected. If the magnets can't be shutdown, natural convection of liquid lithium, which is electrically conductive, will not help to limit the temperature, (see Chapter 4). The plasma is assumed to shut off immediately at the time of the accident. The operating time before the accident is three years.

Figure 3.26 shows the temperature response of Blanket #9 as a function of time after shutdown. The temperature at the front of the shield increases very sharply in the first five hours, and reaches ~450 °C. Then, following a small decrease, it continues to rise at a smaller rate. The temperature at 20 cm from the first wall and at the back of the shield also behave in a similar way.

Figure 3.27 shows the temperature response of Blanket #10 as a function of time after shutdown. Because, the decay heat generation rate is very low in the B_4C shield-layer the temperature at all points in the shield rises at a smaller rate. At five hours after the accident, the highest temperature in the shield is about 175 °C, which is very low compared to more than 450 °C in Blanket #9. Figure 3.28 shows the highest temperatures at the shield and at the first wall of Blankets #9 and #10. The impact of B_4C in the shield even on the first wall temperature response is shown. This is not because of the decrease of neutron flux, but rather because of the lower temperatures in the shield, hence higher heat transfer rate from the first wall to the shield. The first wall temperature of Blanket #10 is 100 °C lower than that of Blanket #9 after about 10 hours, and even lower than its operating temperature.

Figure 3.25 One Dimensional Schematic of Blankets#9 and #10.

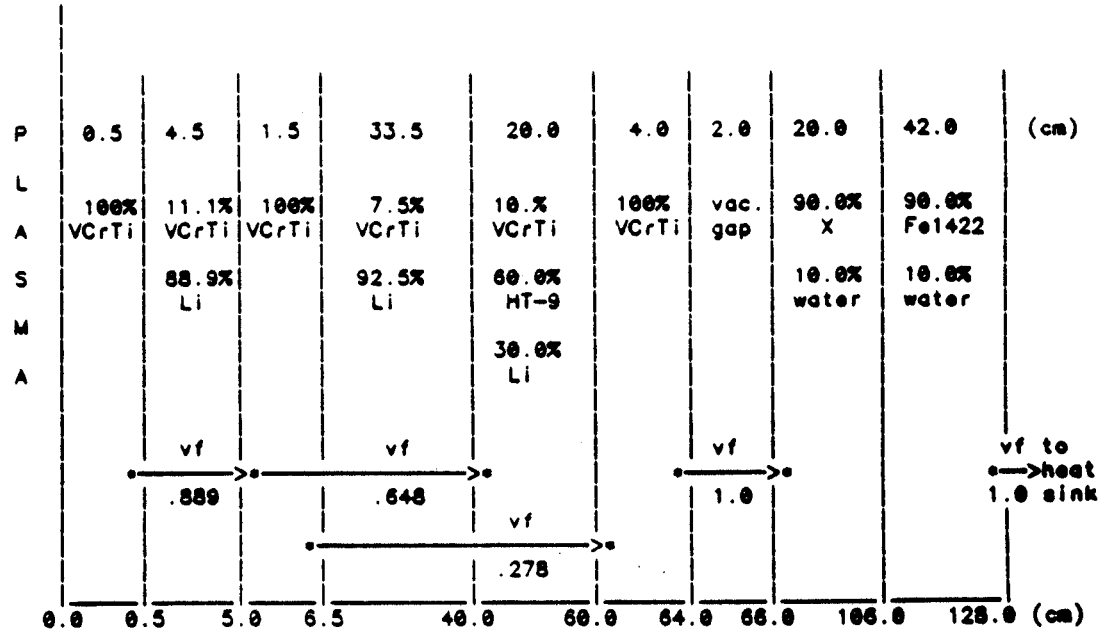

* Arrows connecting asterisks indicate thermal radiation paths in LOCA (complete Lithium drain) case. The vf parameters indicate the view factor for that particular radiation path.

X = Fe1422 for Blanket #9
X = B4C for Blanket #10

Figure 3.26 Temperature Response of Shield of Blanket #9 at Various Locations.

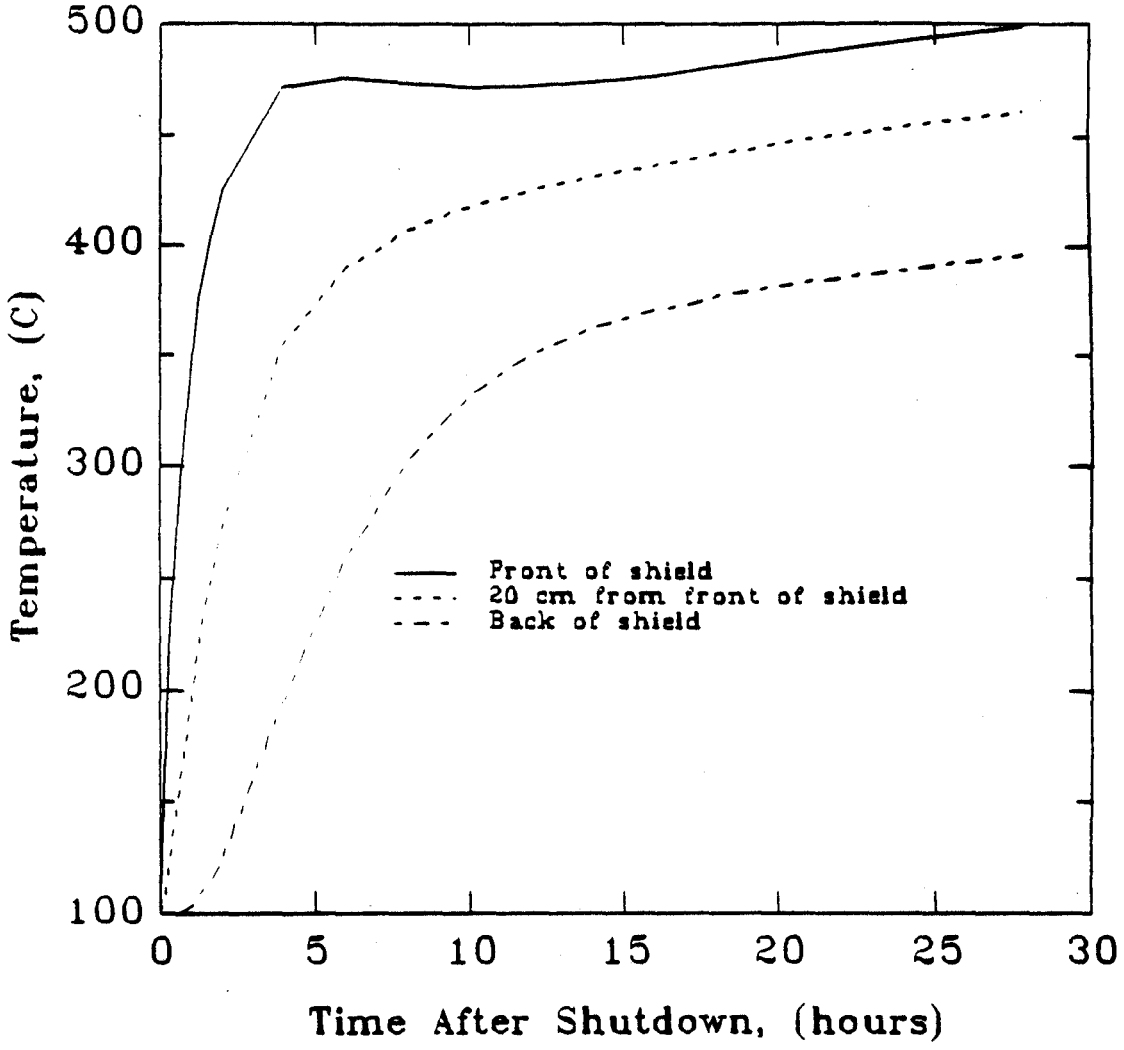

Figure 3.27 Temperature Response of Shield of Blanket #10 at Various Locations.

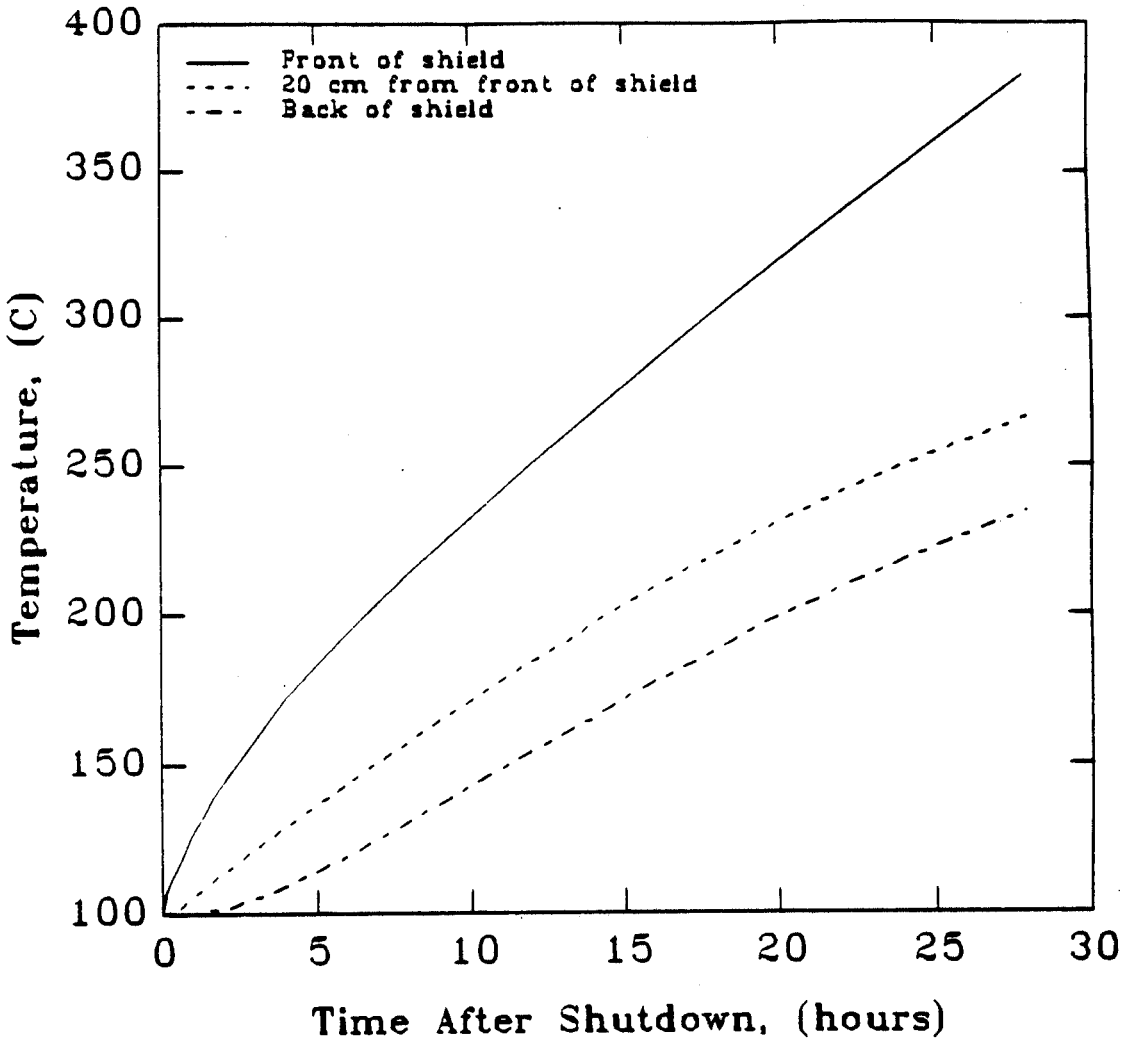

Figure 3.28 Temperature Response of Blankets#9 and #10 at Various Locations

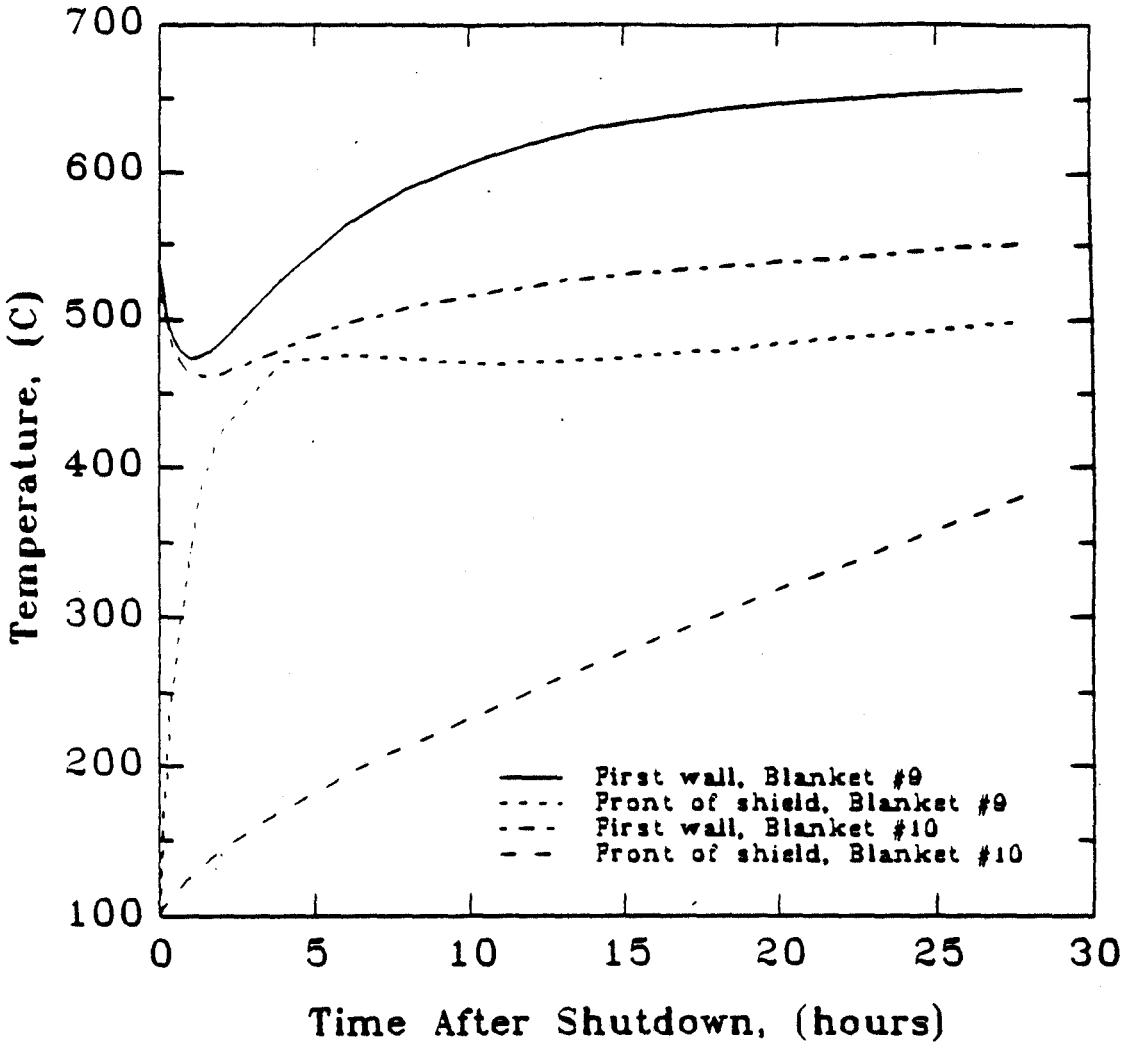

3.6 Conclusions

In this chapter the effects of B_4C on the activation and thermal safety of fusion reactor blankets are analyzed. The neutron absorber is added to the first wall of an experimental reactor and into the shield of a power reactor. Various amounts of B_4C with two different enrichment levels are included in the first wall. It is found that ^{10}B enrichment does not offer any significant advantage over natural boron. The excess amounts of B_4C such as 40% of the fractional volume of the first wall does not bring any significant advantage either. With inclusion of 12.5% B_4C in the first wall (Blanket #2), the activation and temperature of the first wall is limited.

The effects of a graphite tile liner on the thermal response of blankets are also investigated. The temperature peak of Blanket #6 (with liner) is 50 °C less than that of Blanket #1 (no liner). This shows that using graphite liner before the first wall would ease the temperature escalation of experimental reactor blankets.

Several approximations used in this chapter are investigated. The effect of longer operating times, the effect of type of loss-of-cooling accident and the effect of plasma shutdown behavior are all found to be small.

The effect of inclusion of B_4C into the shield of a fusion power reactor shows that the temperature escalation of the shield can be delayed for about a day. The use of B_4C in the shield even lowers the temperature of first wall.

Chapter 4

Impact of Natural Convection Cooling

The thermal analysis presented in Chapter 2 accounted for conductive and radiative heat transfer only. In Chapter 3, that method was applied to several design and accident conditions. In a LOFA, the coolant was assumed to become stagnant at the beginning of the accident, and to stay motionless. However, as the coolant remains inside the coolant tubes there is a possibility that flow would continue at a lower flow rate. This is due to buoyancy effects, and is known as natural convection. The heated fluid thermally expands, and thus becomes less dense than the cooler fluid, and therefore rises, causing a flow.

In this chapter, the impact of natural convection on the temperature response is evaluated. As it is shown in Reference [7], natural convection of gaseous fluids does not affect the temperature response of blankets significantly. However, for liquid metals, natural convection effects may be substantial under certain conditions.

The impact of the behavior of the magnetic field and the initial mass flow rate following a LOFA are analyzed. This analysis is done for a liquid lithium cooled blanket, Blanket #11. The chapter begins with a description of the method of analysis of natural convection. Then, the temperature response of Blanket #11 to a LOFA with various magnetic field and initial mass flow rates is presented.

4.1 Model for Natural Convection Analysis

The model for the natural convection cooling can be divided into two parts: (1) Calculating the flow rate of the coolant under natural convection, (2) Determining the heat transfer charactersitics of the flowing coolant using the flow rate calculated in the

first part. In transient natural convection cases these two parts are coupled to each other; requiring simultaneous solution of two equations derived in both parts.

The flow rate of the coolant under natural convection can be found by a hydraulic balance; total pressure losses are equal to pressure head. There are three components of pressure drop; friction, magnetohydrodynamic (MHD) effects, and inertial effects. The available pressure head is due to buoyancy effects, which is equal to the sum of the pressure drop terms;

$$\Delta P_B = \Delta P_{fric} + \Delta P_{MHD} + \Delta P_T \tag{4.1}$$

The pressure gain by buoyancy head can be expressed as follows:

$$\Delta P_B = \rho g L \beta \Delta T \tag{4.2}$$

where

ρ is the coolant density (500 kg/m^3),

g is the acceleration due to gravity (9.8 m/s^2),

L is the thermal elevation difference (10 m),

$\beta = \frac{-1}{\rho} \frac{\partial \rho}{\partial T}$ is the thermal expansion coefficient of the coolant (1.94 10^{-4} K^{-1}),

ΔT is the temperature rise of the coolant along the channel, (^{o}C).

This pressure gain term is balanced by the pressure drop terms. For high pressure drop caused by MHD effects and small pressure gain by natural convection, the type of flow is expected to be laminar. For such a case the friction pressure drop can be expressed as;

$$\Delta P_f = K_{fric} \dot{m} \tag{4.3}$$

where $\dot{m}$ is mass flow rate and K_{fric} represents the geometry of the flow loop and the properties of the coolant, μ and ρ:

$$K_{fric} = 32 \frac{\mu}{\rho} \frac{l}{A D_e^2} \tag{4.4}$$

where

μ is dynamic viscosity of the fluid (4.0 10^{-4} Pa.s),

ρ is the density of the fluid (kg/m^3),

l is the length of the channel (25 m),

A is the flow area of the channel (0.54 m^2), and

D_e is the hydraulic diameter of the channel (8.0 10^{-3} m for the first wall and 0.3 m for the blanket and manifold).

Sudden expansion or contraction of channels introduce additional pressure drops, which can be added to the factor K_{fric}.

In liquid metal cooled blankets, the MHD effects create a pressure drop. When a liquid metal, which is electrically conductive, flows transverse to a magnetic field, there are electromagnetic forces on the fluid which cause MHD pressure drops. The pressure drop in a flow section can be expressed as:

$$\Delta P_{MHD} = \sigma \frac{\dot{m}}{\rho A} \bar{B}^2 \frac{\Delta l_p}{\alpha} \tag{4.5}$$

where

σ is the conductivity of the coolant channel wall (Ω - m)$^{-1}$,

$\bar{B}$ is the average magnetic field strength (4.75 T),

Δ is the average coolant channel wall thickness (0.005 m),

l_p is the total channel length for flow perpendicular to the B (25 m),

α is the average coolant channel radius or half-width (0.22 m).

The inertial pressure drop term comes from the time dependent accelaration of coolant. Since the coolant initially is flowing by forced convection, its flow rate will decrease after the pump stops, which creates a pressure head. That pressure term can be expressed as:

$$\Delta P_T = \frac{l}{A} \frac{d\dot{m}}{dt} \tag{4.6}$$

where,

l is the length of coolant channel (m),

A is the cross sectional area of coolant channel (m^2), and

$\dot{m}$ is the mass flow rate (kg/s).

By combining equations 4.2, 4.3, 4.5, and 4.6 with equation 4.1, we get the following equation

$$\rho g L \beta \Delta T \;=\; K_{fric}\, \dot{m} \;+ \sigma\, \frac{\dot{m}}{\rho A}\, \bar{B}^2 \;\frac{\Delta l_p}{\alpha} \;+ \frac{l}{A}\frac{d\dot{m}}{dt} \tag{4.7}$$

The above equation involves only two unknowns: $\dot{m}$ and ΔT. ΔT is the temperature rise of the coolant,

$$\Delta T \;=\; T_{out} \;-\; T_{in} \tag{4.8}$$

where

T_{in} is the coolant temperature at the inlet to the blanket, and T_{out} is the coolant temperature at the outlet of the blanket.

The secondary loop which removes heat from the coolant is assumed to remain in operation so that the inlet temperature, T_{in} does not change during the transient (note that this is not an appropriate representation of loss-of-site power accident). Therefore T_{out} remains as the only unknown. T_{out} can be found by calculating the total heat transfer rate to the coolant along the coolant channels. Convective heat transfer from a solid wall to a flowing coolant is described by the equation

$$\dot{q}''_{convection} = h\,(T_s - T_l) \tag{4.9}$$

where

h is the heat transfer coefficient (W/m^2K),

T_s is the temperature of the solid wall, and

T_l is the temperature of the flowing coolant.

There are emprical relations to find h. These relations are based on several non-dimensional parameters representing the physical properties of the coolant and flow characteristics. The Reynolds number, Re, for example defined as

$$Re \;=\; \frac{\rho\, V\, D_e}{\mu} \tag{4.10}$$

where

V is the coolant velocity in the channel(m/s) ,

D_e is the hydroulic diameter of the channel (m), and

μ is the viscosity of the coolant (Pa.s).

The coolant properties are characterized by the Prandtl number, Pr

$$Pr = \frac{c_p \mu}{k} \tag{4.11}$$

where

c_p is the coolant specific heat (J/kg.K), and

k is the coolant thermal conductivity (W/m.K).

The heat transfer characteristics of the coolant in the channel are characterized by the Nusselt number, Nu

$$Nu = \frac{h D_e}{k} \tag{4.12}$$

To calculate h, a relation between Nu and, Re and Pr is needed. For natural convection problems involving liquid metals, the following set of equations can be used [29]

$$Nu = 5.0 + (\psi \, Re \, Pr)^{0.8} \tag{4.13}$$

$$\psi = 1 - \frac{1.82}{Pr \, (\epsilon_m/\nu)^{1.4}_{max}} \tag{4.14}$$

$$(\epsilon_m/\nu)_{max} = 0.029 \, Re^{0.769} \tag{4.15}$$

Then T_{out} can be found by integrating the heat flux along the coolant channel:

$$T_{out} = T_{in} + \frac{1}{\dot{m} c_p} \int_l q"_{convection} \, P_h dl \tag{4.16}$$

where P_h represents the heated perimeter of the channel, and the the integral is taken over the channel length.

The method of solution proceeds as follows. From the previous known value of $\dot{m}$, ΔT can be calculated. In the next time step, by using this ΔT, a new $\dot{m}$ is calculated. Then, ΔT at that time step is calculated, and so on.

All of this analysis is done in another version of THIOD, which has a subroutine called CONVECT [7]. The subroutine calculates $\dot{m}$ and h, and returns those values to

the main code. This version of THIOD solves the following equation which accounts for in the convection heat transfer instead of equation (2.8)

$$\rho(z)\ c_p(z,T)\frac{\partial T(z,t)}{\partial t} + \rho c_p v\frac{\partial \Delta T(z,t)}{\partial z} = \dot{q}'''_{decay} + \nabla.\dot{q}''(z,t). \qquad (4.17)$$

4.2 Results of Natural Convection Analysis

One dimensional schematic of the inboard side of Blanket #11 is shown in Figure 4.1. Its operating conditions and design parameters are shown in Table 2.4. This blanket uses liquid lithium coolant. In this part of the study the copper magnets are also included in the neutronic and thermal analysis.

The impact of natural convection on the temperature response of Blanket #11 is investigated in different LOFA cases. Those cases summarized in Table 4.1. The varying conditions are the magnetic field behavior and the initial mass flow rate.

Table 4.1 Summary of Different Convection Cases Analyzed

CASE #	Initial Magnetic Field (Tesla)	Initial Mass Flow Rate (kg/s)	Magnetic Field Decay Constant (λ) (s^{-1})	Remarks
1	4.75	0.0	0.0	
2	0.0	0.0	—	
3	4.75	0.0	$1.28\ 10^{-2}$	
4	—	—	—	No Nat. Conv.
5	4.75	0.0	$1.15\ 10^{-3}$	
6	0.0	$1.4\ 10^{4}$	—	

* $B(t) = B(0)\ \exp(-\lambda \times t)$

$\lambda = 1.28\ 10^{-2}\ s^{-1}$ corresponds to a decay of 10^{-4} in 10 min.

$\lambda = 1.15\ 10^{-3}\ s^{-1}$ corresponds to a decay of factor of two in 10 min.

Figure 4.1 Blanket #11.

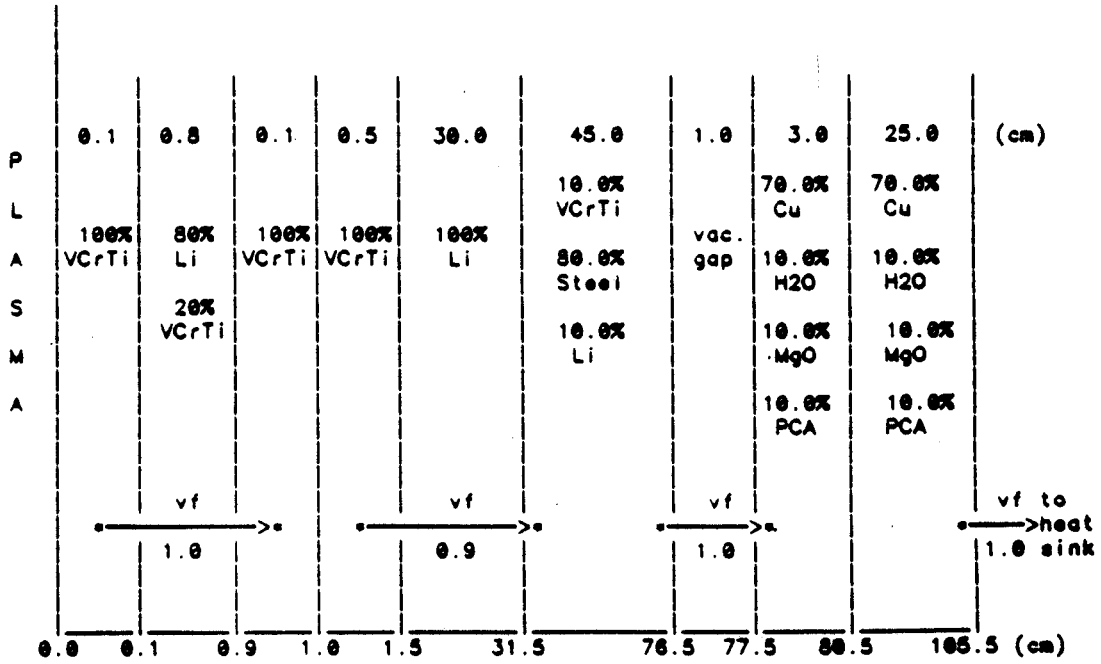

One-dimensional schematic of Los Alamos RFP Li/Li/V blanket for neutronics and 1-D thermal transport modeling.

Numbers at top are zone thicknesses in centimeters.

Arrows connecting asterisks indicate radiation paths in LOCA (complete Lithium drain) case. The vf parameters indicate the view factor for that particular radiation path.

The pressure drop due to magnetohydrodynamics effects is the dominant one. In a LOFA, if the magnets can't be shut down in a short time, MHD pressure drop will prevent the coolant from flowing. Then the effects of natural convection is negligible. This is shown in Figure 4.2. A temperature peak is observed at about 1040 °C, which may cause a structural failure, for both cases. Case 1 corresponds to the case in which the magnets are on during the transient. In Case 4, an older version of THIOD which does not allow natural convection calculations is used. The temperature response of the blanket is very similar in both cases, meaning natural convection is negligible due to high MHD pressure drop.

The effect of magnet shutdown behavior is also analyzed. The magnetic field is assumed to die off exponentially. Two different decay constants corresponding to a decay factor of four orders of magnitude in 10 minutes (Case 3), and a decay of factor of two in 10 minutes (Case 5) are considered. In Case 2 the magnetic field is assumed to shut off immediately after the accident. The temperature responses of Blanket #11 to those cases are shown in Figure 4.3 together with the Case 1 which corresponds to an operational magnetic field during the transient. Effects of natural convection are noticable. Cases 1, 2, and 3 exhibit a temperature peak of 900 °C just few seconds after the accident due to assumed continued plasma burn behavior in the first five seconds, (Figure 2.4). Case 5 has a temperature peak of about 700 °C. The temperature response of Cases 2 and 3 overlap each other which means the decay rate of the magnetic field in Case 2 is high.

The effect of the initial mass flow rate can be seen from Figure 4.4. In both cases, Case 2 and 6, the magnetic field is assumed to shut off immediately after the accident. Case 2 corresponds to a nil initial mass flow rate, whereas Case 6 corresponds to an initial upward operational mass flow rate of 10,000 kg/sec. The effect of initial mass flow rate can be seen up to 3 hours after the accident. As explained in the last section, inertial pressure drop is actually a pressure gain, because the term $\frac{d\dot{m}}{dt}$ is negative. Therefore, this initial mass flow reduces the first wall temperature to about 300 °C

Figure 1.2 First Wall Temperature Response of Blanket #11.

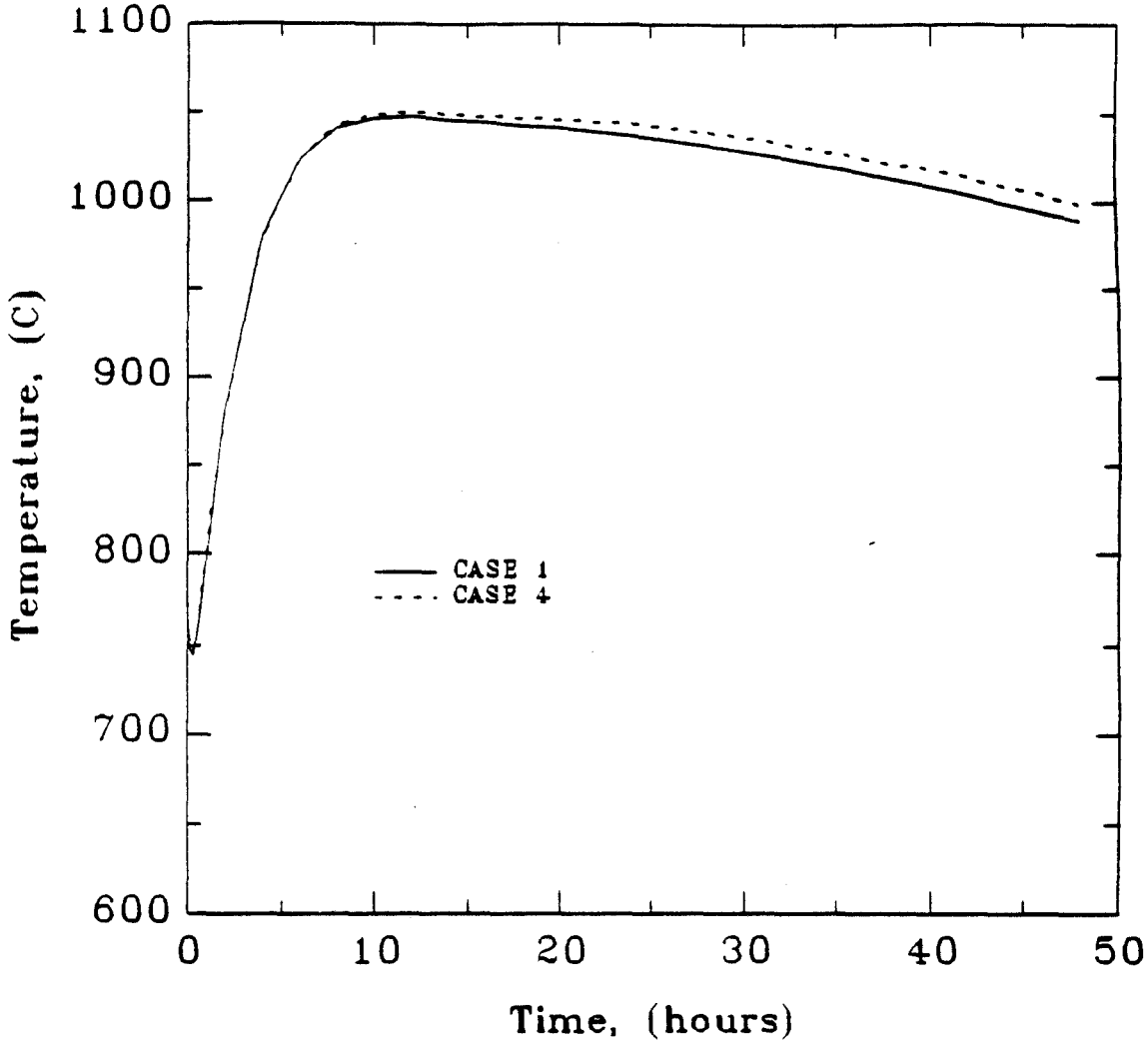

Figure 4.3 First Wall Temperature Response of Blanket #11.

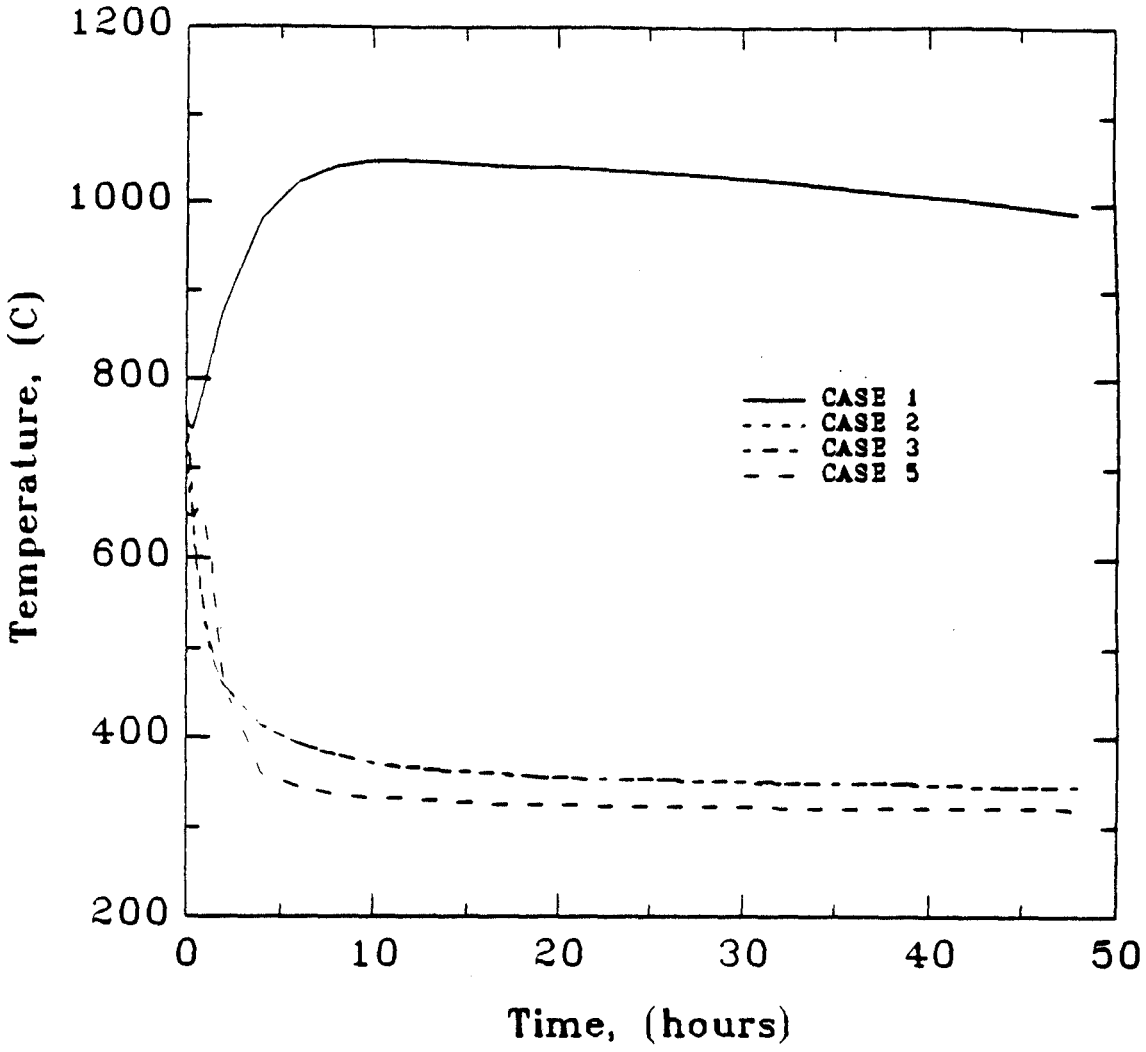

Figure 4.4 First Wall Temperature Response of Blanket #11.

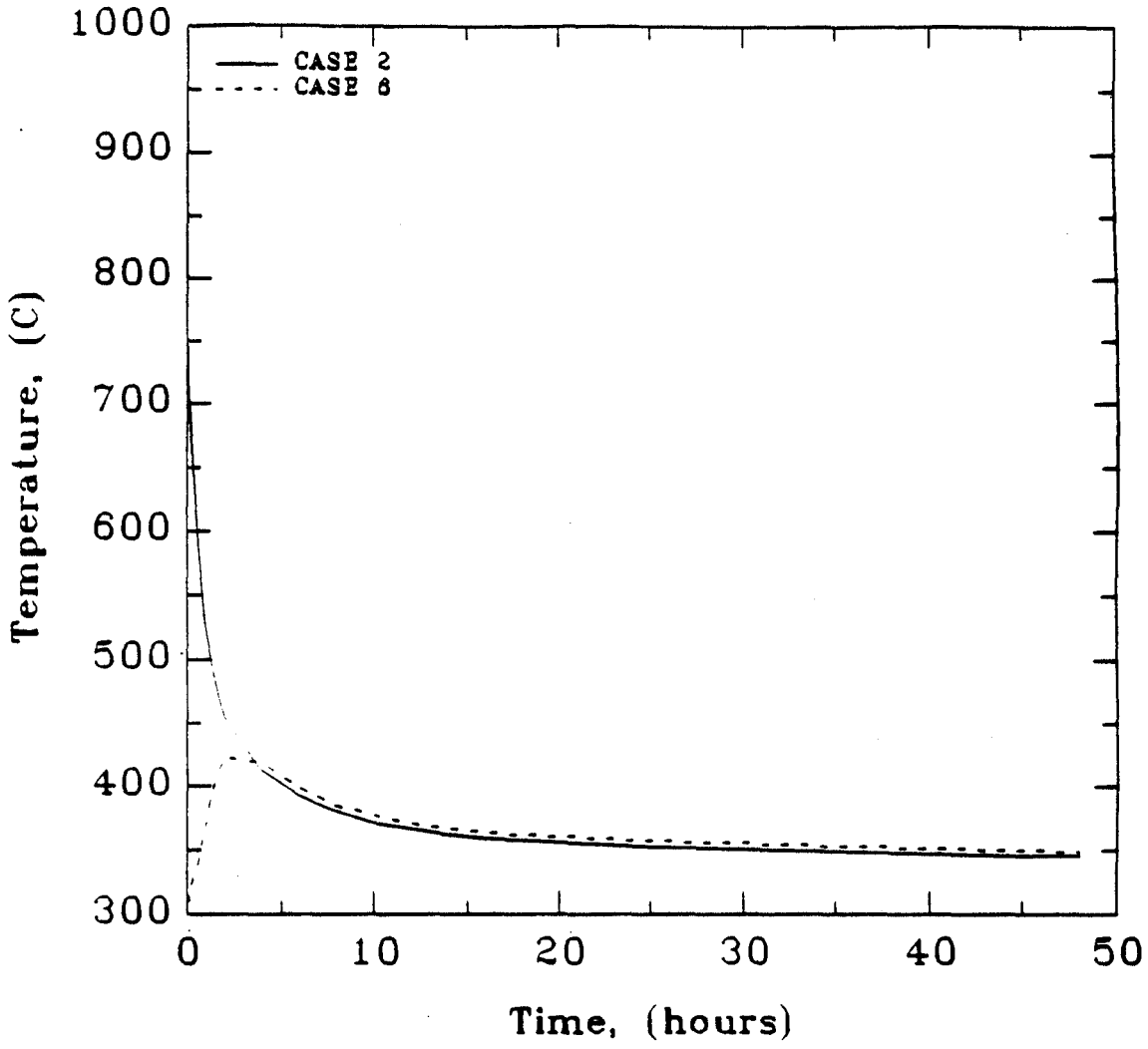

from an initial value of 600 °C few seconds after the accident.

4.3 Summary and Conclusions

The impact of natural convection is analyzed. The method of analysis used in the newer version of THIOD is explained. Temperature responses of a liquid lithium cooled blanket to various cases are compared. MHD effects cause a very high pressure drop so that the impact of natural convection is negligible. The initial upward mass flow rate helps drop the temperature to very low values for about 3 hours after the accident.

Chapter 5

Impact of Structural Material on Activation

In this chapter, the impact of the choice of the structural material on activation levels is investigated. Long-term activation of radionuclides created by elements in the structural material as a result of neutron interactions is a concern from a waste disposal point of view. Short-term activation, on the other hand, creates maintenance and safety problems. Therefore, the choice of structural material is an important consideration.

Several materials are proposed for use as structural materials. Most commercial metals are not low-radioactive materials. New alloys have been developed for low-activation purposes. A solution is the use of very-low-activation materials such as SiC, graphite or various aluminum alloys. These materials, however, require further development. Another way of solving the activation problem is elemental or isotopic tailoring of currently commercial steels, or using advanced relatively low-activation alloys such as VCrTi.

In the following section, results of a comparative activation analysis is presented. Three structural materials are compared from an activation standpoint. These materials are O3X11H1OM2 steel (a Soviet steel), SS-316, and VCrTi.

5.1 Results of Structural Activation Analysis

The blanket used in this part of the study is developed as part of ITER study [17,18,19]. Table 2.5 shows the design parameters and operating conditions. Figure 5.1 shows a one dimensional schematic of this blanket. Structural materials of Blanket #12, #13, and #14 are O3X11H1OM2, SS-316 and VCrTi, respectively. These blankets are cooled by water. Pb in pure form or in $Li_{17}Pb_{83}$ form is used for neutron multiplication. The inboard side of the blanket is 20 cm less thick than the outboard side.

Figure 5.1 Blankets #12 through #14.

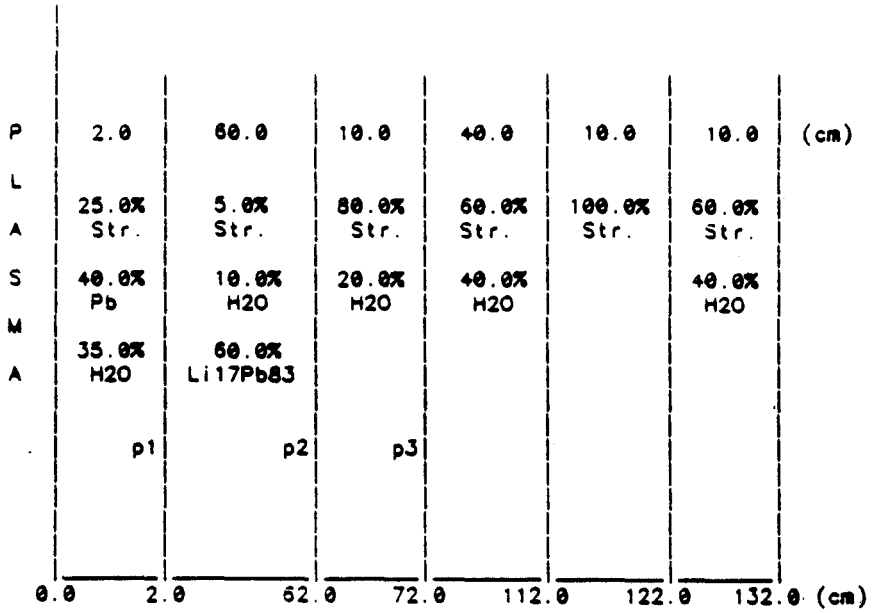

One-dimensional schematic of Blankets #12-14 outboard blanket for neutronics and activation modeling.
p1: point 1
p2: point 2
p3: point 3

Str. : Structural material

Blanket #12	03X11H10M2 Steel	(See Table 2.6)
Blanket #13	SS-316	(See Table 3.1)
Blanket #14	VCrTi	(See Table 3.1)

A one-dimensional neutronic analysis in cylindrical geometry is performed for this blanket. However, the D-shaped geometry of the plasma and surrounding blanket is assumed to be a one dimensional cylinder. Therefore, the radius of the cylinder is equal to the minor radius. In previous chapters, it was the total of major and minor radii.

The time dependent total specific activation levels are calculated at three locations which are shown in Figure 5.1. In Figure 5.2 through 5.4, these levels are plotted as a function of cooling time (time after shutdown). Points 1, 2, and 3 correspond to 2 cm from first wall (back of first wall), 62 cm from first wall (back of breeder), and 72 cm from first wall, respectively.

The activity levels of Blanket #12 and #13 are very close to each other for all locations. That is because of the structural materials containing similar elements used in these blankets. At Point 2, the activation levels depend on the breeder/multiplier $Li_{17}Pb_{83}$ (60% volumetric fraction) rather than structural material (5% volumetric fraction). Tritium activity from lithium is also shown in Figure 5.3. Tritium activity constitutes a large part of the total specific activity, and goes to zero after 30 years. Tritium activity should not be included in waste management considerations. Because, in normal operation, tritium will be removed from the blanket and coolant for reprocessing. But, a fraction of it, correponding to the steady state concentration, must be included in decay heat calculations.

The activity of Blanket #14 is higher than those of Blankets #12 and #13 until 10 minutes after shutdown, then becomes less active by about two orders of magnitude less after one year ($3.16\ 10^7$ sec). Figure 5.5 shows the first wall structural material activation as a function of cooling time. Total activation and structural material activation are almost equal to each other. Pb and H_2O do not affect the level of activation.

Behind the breeding/multiplier zone, the activity of structural materials is very low compared to that of the first wall. Although, structural material volume fraction is 80.0% at Point 3 which is higher than that of the first wall (25.0%), the activity of steels in the first wall are 100 times more, and the activity of VCrTi is 10 times more

Figure 5.2 Total Activation at Point 1.

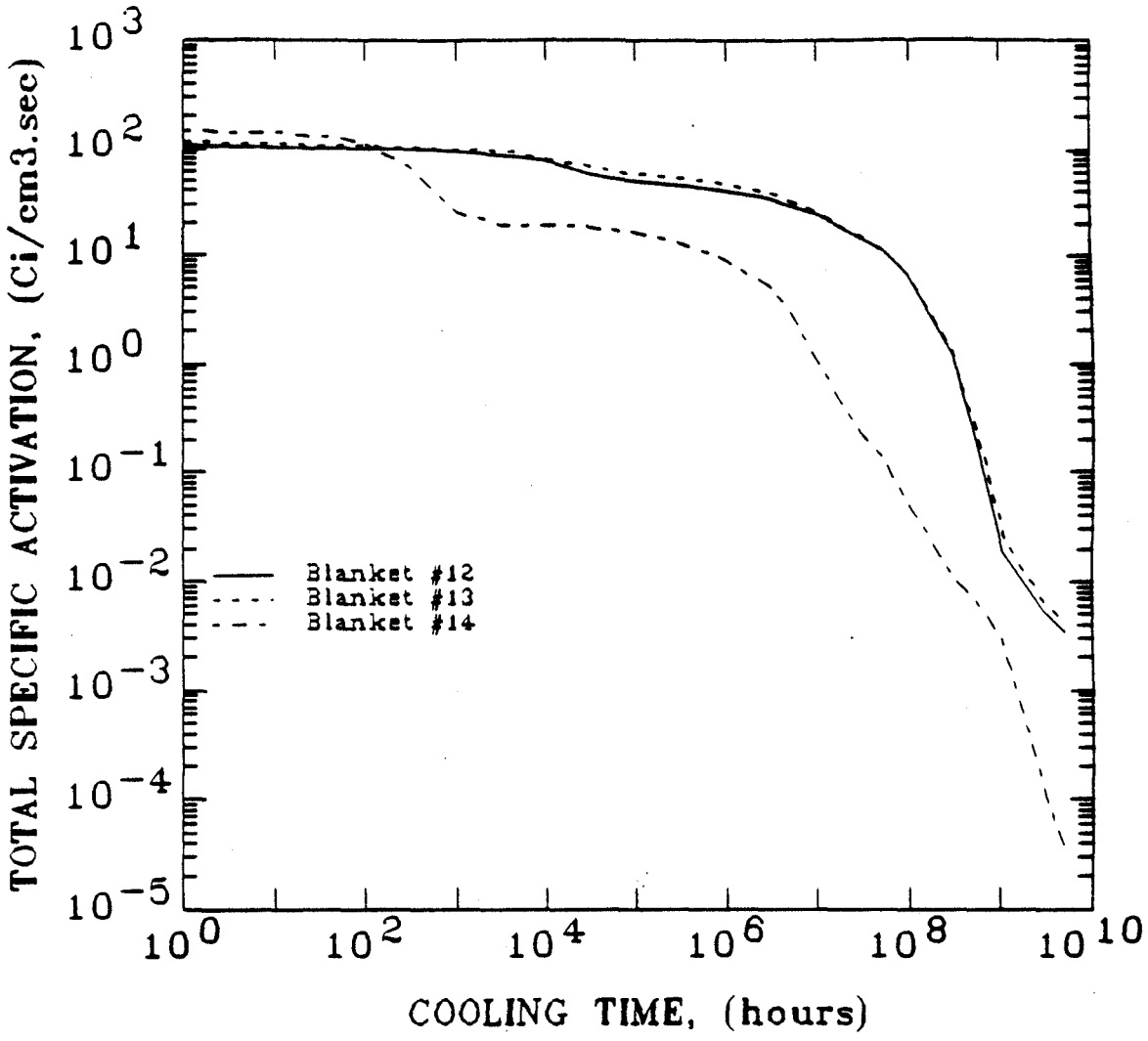

Figure 5.3 Total and Tritium Activation at Point 2.

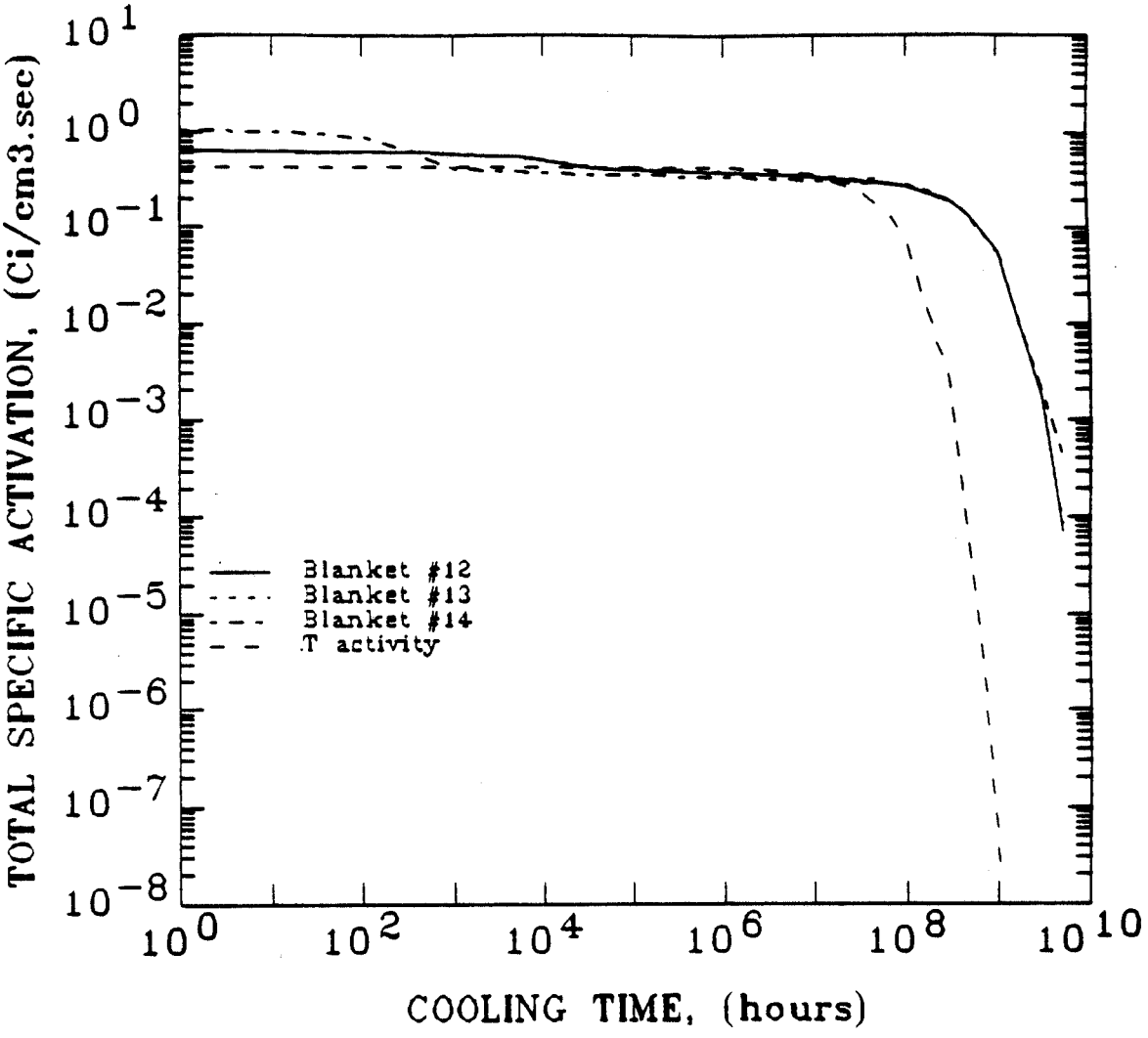

Figure 5.4 Total Activation at Point 3.

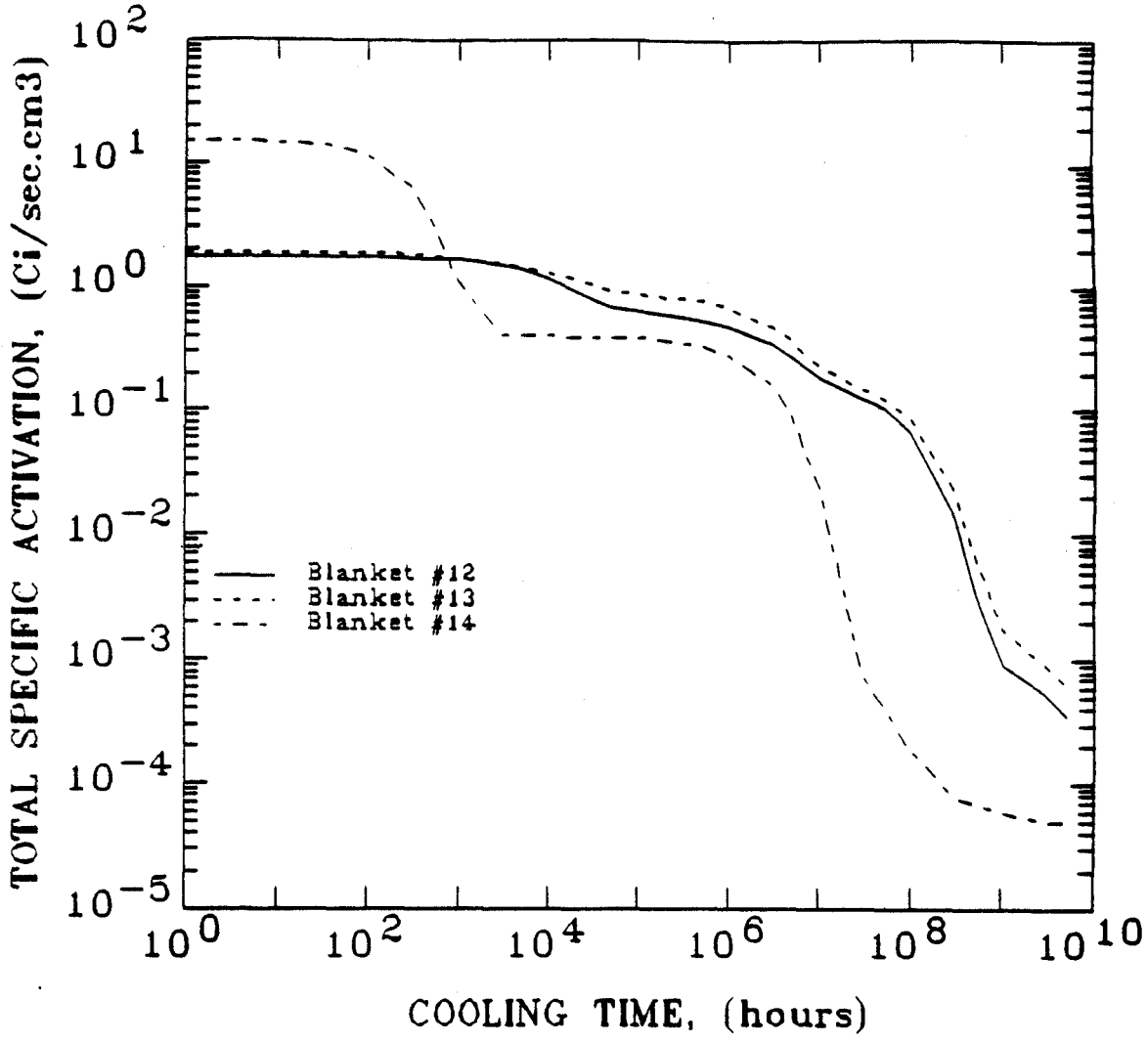

Figure 5.5 Structural Activation at Point 1.

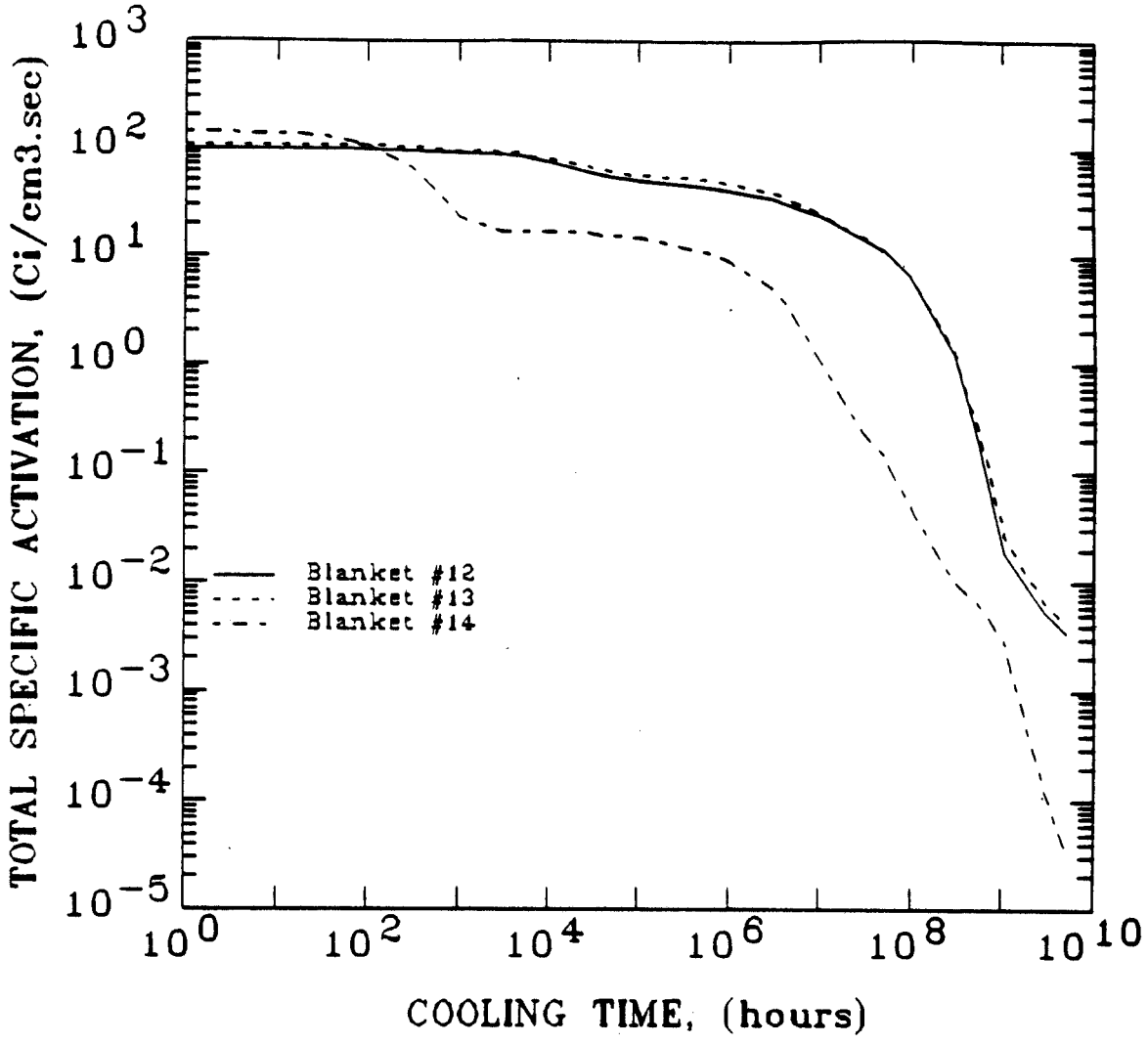

than those at Point 3.

5.2 Conclusions

The two steels have very similar activation characteristics. They are favorable to VCrTi from a thermal safety point of view. However, VCrTi has a lower activity than the steels two hours after shutdown, and therefore is more favorable from a maintenance point of view. VCrTi has also lower activity than the two steels in the long-term, and hence is better from a waste management standpoint.

Chapter 6

Summary and Conclusions

Use of the D-T fusion fuel cycle will cause induced radioactivity in materials surrounding the plasma, especially the structural first wall and blanket. One resulting problem is the potential for public exposure to the radioactive material due to a possible accidental release. A proper development path will reduce the potential hazards of future fusion power plants. Acceptance of fusion for commercial energy production will be influenced by environmental considerations.

Keeping the activation levels low in the blanket and in the shield is very important for several reasons:

- To minimize the dose rate around the reactor and to maintenance workers;
- To diminish the problems of waste handling;
- To limit the potential escalation of temperature following shutdown; and
- To lower the potential adverse health effects in case of a severe accident.

The function of the primary system of a fusion reactor is to remove the energy deposited in the first wall/blanket region surrounding the plasma. Conduits within the blanket structure contain the primary coolant to which the energy deposited in the blanket is transferred. A Loss-of-Cooling accident may result from a pump failure or a break of a coolant boundary. This will cause a termination of active cooling, and a blanket temperature rise.

Loss-of-Cooling accidents can be divided into two groups: Loss-of-Flow Accidents (LOFA) and Loss-of-Cooling Accidents (LOCA). In a LOFA, it is assumed that the coolant immediately stops at accident initiation and remains stagnant in an entire

module. In a LOCA, the coolant is assumed to be drained out immediately at accident initiation leaving a void in its place in an entire module. However, the possible heat transfer in the azimuthal direction is not allowed by the code which is used for temperature calculations in this study.

Subsequent to a loss of cooling accident, there are two heat sources of concern. If the plasma is not extinguished, it will continue to deposit energy in the blanket. The decay afterheat due to induced structural activity will also exist as a heat source in the blanket.

6.1 Summary of Method of Analysis

The first step in calculating the temperature is to determine the heat source present within the system. The temperature distribution calculation is needed to predict whether a structural failure will occur and to improve the design of blankets from the thermal safety point of view. Three computer codes are run successively to find the temperature responses of the blankets. These are ONEDANT [13], REAC [14] and THIOD [7].

ONEDANT is employed for the calculation of the neutron fluxes. Calculation of the activation is performed by running the activation/transmutation code REAC. The THIOD code is used for temperature response of the blankets.

Neutron flux calculations are performed in one-dimensional cylindrical geometry, and temperature calculations are performed in one-dimensional slab geometry.

The version of THIOD which is used in Chapter 3 only accounts for conduction and radiation heat transfer. The heat deposited in the blanket flows to the magnet coils by radiation.

6.2 Conclusions of the Effects of B_4C

The effects of B_4C on activation and thermal response of blankets are analyzed in Chapter 3. By including B_4C into the blanket-shield of an experimental type reactor, the activation and decay heat level can be limited. Hence, possible safety, maintenance and waste disposal problems are eased. Furthermore, including a graphite tile liner before the first wall does also help achieving low activation and better temperature response.

The inclusion of various amounts of B_4C with two different enrichment levels in the in the steel blanket of an experimental reactor are studied. Activation, decay heat density and temperatures after a LOCA are calculated for Blanket #1 through #8 for a neutron wall loading of 0.84 MW/m^2 for 1 year. It is found that ^{10}B enrichment does not offer any significant advantage over natural boron (Blanket #3 and #5). Excess amounts of B_4C such as 40% of the fractional volume of the first wall do not bring any significant advantage either, (Blanket #4, #5 and #8). The optimum B_4C (Blanket #2 and #7) volumetric fraction is 12.5% or lower, and brings significant advantages over the blankets without B_4C from a safety standpoint. Even under most severe LOCA, the temperature of the first wall never exceeds the operating temperature.

A graphite tile liner before the first wall, helps limit the temperature escalation of the first wall. Comparison of the highest temperatures of Blanket #2 and #7 shows that using the neutron absorber and the graphite tile liner at the same time results in an advantage of a difference of 50 °C in the temperature response over only using the neutron absorber. Therefore, if it is feasible from other viewpoints, such as strength, fabricability and irradiation resistance, the use of B_4C and a graphite tile liner at the same time are recommended. If one of them is not feasible to use, the other can still bring advantages alone.

The effects of the type of Loss-of-Cooling accident, of the plasma shut-down behavior and of the operating time are investigated. The temperature response of Blanket #5 to LOCA and LOFA overlap each other. Longer operating lifetimes cause a very minor

increase in temperature after five hours the accident, and continued plasma burn cause also a minor increase in temperature till one hour after the accident.

The effect of B_4C on a fusion power reactor shield is investigated. A 20 cm section of a 62 cm steel shield is replaced by B_4C. Then the temperature transients of the original blanket (Blanket #9) and the modified blanket (Blanket #10) with B_4C in case of LOCA are compared. The shield temperature of the modified blanket increases at a much slower rate than the original blanket does. The first wall temperature of Blanket #10 is 100 °C lower than that of Blanket #9 after about 10 hours, and even lower than its operating temperature.

6.3 Impact of Natural Convection Cooling

In LOFA, as the coolant remains inside the coolant tubes, there is a possibility that the coolant flow would continue at a lower rate. This is due to buoyancy effects and known as natural convection. The effects of magnetic field on the temperature response of a liquid lithium cooled blanket is investigated. The effect of the initial mass flow rate/direction is also analyzed.

The flow rate of coolant under natural convection is found by hydraulic balance; total pressure losses are equal to the available pressure head. There are three components of the pressure drop: friction, MHD effects and inertial effects. The available pressure head is due to the buoyancy effects. The pressure balance equation is solved for coolant mass flow rate, and then, the heat removal rate from the blanket to the coolant can be calculated.

The pressure drop due to MHD effects is the dominant one if the magnets can't be turned off. In this case, natural convection will have no impact at all. However, by rapid decay of the magnetic field, temperature escalation of the first wall would be limited.

The effect of initial mass flow rate can be seen only if the magnets can be shut off quickly. An initial upward mass flow rate helps to drop the temperature to very low

values for about 2 hours after the accident. Therefore, a blanket design which employs downward mass flowrate has adverse effects on the safety of the blanket, and hence, it is not recommended.

6.4 Impact of Structural Materials on Activation

The impact of the choice of the structural material on activation levels is investigated. Long-term activation of radionuclides created by elements in the structural material is a concern from a waste disposal point of view. Three materials, O3X11H1OM2 (a Soviet steel), SS-316 and VCrTi are compared from an activation standpoint.

The activity levels of the two steels are very close to each other. Because, these materials contain similar elements. The activity of VCrTi is about 2-10 times higher than that of the steels for the first two hours after the accident. It becomes 1-2 order of magnitude less than those of the steels two hours after the accident.

In the breeding/multiplication zone, activity level is governed by the breeder/multiplier $Li_{17}Pb_{83}$, and in other zones, it is governed mainly by the structural material.

References

1. M.S. Kazimi, 'Risk Considerations for Fusion Energy,' Nuclear Technology/Fusion, Vol. 4, 527, September 1983.

2. S. Fetter, 'A Calculational Methodology for Comparing the Accident, Occupational, and Waste-Disposal Hazards of Fusion Reactor Designs,' Fusion Technology, Vol. 8, 1359, July 1985.

3. J.P. Holdren, 'Fusion Energy in Context,' Science, No. 200, 168, April 1978.

4. S.J. Piet, *et al.*, 'Relative Public Effects from Accidental Release of Fusion Structural Radioactivity,' Nuclear Technology/Fusion, Vol. 4, 533, September 1983.

5. D.L. Smith *et al.*, 'Blanket Comparison and Selection Study (BCSS) - Final Report, Argonne National Laboratory,' ANL/FPP-84-1, Sept. 1983.

6. S.J. Brereton, and M.S. Kazimi, 'Safety and Economic Comparison of Fusion Fuel Cycles,' PFC/RR-87-7, Aug. 1987.

7. J.E. Massidda, and M.S. Kazimi, 'Thermal Design Considerations for Passive Safety of Fusion Reactors,' PFC/RR-87-18, Oct. 1987.

8. J.E. Massidda, *et al.*, 'Passive Safety Considerations in Thermal Design of Fusion Blankets,' to be published, submmitted to NURETH-4 conference, Jan. 1989.

9. J.A. Blink, and G.P. Lasche, 'The Influence of Steel Type on the Activation and Decay of Fusion Reactor First Walls,' Nuclear Technology/Fusion, Vol. 4, 1146, Sept. 1983.

10. E.T. Cheng, *et al.*, 'Low Activation Burning Core Reactor Design Studies' Fusion Technology, Vol. 8, 1408, July 1985.

11. G. Hopkins, *et al.*, 'Low Activation Fusion Design Studies, Annual Report for FY 1983' GA Technologies Report GA-A17389, Oct. 1984.

12. S.J. Piet, *et al.*, 'Potential Consequences of Tokamak Fusion Reactor Accidents: The Materials Impact,' PFC/RR-82-19, June 1982.

13. R.D. O'Dell *et al.*, 'User's Manual for ONEDANT: A Code Package for ONE-Dimensional, Diffusion-Accelerated, Neutral-Particle Transport, Los Alamos National Laboratory, LA-9184-M, Feb. 1982.

14. F.M. Mann, Transmutation of Alloys in MFE Faciliteis as Calculated by REAC (A Computer Code System for Activation and Transmutation), Hanford Engineering Development Laboratory, HEDL-TME-81-37, Aug. 1982.

15. J.D. Lee, editor, 'TIBER II/ETR Final Design Report,' UCID-21150, Volumes 1, 2, and 3, Sept. 1987.

16. B.N. Kolbasov, *et al.*, 'Summary of Soviet Works on ITER Safety and Environmental Impact (S+E) Work Packages for Definition Phase,' ITER-TN-SA- 8-S-1, May1988

17. J. Raeder, *et al.*, 'S& E for ITER Specalists Meeting,' ITER-TN-SA-8-3, Aug. 1988.

18. A. Kashirskij, Personnel communication, Oct. 1988.

19. N.E. Todreas, and M.S. Kazimi, 'Nuclear Systems,' Hemisphere, to be published 1989.

20. Classnotes of Subject 22.63, MIT, 1989.

21. J.E. Chafey, and J.B. Wattier, 'Estimation of Allowable Design Stress Values for 12Cr-1Mo-0.3V Steel, General Atomic Project 4230, GA-A14610, Feb. 1978.

22. J.A. Collins, 'Failure of Materials in Mechanical Design,' John Wiley & Sons, 1981.

23. J.F. Harvey, 'Theory and Design of Pressure Vessels,' N.Y., Van Nostrand, 1985.

24. Classnotes of Subject 22.314J, MIT, 1988.

25. J.H. Lienhard, 'A Heat Transfer Textbook,' Prentice Hall, Inc., Englewood Cliffs, N.J., 1981.

26. F.M. Mann, Personal Communication, 1988.

27. W.E. Meyerhof, 'Elements of Nuclear Physics,' New York, Mc Graw Hill, 1967.

28. 'Marks' Standard Handbook for Mechanical Engineers,' 7^{th} ed., Mc Graw Hill, 1967.

29. O.E. Dwyer, 'Liquid Metal Heat Transfer,' Gordon and Breach, 1976.